



Factors affecting the excitability of skinned fibres of the rat

Submitted by

Craig Andrew Goodman B. Sc. (Hons.)

A thesis submitted in the total fulfillment of the requirement for
the degree of

Doctor of Philosophy

Muscle Cell Biochemistry Laboratory, School of Biomedical Sciences

Footscray Park Campus, Victoria University

PO Box 14428 Melbourne City Mail Centre

Victoria, 8001, Australia

December 2003

FTS THESIS
573.751935 GOO
30001008089155
Goodman, Craig Andrew
Factors affecting the
excitability of skinned
fibres of the rat



Table of Contents

Summary	x
Declaration	xiv
Acknowledgements	xv
List of publications	xvi
List of abbreviations	xviii
List of figures	xxii
List of tables	xxv
Chapter 1.	
GENERAL INTRODUCTION	1
The Excitation-Contraction-Relaxation cycle – an overview	1
Structures and molecular events involved in the E-C-R cycle	2
<i>Transverse-tubular system</i>	3
<i>Dihydropyridine receptor/voltage sensor</i>	5
<i>Sarcoplasmic reticulum</i>	7
<i>Ryanodine receptor/calcium release channel</i>	8
<i>RyR isoforms and splice variants</i>	10
<i>Putative endogenous regulators of the skeletal muscle RyR1 isoform</i>	12
<i>Ca and Mg ions</i>	12
<i>ATP</i>	14
<i>Calmodulin</i>	14

<i>Other triadic proteins</i>	15
<i>FKBP12</i>	15
<i>Triadin</i>	15
<i>Junctin</i>	16
<i>SR Ca²⁺ ATPase/SR Ca²⁺ pump</i>	16
<i>The contractile apparatus</i>	17
<i>Thin filament structure at rest</i>	17
<i>Thin filament activation and muscle contraction</i>	19
<i>Thick filament structure</i>	20
<i>Isoforms of the contractile and regulatory proteins of the thin and thick filaments</i>	20
<i>Myosin heavy chain isoforms</i>	22
<i>Calcium up-take by the SR calcium ATPase/Pump</i>	23
<i>Signal transduction between the DHPR and RYR</i>	24
<i>Protein-protein interaction</i>	24
<i>IP₃ mediated coupling</i>	25
<i>Ca²⁺ mediated coupling</i>	26
Skeletal muscle fibre diversity	27
<i>Methods of classifying muscle fibre types</i>	28
<i>Immunohistochemical determination of MHC isoforms</i>	31
<i>Determination of MHC isoforms using SDS-PAGE</i>	31
Aspects of postnatal development of rat skeletal muscle relevant to the R cycle	E-C-32
<i>Growth of whole muscle and individual fibres</i>	33

<i>T-system and SR</i>	35
<i>DHPR/voltage sensors and RyR/calcium release channels</i>	35
<i>E-C coupling</i>	36
<i>Myosin heavy chain isoforms</i>	38
<i>Contractile properties</i>	39
<i>Concluding remarks</i>	39
Use of skinned fibres for studying E-C coupling	41
<i>Advantages of the mechanically skinned fibre preparation</i>	44
<i>Disadvantages of the mechanically skinned fibre preparation</i>	45
Skeletal muscle glycogen	45
<i>Glycogen particle structure</i>	45
<i>Location of skeletal muscle glycogen and glycogenolytic enzymes</i>	49
<i>Glycogenolysis</i>	51
<i>Glycogen phosphorylase</i>	52
<i>Phosphorylase kinase</i>	52
<i>Glycogen and muscle fatigue</i>	53
<i>Energy related role of glycogen in fatigue</i>	54
<i>Non energy related role of glycogen in fatigue</i>	55
Aims of this study	58
Chapter 2.	
GENERAL MATERIALS AND METHODS	59
<i>Animals</i>	59

	<i>Muscle dissection</i>	59
	<i>Single muscle fibre dissection</i>	
60		
	<i>Mechanical skinning</i>	60
	<i>Measurement of muscle fibre dimensions</i>	62
	<i>Mounting the skinned muscle fibre preparation to the force measuring system</i>	62
	<i>Force measurements and recording apparatus</i>	64
	<i>Force transducer calibration</i>	66
	<i>The protocol for T-system depolarization induced activation</i>	66
	<i>Parameters describing skinned fibre responsiveness to T-system depolarization</i>	67
	<i>Force detection limit</i>	70
	<i>Solution composition</i>	70
	<i>Free $[Ca^{2+}]$ in the Polarizing solution</i>	74

Chapter 3.

DEVELOPMENTAL AGE AND E-C COUPLING CHARACTERISTICS OF MECHANICALLY SKINNED MUSCLE FIBRES OF THE RAT

	Introduction	76
	Materials and Methods	77
	<i>Animals</i>	77

<i>Skinned fibre preparation</i>	77
<i>Skinned fibre solutions</i>	77
<i>T-system depolarization and E-C coupling parameters</i>	78
<i>Contractile apparatus experiments</i>	78
<i>Data analyses and statistics</i>	82
Results	82
<i>Age related differences in E-C coupling characteristics</i>	82
<i>Maximum depolarization-induced force response</i>	82
<i>75% run-down</i>	89
<i>Stability of responsiveness to T-system depolarization</i>	
92	
Discussion	92
<i>Age related differences in E-C coupling characteristics</i>	94
<i>Maximum depolarization-induced force response</i>	94
<i>Run-down</i>	96
<i>Methodological comments</i>	97
Chapter 4.	
MHC-BASED FIBRE TYPE AND E-C COUPLING CHARACTERISTICS OF MECHANICALLY SKINNED MUSCLE FIBRES OF THE RAT	
Introduction	99
Materials and Methods	101
<i>Animals and muscles</i>	101
<i>Mechanically skinned single fibre preparations and T-system depolarization experiments</i>	102
<i>Skinned fibre solutions</i>	102

<i>Myosin heavy chain analysis</i>	102
<i>Sample preparation</i>	102
<i>Electrophoretic set up</i>	102
<i>Staining of polyacrylamide gels</i>	104
<i>Statistics</i>	105
Results	105
<i>Profiles of T-system depolarization induced force responses developed by electrophoretically typed single fibre preparations from EDL, SM and SOL</i>	105
<i>Relationship between quantitative E-C coupling characteristics</i>	110
<i>Quantitative E-C coupling characteristics in electrophoretically typed single fibres from EDL, SM and SOL</i>	113
<i>Type IIB EDL fibres vs type IIB SM fibres</i>	113
<i>Type IIB EDL and type IIB SM fibres vs Type I SOL fibres</i>	116
<i>Type IIB/D SM fibres vs type IIB SM fibres; type I/IIA SOL fibres vs type I SOL fibres</i>	116
<i>Type I SOL fibres</i>	118
Discussion	118
<i>$_{max}DIFR$ and MHC-based fibre type</i>	119
<i>$_{75\%R-D}$ and MHC-based fibre type</i>	121
<i>Profile of T-system depolarization induced force responses produced by mechanically skinned fibres from EDL, SM and SOL muscles</i>	123
<i>Are functional characteristics of the T-system and SR compartments related to MHC-based fibre type?</i>	126

Chapter 5.

GLYCOGEN STABILITY AND GLYCOGEN PHOSPHORYLASE ACTIVITIES
IN ISOLATED SKELETAL MUSCLES FROM RAT AND TOAD

Introduction	130
Materials and Methods	131
<i>Animals</i>	131
<i>Muscle preparation</i>	132
<i>Muscle storage</i>	133
<i>Glycogen determination</i>	133
<i>Wet weight/dry weight conversion</i>	135
<i>Phosphorylase activities</i>	135
<i>Statistics</i>	136
Results	137
<i>Glycogen content in control muscles</i>	137
<i>Glycogen content in muscles stored under oil at RT</i>	137
<i>Glycogen content in muscles stored under oil at 4°C</i>	139
<i>Phos_{total} and Phos a activities in control muscles</i>	140
<i>Phos_{total} and Phos a activity in muscles stored under oil at RT 4°C</i>	and 140
Discussion	144
<i>Glycogen content and phosphorylase activities in freshly dissected (control) muscles</i>	144
<i>Glycogen loss and phosphorylase activities in muscles stored under oil at RT and at 4°C</i>	149

Chapter 6.

GLYCOGEN CONTENT AND RESPONSIVENESS TO T-SYSTEM

DEPOLARIZATION IN RAT MECHANICALLY SKINNED MUSCLE FIBRES

Introduction	153
Materials and Methods	154
<i>Animals and muscles</i>	154
<i>Skinned fibre responsiveness to T-system depolarisation</i>	155
<i>Skinned fibre solutions</i>	155
<i>Glycogen analysis in single fibre segments</i>	155
<i>Preparation of Petri dishes for enzymatic reactions in μl volumes</i>	157
<i>Solutions</i>	157
<i>Reaction steps</i>	157
<i>Preparation of reaction droplets</i>	158
<i>Determination of SFGlyc in washed fibre segments</i>	158
<i>Determination of fluorogenic material in washing solution</i>	160
<i>Determination of NGlyc material in the washing solution</i>	160
<i>Microfluorometric reading of samples</i>	160
<i>STD curves</i>	162
<i>Glucose and insulin treatment</i>	164
<i>Statistics</i>	164
Results	164
<i>Glycogen content in mechanically skinned fibres from rat EDL muscle</i>	164
<i>The contractile responsiveness to T-system depolarization of mechanically skinned fibres from rat EDL muscles</i>	165

SR Ca²⁺-release induced by T-system depolarization in mechanically skinned fibres from rat EDL muscle is not accompanied by detectable loss of fibre glycogen 168

Initial SFGlyc and response capacity in mechanically skinned fibres from rat EDL muscle 170

Discussion 170

CONCLUDING REMARKS 180

REFERENCES 183

Summary

During the last decade, the rat mechanically skinned fibre preparation has been used with increasing frequency to investigate cellular aspects of excitation-contraction (E-C) coupling processes in mammalian skeletal muscle. The main aim of this PhD project was to increase awareness of factors that affect the contractile responsiveness of rat mechanically skinned fibre preparations to T-system depolarization, a functional parameter of E-C coupling referred to, sometimes, as skinned fibre excitability. More specifically, the work presented in this thesis is concerned with the relationship between rat skinned fibre excitability and (i) developmental age (*Chapter 3*), (ii) MHC composition, muscle of origin (*Chapter 4*) and (iii) glycogen content (*Chapter 6*). Below are summarized the specific aims of the individual studies carried out within the scope of this project, and the major findings produced.

1. This study was undertaken to examine whether the responsiveness to T-system depolarization in mechanically skinned fibres from rat fast-twitch skeletal muscle varies with the developmental age of the animal. Three descriptors of skinned fibre excitability, (i) the amplitude of the maximum depolarization-induced force response (maxDIFR); (ii) the number of depolarization-induced force responses elicited before 75% run-down ($75\%R-D$); and (iii) the stability of the responsiveness to T-system depolarization ($\#DIFR_{80-100\%}$) were determined in Long Evans (LE) rats aged 4 to 21 wks. Rats belonging to this age range are commonly used in investigations of 'adult' rat skeletal muscle contractility. The data show for the first time that the contractile

responsiveness of mechanically skinned fibre preparations from rat extensor digitorum longus (EDL) muscle to T-system depolarization varies with the developmental age of the animal. More specifically it was found that mechanically skinned fibres from 21 wk old rats performed well with respect to all descriptors of E-C coupling (maxDIFR , $75\%R-D$, $\#DIFR_{80-100\%}$) examined, while fibres from 4 wk old rats were the poorest performers for all three parameters. By comparison, fibres from 10 wk old rats performed as well as 21 wk fibres with respect to maxDIFR but not with respect to $75\%R-D$ or $\#DIFR_{80-100\%}$.

2. In this study, it was investigated whether the previously established differences between fast- and slow-twitch single skeletal muscle fibres of the rat, in terms of myosin heavy chain (MHC) isoform composition and contractile function, are paralleled by differences in E-C coupling. Characteristics of contractile responsiveness to T-system depolarization-induced activation of electrophoretically typed, mechanically skinned single fibres from the soleus (SOL), EDL, and the white region of the sternomastoid (SM) muscle were determined and compared. The quantitative parameters assessed were maxDIFR and $75\%R-D$. The mean maxDIFR values for type IIB EDL and type IIB SM fibres were not statistically different, and both were greater than the mean maxDIFR for type I Sol fibres. The mean $75\%R-D$ for type IIB EDL fibres was greater than that for type I Sol fibres as well as type IIB SM fibres. These data suggest that E-C coupling characteristics of mechanically skinned rat single muscle fibres are related to MHC based fibre type and the muscle of origin.

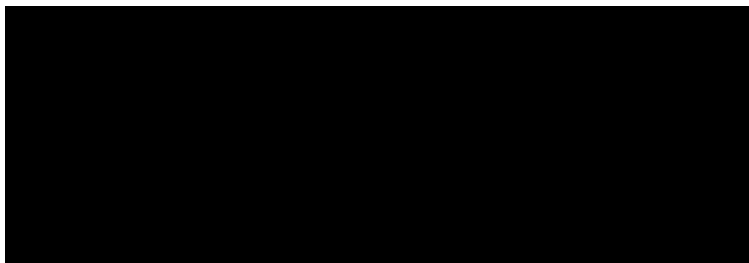
3. This study was concerned with the stability of glycogen in isolated EDL and SOL muscles of the rat and iliofibularis (IF) muscles of the toad during storage conditions commonly used in experiments involving mechanically skinned single fibre preparations. Glycogen content was determined fluorometrically in homogenates prepared from whole muscles stored under paraffin oil for up to 6 hrs at RT (20-25°C) or 4°C. Control muscles and muscles stored for 0.5 hr and 6 hrs were also analysed for total phosphorylase and phosphorylase a activities. No significant change was observed in the glycogen content of EDL and SOL muscles stored at RT for 0.5 hr. In rat muscles stored at RT for longer than 0.5 hr, the glycogen content decreased to 67.6 % (EDL) and 78.7 % (SOL), when compared to controls, after 3hrs and to 25.3 % (EDL) and 37.4 % (SOL) after 6 hrs. Rat muscles stored at 4°C retained 79.0 % (EDL) and 92.5 % (SOL) of glycogen after 3hrs and 75.2 % (EDL) and 61.1 % (SOL) after 6 hrs. The glycogen content of IF muscles stored at RT or 4°C for 6 hrs was not significantly different from controls. Taken together, these results indicate that storage under paraffin oil for up to 6 hrs at RT or 4°C is accompanied by a time- and temperature-dependent glycogen loss in EDL and SOL muscles of the rat and by minimal glycogen loss in toad IF muscles.
4. Glycogen content (determined microfluorometrically), response capacity to T-system depolarization (a composite parameter describing the amplitude of force responses and the number of responses to 'run-down') and the relationship between these two parameters were examined in single

mechanically skinned fibres from rat EDL muscle in the presence of high and constant [ATP] and [creatine phosphate]. These experiments were carried out within 3 hours of muscle dissection. Total glycogen content (tGlyc) in freshly dissected fibres was 58.1 ± 4.2 mmol glucosyl units/l fibre ($n = 53$), with a large proportion being retained in the skinned fibres (SFGlyc) after 2 min (73.1 ± 2.8 %) and 30 min (64 ± 12.3 %) exposure to an aqueous relaxing solution. The proportion of SFGlyc was markedly lower ($\sim 28\%$) after 30 min incubation of the fibre in a high ($30 \mu\text{M}$) Ca^{2+} solution, which suggests that rat skinned fibres contain a Ca^{2+} -sensitive glycogenolytic system. In rat skinned fibres there was no detectable loss of glycogen associated with T-system depolarization-induced Ca^{2+} release and there was no correlation between response capacity and initial SFGlyc, indicating that other factors, unrelated to glycogen depletion, ultimately limited the capacity of rat skinned fibres to respond to T-system depolarization. These data indicate that rat mechanically skinned fibre preparations are well suited for studies of glycogenolysis at a cellular level and that with further refinement of the depolarization protocol may be suitable for studies of the non-metabolic role of glycogen in mammalian skeletal muscle contractility.

Knowledge of the contribution of animal age and MHC isoform composition to inter-fibre variability, with respect to skinned fibre responsiveness to T-system depolarization, has direct practical value for single fibre studies of E-C coupling in mammalian muscle which use the mechanically skinned fibre preparation.

Declaration

This thesis contains no material that has been presented or accepted for the award of any other degree or diploma in this or any other university. Except where specifically indicated in the text, the data presented herein is the result of work of the author, and to the best of my knowledge and belief, has not been previously written or published by any other person.



Craig Andrew Goodman

Acknowledgements

I would like to acknowledge and thank my supervisor Professor Gabriela Stephenson for her support, commitment, patience and insight. I am forever indebted for all that I have learned, professionally and personally, over the past few years.

I also thank current (Dr Ronnie Blazev, Mr Brett O'Connell and Mr Justin Kemp) and past members (Dr Susie Bortolotto, Dr Long Nguyen and Dr Michael Patterson) of the Muscle Cell Biochemistry Laboratory for their support, guidance, and for many funny moments.

To the guys 'down stairs' in the Exercise Metabolism Unit (Assoc. Prof Michael Carrey, Dr Alan Hayes and Mr Andy Williams) thanks for your friendship, for great debates and lunch time quizzes.

To my family and friends, I thank you for all your encouragement and prayers over the years. A big 'thank you' to my Dad for helping edit the final manuscript.

Finally, I would like to acknowledge my wife, Katrina, for her emotional, spiritual and financial support over the past decade that has allowed me to follow my dream. Your patience, encouragement and dedication have been a life line in times of doubt. I promise that I will spend more time with you and our beautiful Audrey.

List of Publications

Refereed papers

1. **Goodman CA & Stephenson GMM (2000).** Glycogen stability and glycogen phosphorylase activities in isolated skeletal muscles from the rat and toad. *J Muscle Res Cell Motil* **21**, 655-662.
 2. **Goodman CA, Patterson MF & Stephenson GM (2003).** MHC-based fibre type and E-C coupling characteristics in mechanically skinned muscle fibres of the rat. *Am J Physiol* **284**, C1448-C1459.
-

Goodman CA, Blazev R & Stephenson GMM. Glycogen content and contractile responsiveness to T-system depolarization in skinned muscle fibres of the rat. *Cell Physiol Biochem* (under review, Ms no. 2003MS078).

Blazev R, Goodman CA & Stephenson GMM. The effect of age and strain on E-C coupling characteristics of rat mechanically skinned skeletal muscle fibres. (in preparation).

Conference Presentations

1. **Goodman CA & Stephenson GMM (1999).** Glycogen stability in isolated muscles from toad and rat. *Proceedings of the Australian Physiological and Pharmacological Society.* 30 (2): 38P.

2. **Goodman CA, Patterson MF, Cellini M & Stephenson GMM (2000).** MHC isoform expression and EC-coupling in mechanically skinned muscle fibres of the rat. *Proceedings of the Australian Physiological and Pharmacological Society.* 31(2): 102P.

3. **Goodman CA, Patterson MF, Cellini M & Stephenson GMM (2000).** MHC isoform expression and EC-coupling in mechanically skinned muscle fibres of the rat. *The Physiologist.* 43(4): 357.

4. **Goodman CA, Nguyen LT & Stephenson GMM (2001).** A study of the relationship between glycogen content and excitation-contraction coupling in mechanically skinned muscle fibres of the rat. *Proceedings of the XXXIV International Congress of Physiological Sciences.* IUPS 2001 Christchurch, NZ. CD-ROM Abstract 750.

List of abbreviations

ADP – adenosine diphosphate

AMP – adenosine monophosphate

ANOVA – analysis of variance

ATP – adenosine triphosphate

ATPase – adenosine triphosphatase

cAMP – cyclic adenosine monophosphate

C – the proportion of total acrylamide monomer (acrylamide & methylenebisacrylamide) represented by methylenebisacrylamide

°C – degrees celcius

CaM – calmodulin

Ca²⁺ - calcium ion

[Ca²⁺] – concentration of ion X. e.g. [Ca²⁺] – concentration of calcium ions

cDNA – complementary deoxyribonucleic acid

CICR – calcium-induced calcium release

cm - centimeter

CP – creatine phosphate

C-terminal – carboxyl terminal

d - diameter

Da – Daltons

DHP - dihydropyridine

DHPR – dihydropyridine receptor

DIFR – depolarization-induced force response

E-C coupling – excitation contraction coupling

E-C-R cycle – excitation-contraction-relaxation cycle

EDL – extensor digitorum longus

EDTA - ethylenediaminetetraacetic acid

EGTA - ethyleneglycol-bis(β-aminoethylether)-N,N'-tetraacetic acid

Em – membrane potential

FT – fast twitch

G-6-P – gluocse-6-phosphate

GP – glycogen phosphorylase

g – gram

HDTA – hexamethalenediamine N,N,N',N'-tetraacetic acid

HEPES - N-2-hydroxyethyl-piper-azine-N'-2-ethylsulphonic acid

HMM – heavy meromyosin

hr - hour

IF - iliofibularis

IP₃ – inositol trisphosphate

K⁺ - potassium ion

K_{app} – apparent affinity constant

K_D – apparent dissociation constant

kDa – kilodaltons

kg - kilogram

K_m – Michaelis-Menton constant

l – length

LE – Long Evans

LMM – light meromyosin

M – molar

$_{\max}CaF$ – maximum Ca²⁺-activated force

$_{\max}DIFR$ – maximum depolarization-induced force response

mg - milligram

MG - macroglycogen

Mg²⁺ - magnesium ion

MHC – myosin heavy chain

ml – milliliter

MLC – myosin light chain

mm - millimeter

mM – millimolar

mosmol - milliosmols

mRNA – messenger ribonucleic acid

mV - millivolt

MW – molecular weight

Na⁺ - sodium ion

NADH - nicotine adenine dinucleotide (reduced form)

NAD⁺ - nicotine adenine dinucleotide (oxidized form)

NaN_3 – sodium azide

nF – no force response

nl - nanoliter

nm - nanometer

nM – nanomolar

N-terminal – amino terminal

pCa - $-\log_{10}[\text{Ca}^{2+}]$

pF – prolonged force response

PG - proglycogen

pH - $-\log_{10}[\text{H}^+]$

PhK – phosphorylase kinase

Phos a – phosphorylase a

Phos b – phosphorylase b

Phos_{total} – phosphorylase total

Pi – inorganic phosphate

PIP₂ - phosphatidylinositol 4,5-bisphosphate

pmol - picomol

PP1 – protein phosphatase 1

r – correlation co-efficient

r^2 – co-efficient of determination

75% R-D- number of depolarization-induced force responses to 75% run-down

RT – room temperature (20-25°C)

rtF – rapid transient force

RYR – ryanodine receptor

RYR1 – skeletal muscle ryanodine receptor isoform

RYR2 – cardiac muscle ryanodine receptor isoform

RYR3 – brain ryanodine receptor isoform

s - second

S1 – myosin subfragment 1

S2 – myosin subfragment 2

SDS-PAGE - sodium dodecyl sulfate-polyacrylamide gel electrophoresis

SEM – standard error of the mean

SM - sternomastoid

SOL - soleus

SR – sarcoplasmic reticulum

ST – slow twitch

T – the total concentration of monomer used to produced a polyacrylamide gel
(expressed as % w/v)

TC – terminal cisternae

TCA – trichloroacetic acid

Tm – tropomyosin

Tn - Troponin

TnC – troponin C

TnI – troponin I

TnT – troponin T

T-system – transverse tubular system

t-tubule – transverse tubule

μg – microgram

μl - microliter

μm - micrometer

μM – micromolar

μN - micronewton

V – volume

w – width

wks – weeks

List of Figures

Figure No.	Figure Title	Page
1.1	Skeletal muscle triad	4
1.2	The t-tubular DHPR/voltage sensor	6
1.3	Diagram of the molecular structure of the SR RyR/Ca ²⁺ release channel	9
1.4	Triad proteins involved in skeletal muscle E-C coupling	11
1.5	RyR/Ca ²⁺ release channel regulation	13
1.6	The ultrastructure of the thin filament in vertebrate skeletal muscle	18
1.7	Myosin heavy chain	21
1.8	Changes in rat body mass, muscle length and muscle girth with age	34
1.9	The mechanically skinned muscle fibre	43
1.10	The glycosome	47
1.11	The molecular structure of a glycogen particle	48
1.12	Correlation between toad fibre capacity to respond to T-system depolarization and initial fibre glycogen concentration	57
2.1	Dissecting microscope with video monitor system used for dissection, skinning and measuring single muscle fibres	61
2.2	Force measurement and recording apparatus	63
2.3	Circuit diagram of the Wheatstone bridge	65
2.4	Force transducer calibration curve	71
3.1	Representative chart recording of force response by a 10 week rat EDL fibre exposed to solutions with varying free Ca ²⁺ concentrations	81
3.2	T-system depolarization-induced force responses elicited in single mechanically skinned EDL fibres from Long Evans rats of different ages	83

3.3	Summarized data for (A) the maximum depolarization-induced force response and (B) the number of responses to depolarization obtained before 75% run-down in skinned fibres from 4-wk, 8-wk, 10-wk, 15-wk, and 21-wk Long Evans rats	87
3.4	Averaged force/pCa curves for 4 week (■; n = 16) and 10 week (○; n = 21) EDL fibres	88
3.5	Correlation between fibre cross-sectional area and the number of depolarization-induced force responses obtained before 75% run-down	93
4.1	Electrophoresis equipment	103
4.2	An example of a rapid transient force (<i>rtF</i>) response developed by type IIB EDL muscle fibre	a 106
4.3	Sample force responses produced by soleus fibres	107
4.4	An example of a trace from a soleus fibre that produced no force (<i>nF</i>) in response to T-system depolarisation	109
4.5	Representative electrophoretogram of the muscle fibre types from extensor digitorum longus (EDL), sternomastoid (SM) and soleus (SOL).	112
4.6	Relationship between the maxDIFR and $75\%R-D$ for type IIB EDL fibres, type IIB sternomastoid (SM) fibres, and type I SOL fibres	114
4.7	(A) The amplitude of the maximum depolarization induced force response (maxDIFR ; expressed as a % of the maximum Ca^{2+} activated force) for type IIB EDL, type IIB sternomastoid (SM) and type I SOL mechanically skinned muscle fibres. (B) The number of depolarization induced force responses to 75 % run-down ($75\%R-D$) in type IIB EDL, type IIB sternomastoid (SM) and type I SOL mechanically skinned muscle fibres.	117
5.1	The time course of glycogen loss in rat EDL, SOL and IF muscles stored under oil at room temperature (20 – 25°C) (A) and 4°C (B)	138
5.2	(A) Total phosphorylase activities ($\mu\text{mol}/\text{min}/\text{g}$ dry weight) in rat EDL and SOL and toad IF control muscles. (B) Phosphorylase a activities (expressed: $\text{mol}/\text{min}/\text{g}$ dry weight and as % of total phosphorylase) in rat EDL and SOL and toad IF control muscles	141
5.3	Phosphorylase 'a' activities (expressed as % of total phosphorylase) in rat EDL and SOL and toad IF muscles stored under oil at room temperature (20 – 25°C) (A) and 4°C (B) for up to 6 hrs	145
6.1	Arrangement of reagent droplets under a layer of mineral oil on the bottom of a Petri dish	159

6.2	Custom designed brass frame with two microcells	161
6.3	Microfluorimetric system used in single fibre glycogen content experiments	163
6.4	An example of the depolarization induced force responses developed by an EDL muscle fibre to 75 % run-down	167
6.5	Correlation between initial fibre glycogen concentration and fibre response capacity in mechanically skinned fibres	171

List of Tables

Table No.	Table Title	Page
1.1	Fibre type differences in structures and molecular species involved in the E-C-R cycle	29
1.2	Summarized information on the time taken by various structures and processes involved in the E-C-R cycle to reach adult values	40
2.1	Essential positive contributors to the upstroke and downstroke of T-system depolarization induced force responses in mechanically skinned fibre preparations	69
2.2	Solutions used in E-C coupling experiments	72
3.1	Volumes of relaxing (high EGTA) and maximum Ca^{2+} activation (high Ca-EGTA) solutions required to obtain Ca^{2+} -activation solutions used in force/pCa experiments	80
3.2	Mean summarized data for E-C coupling (and other) parameters examined in skinned fibres of different aged Long Evans rats	91
4.1	Profiles of T-system depolarisation induced force responses and the magnitude of low Mg^{2+} -induced force responses developed by electrophoretically typed single fibre preparations from EDL, SM and SOL	111
5.1	Ratio $\text{Phos}_{\text{total}} 6 \text{ hrs} / \text{Phos}_{\text{total}} \text{ control}$ for EDL, SOL and IF	143

Chapter 1

GENERAL INTRODUCTION

The Excitation-Contraction-Relaxation cycle – an overview

The term excitation-contraction relaxation cycle (E-C-R cycle) describes the process initiated by an electrical signal produced by normal nervous transmission or by direct stimulation, which involves excitation of the membraneous interface between myoplasm and extracellular fluid [sarcolemma and transverse (t)-tubular system (T-system)], activation of the contractile apparatus, deactivation of the contractile apparatus and muscle relaxation (Sandow, 1965; Stephenson *et al.*, 1998). More specifically for vertebrate skeletal muscle, the E-C-R cycle comprises the following events: 1) initiation and propagation of an action potential along the sarcolemma and into the T-system; 2) action potential induced depolarisation of the t-tubular membrane; 3) dihydropyridine receptor (DHPR)/voltage sensor activation associated with the T-system depolarization; 4) transmission of the signal from the T-system to the sarcoplasmic reticulum (SR) where Ca^{2+} is stored; 5) activation of the ryanodine receptor (RyR)/ Ca^{2+} release channel and release of Ca^{2+} from the SR into the myoplasm; 6) the rise in myoplasmic $[\text{Ca}^{2+}]$, binding of Ca^{2+} to the regulatory proteins on the thin filament and activation of the contractile apparatus, and 7) the reuptake of Ca^{2+} into the SR and muscle relaxation (Stephenson *et al.*, 1998).

Most of these events can be investigated at the cellular level using mechanically skinned fibre preparations, i.e. single muscle fibres demembrated under oil with a pair of fine forceps and incubated under controlled conditions in carefully designed

aqueous solutions. This thesis is concerned with the relationship between the responsiveness to T-system depolarisation (also referred to as fibre excitability; Barnes *et al.*, 2001) of rat mechanically skinned fibres and the developmental age of the rat, myosin heavy chain composition (MHC) of the fibre and fibre glycogen content. Accordingly, this chapter will briefly survey current knowledge on selected structures and events in the E-C-R cycle, the polymorphic nature of muscle proteins (with emphasis on MHC), the molecular diversity of skeletal muscle cells, the postnatal development of the rat and skeletal muscle glycogen.

Structures and molecular events involved in the E-C-R cycle

In the first step, there is a local change in the membrane potential (which becomes more positive inside) above a critical value known as 'threshold'. This event activates voltage-gated Na^+ - (and K^+ -) channels, triggering a wave of depolarizations (known as an 'action potential') which spread along the sarcolemma and into the T-system.

In the second step, the action potential is detected by a voltage sensitive protein complex (known as 'voltage sensor') located at the junction of the T-system and the SR. This protein, also referred to as the dihydropyridine receptor (DHPR), transmits the electrical signal to Ca^{2+} release channels located in the SR membrane. Once the Ca^{2+} release channel is activated, Ca^{2+} is rapidly released from the SR into the sarcoplasm causing a transient increase in the myoplasmic $[\text{Ca}^{2+}]$ from about $0.1 \mu\text{M}$ at rest to about $10 \mu\text{M}$ (Bagshaw, 1993). According to the current paradigm for the mechanism involved in the shortening or contraction of skeletal muscle, Ca^{2+} diffuse rapidly into the myofibrillar lattice and bind to the troponin C (TnC) protein on the actin thin filament. The binding of Ca^{2+} to TnC results in the removal of the inhibitory

action of TnI on tropomyosin and the movement of tropomyosin along the thin filament, which exposes the myosin binding sites on actin (Bagshaw, 1993). Myosin S1 heads can now bind to the thin filaments. Using the free energy released from the hydrolysis of ATP by the myosin ATPase, myosin swivels or rotates at the S2 flexible hinge, causing the actin filaments to slide over the myosin filaments. Once the electrical signal initiating SR Ca^{2+} release ceases the intracellular $[\text{Ca}^{2+}]$ must be lowered back to resting levels ($0.1 \mu\text{M}$) to induce muscle relaxation. This is accomplished in part by Ca^{2+} binding to myoplasmic Ca^{2+} binding proteins such as parvalbumin. Most Ca^{2+} however is actively 'pumped' back into the SR by the Ca^{2+} ATPase- Ca^{2+} pump. Once intracellular $[\text{Ca}^{2+}]$ has been lowered and TnC proteins are no longer occupied by Ca^{2+} , TnI resumes its inhibitory influence on tropomyosin, which in turn blocks the myosin binding sites on the thin filament.

Transverse-tubular system

The T-system is composed of a network of tubular invaginations (t-tubules) originating from the plasma membrane that project transversely into the cell interior making contact with every myofibril. The t-tubules enter mammalian muscle fibres at the region corresponding to the overlap between the actin and myosin filaments and hence occur twice every sarcomere. The major role of the T-system is to allow the propagation of an action potential from the plasma membrane into the core of the fibre and facilitate the activation of myofibrils deep within the muscle cell. The majority of the T-system is located in direct apposition to the terminal cisternae (TC) region of the SR. A triad (see Figure 1.1) is formed when a TC is located on either side of one t-tubule.

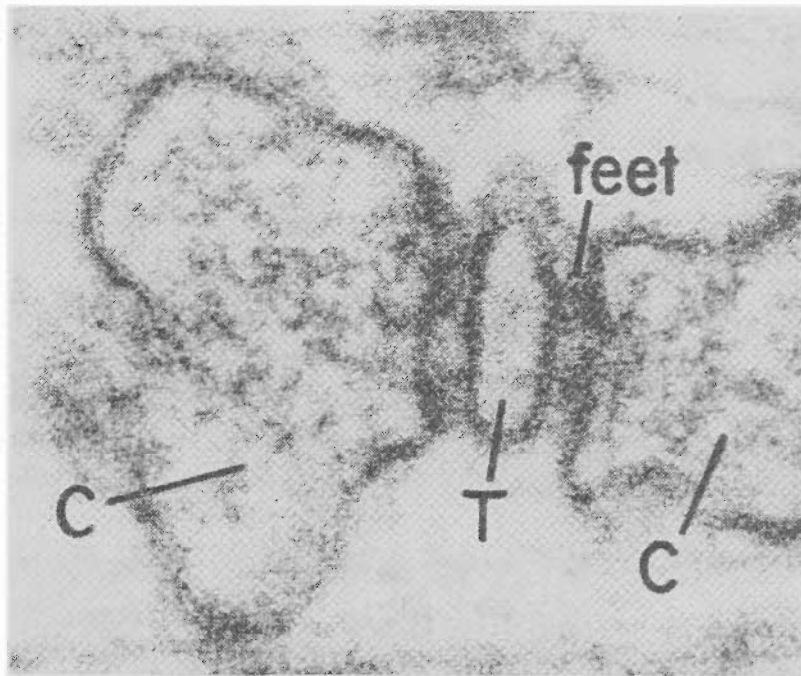


Figure 1.1. Skeletal muscle triad (cross-sectional view).

An SR terminal cisternae (C) is located on either side of a transverse tubule (T). The electron dense 'feet' structures represent the myoplasmic domain of the RyR/Ca²⁺ release channels. (Reproduced from Martonosi, 1994)

Dihydropyridine receptor/voltage sensor

The skeletal muscle t-tubule membrane is a rich source of DHPRs (Fosset *et al.*, 1983). The DHPR has the potential to act as a voltage-dependent L-type Ca^{2+} channel (Curtis & Catterall 1983, 1986) but less than 5 % of total appear to perform this function (Schwartz *et al.*, 1985). As shown in Figure 1.2A, the DHPR is made up of a large α_1 subunit (185 kDa) and several smaller subunits known as the α_2 (143 kDa), β (54 kDa), γ (30 kDa) and δ (26 kDa) (for reviews see Dulhunty, 1992, Aidely, 1998). The exact functions of these smaller subunits remain unclear but the α_1 subunit appears to contain the channel pore, the DHP binding sites and the voltage sensor. (Dulhunty *et al.*, 2002). There exist two molecular forms (isoforms) of the DHPR α_1 subunit, the α_{1S} (skeletal isoform) and α_{1C} (cardiac isoform). The α_{1S} is the most common isoform found in fast and slow skeletal muscle. The α_{1C} has been found in the heart, neonatal skeletal muscle, and in adult slow-twitch skeletal muscle (e.g. soleus) and in the diaphragm (Froemming *et al.*, 2000). The presence of the α_{1C} isoform may confer cardiac-type E-C coupling characteristics to skeletal muscle fibres (Tanabe *et al.*, 1990).

The molecular structure of the DHPR is very similar to that of the voltage dependent Na^+ channel, containing four membrane spanning repeat domains (I–IV), each of which contains six transmembrane α -helices (S1–S6) (Figure 1.2B). The fourth α -helix of each domain (S4) contains numerous positive charges and is thought to form the voltage sensor and be responsible for the asymmetrical charge movement observable upon membrane depolarization. The peptide loop located between ‘repeat’ domains II and III on the myoplasmic side of the t-tubular membrane appears to be essential for signal transmission between the T-tubule and the SR (Dulhunty, 1992;

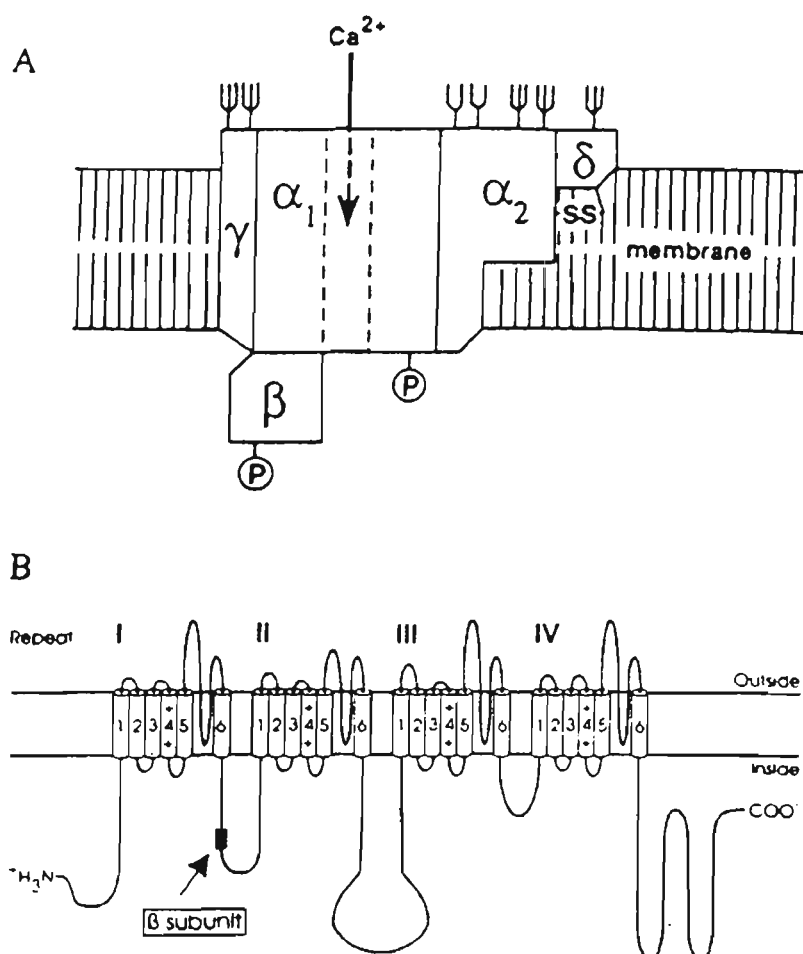


Figure 1.2 The t-tubular DHPR/voltage sensor.

A. The protein subunits that make up the t-tubular DHPR/voltage sensor L type Ca^{2+} channel. B. The molecular structure of the t-tubular DHPR/voltage sensor L type Ca^{2+} channel. (Reproduced from Melzer, 1995)

Matterson, 1994; see also section on *Signal transduction between the DHPR and RyR*, page 24). DHPRs are arranged in symmetrical groups of four called tetrads. Each DHPR tetrad is directly apposed to a RyR/Ca²⁺ release channel homotetramer. As already mentioned, although the DHPR is an L-type Ca²⁺ channel, the entry of Ca²⁺ through the channel from the extracellular fluid is not essential, in skeletal muscle, for an action potential or for muscle contraction (Luttgau & Spiecker, 1979; Dulhunty & Gage, 1988). Instead it seems that the major role of the DHPR in skeletal muscle is as a t-tubule membrane-bound voltage sensor. Indeed, dysgenic mice that do not express the $\alpha 1$ subunit display a lack of E-C coupling and DHP sensitive Ca²⁺ channels (Beam *et al.*, 1986) both of which can be restored by the microinjection of the $\alpha 1$ cDNA (Tanabe *et al.*, 1988).

Sarcoplasmic reticulum

The internal membrane system called the SR is the muscle cell equivalent of smooth endoplasmic reticulum and is separate from the outer plasma membrane and t-tubules (Peachy & Franzini-Armstrong, 1980). The two major regions of the SR relevant to the E-C-R cycle are the TC and the longitudinal tubules. The TC, also known as junctional SR, is involved in forming the triad (see Figure 1.1) whereby a TC is located on each side of a t-tubule (Franzini-Armstrong, 1994), while longitudinal SR run parallel to the muscle filaments and connect two TC together medially. The junctional surface of the SR is covered with regularly arranged and electron dense 'feet' structures (Figure 1.1) while non-junctional surfaces, including the longitudinal SR contain a high density of ATP-dependent Ca²⁺ pumps (Franzini-Armstrong, 1994).

The basic function of the SR is to regulate the $[Ca^{2+}]$ in the myoplasm and as a consequence regulate the activation state of the contractile apparatus (Peachy & Franzini-Armstrong, 1980). A resting myoplasmic $[Ca^{2+}]$ of $0.1 \mu M$ is maintained by the SR Ca^{2+} pumps which actively transports Ca^{2+} into the SR against a concentration gradient (Gillis, 1985). The glycoprotein calsequestrin, located within the TC, has a high capacity and medium affinity for Ca^{2+} binding and acts primarily as a Ca^{2+} buffer helping to reduce the SR lumen/myoplasm Ca^{2+} gradient (Yano & Zarain-Herzberg, 1994). When the muscle cell is stimulated Ca^{2+} is rapidly released from the SR via Ca^{2+} release channels located in the SR TC.

Ryanodine receptor/calcium release channel

The skeletal muscle Ca^{2+} release channel is also known as the ryanodine receptor (RyR) due to its ability to bind with high affinity the plant alkaloid ryanodine from the South American plant *Ryania speciosa* (Fill & Copella, 2002). When these ryanodine binding proteins were first purified and visualized by electron microscopy, they were found to be of similar size and shape as the 'feet' proteins observed to project out from the junctional SR into the gap between the TC and t-tubules. Subsequent incorporation of this protein into lipid bilayers revealed that it was an ion channel (Fill & Copello, 2002). As shown in Figure 1.3, mammalian RyRs are homotetramers each made up of 4 polypeptides, each with a molecular mass of ~ 560 kDa (Meissner, 1994). The RyR displays four-fold symmetry owing to its formation by four RyR protein monomers. The C-terminal portion of the RyR peptide contains four transmembrane segments while the N-terminus makes up the large ($\sim 80\%$ of protein RyR mass) myoplasmic domain and contains the binding sites for nucleotides, calmodulin, FK binding protein 12 (FKBP12) and Ca^{2+} , as well as potential

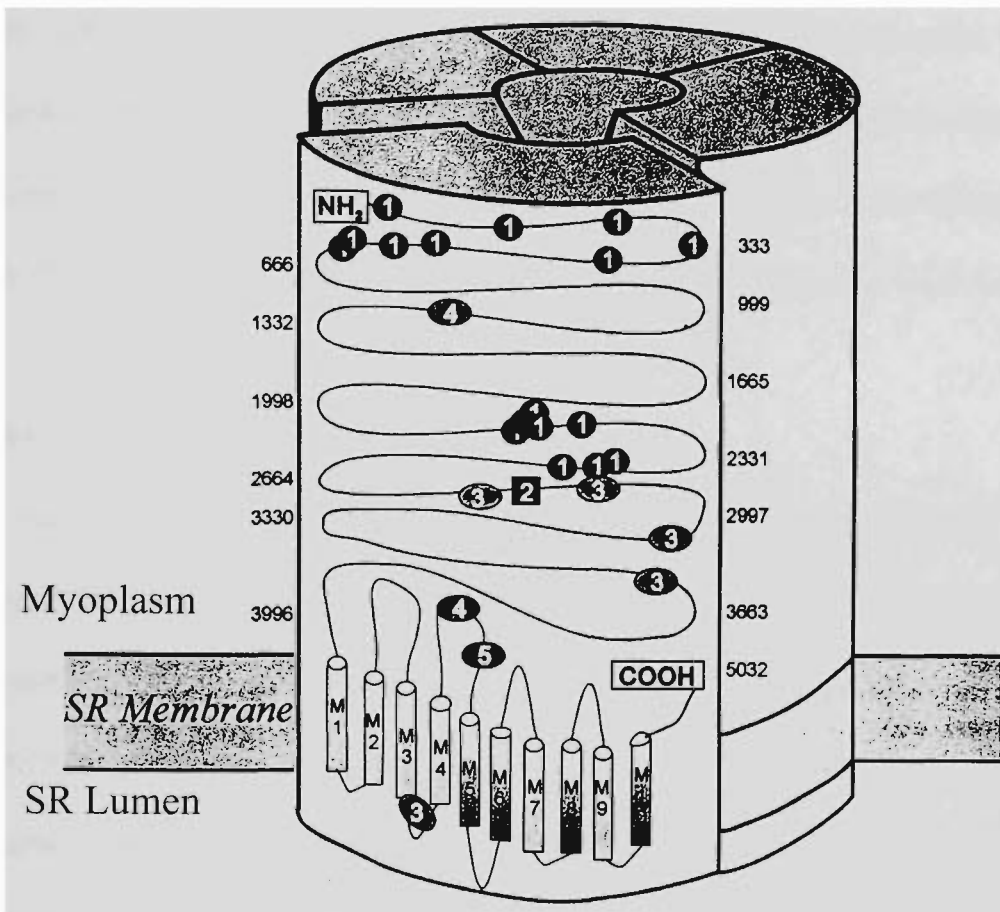


Figure 1.3 Diagram of the molecular structure of the SR RyR/Ca²⁺ release channel. (1. malignant hyperthermia mutations; 2. phosphorylation site; 3. potential calmodulin binding sites; 4. potential nucleotide binding sites; 5. Ca²⁺ activation site) (Modified from Hermann-Frank *et al.*, 1999).

phosphorylation sites (Melzer, 1995). It is these large N-terminal domains that are responsible for the 'feet' projections into the triadic gap region that are visible in electron micrographs. In mammalian skeletal muscle every second RyR homotetramer in the SR membrane faces a DHPR tetrad on the apposite t-tubule membrane (Figure 1.4A). In negative stained samples the RyR has been shown to have a four leaf clover-like (quarter foil) appearance which is likely due to four identical radial 'sub' channels branching from a central common channel (Melzer, 1995). Upon stimulation, it is thought that Ca^{2+} diffuses through the main centre channel and then out the side of the protein complex via the four radial channels (Fill & Copello, 2002).

RyR isoforms and splice variants

In mammals there are three genetically distinct RyR isoforms: RyR1, RyR2 and RyR3. Each of these three mammalian isoforms show a high degree of sequence homology sharing 66-70% amino acid sequence identity (Rossi & Sorrentino, 2002).

RyR1 is the primary isoform found in skeletal muscle, RyR2 is the main isoform found in cardiac muscle (and to a lesser extent in the brain), while the RyR3 isoform was first found in the brain but appears to be present in very small amounts in skeletal muscle (for reviews see Sutko & Airey, 1996 and Murayama & Ogawa, 2002).

Although the RyR3 represents only a few percent of total RyR in adult diaphragm and close to nil in other mature skeletal muscles, it is more abundant in the late embryonic and early neonatal developmental periods. Alternative splice variants for each of the three mammalian RyR isoforms have been identified at the mRNA level (Zorato *et al.*, 1994 & Futatsugi *et al.*, 1995). To date, no direct evidence exists to verify any functional differences between the protein products of these mRNA species (Rossi &

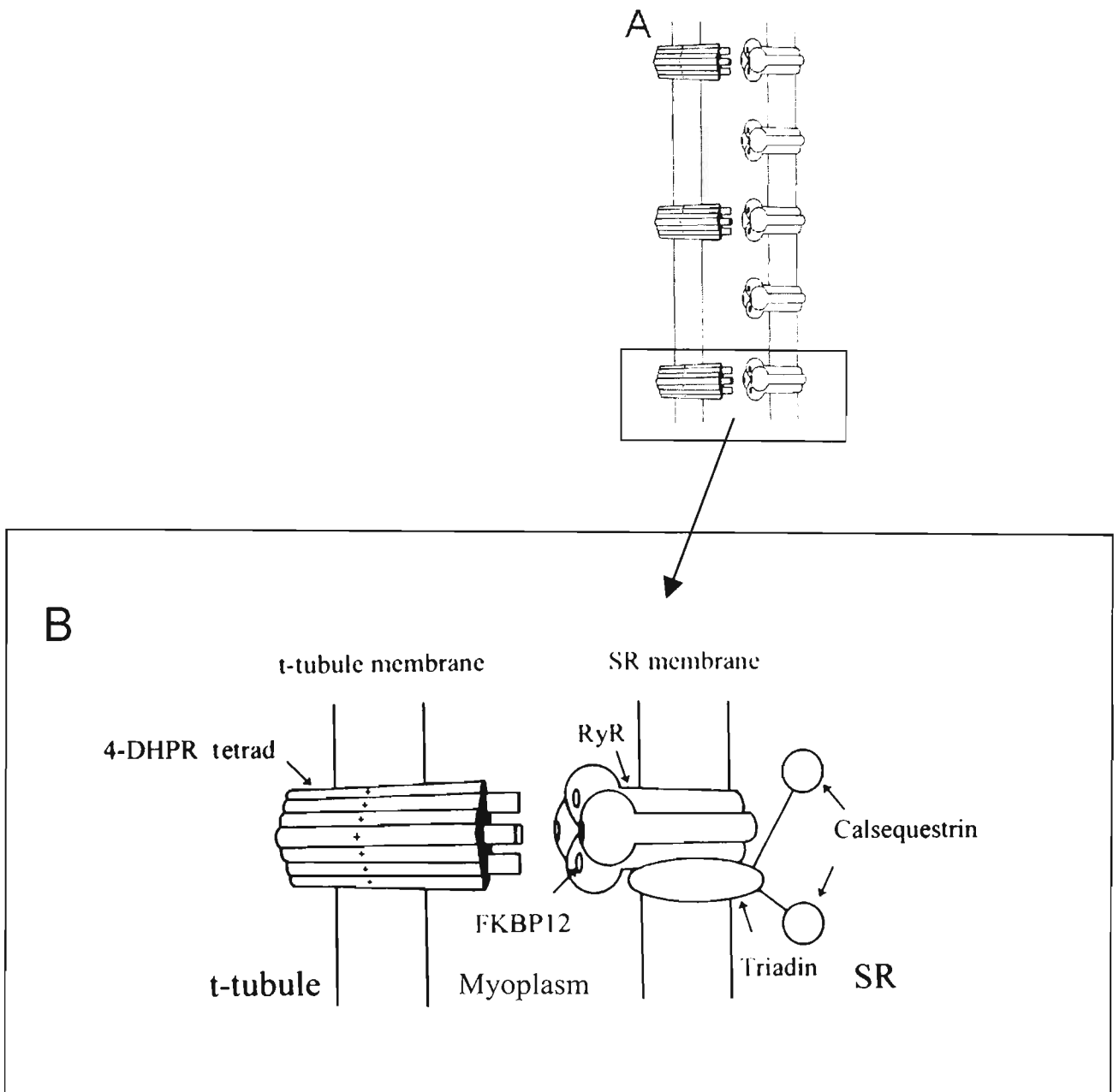


Figure 1.4 Triad proteins involved in skeletal muscle E-C coupling.

A. Diagram showing every second SR RyR/ Ca^{2+} release channel directly apposed to a t-tubular DHPR/voltage sensor. B. Diagram of the various membrane associated proteins proposed to be involved in the transduction of t-tubular membrane depolarisation to the release of Ca^{2+} from the SR. (Modified from Hermann-Frank *et al.*, 1999)

Sorrentino, 2002). However, some of the predicted amino acid variations occur in regions containing putative binding sites for ATP, calmodulin, Ca^{2+} and sites for phosphorylation, which suggests the potential for differences in function and regulation (Sutko & Airey, 1996).

Putative endogenous regulators of the skeletal muscle RyR1 isoform

The RyR1/ Ca^{2+} release channel is primarily affected by four endogenous regulators: Ca^{2+} , Mg^{2+} , ATP and calmodulin.

Ca and Mg ions

Myoplasmic Ca^{2+} has the potential to regulate the RyR1/ Ca^{2+} release channel in a biphasic manner. Ca^{2+} activates the RyR1 by binding to a high affinity activation site (K_D - $1\mu\text{M}$; see Figure 1.5) causing a Ca^{2+} -induced Ca^{2+} release (CICR) effect (Lamb, 1993). However, at physiological levels of free Mg^{2+} ($\sim 1\text{mM}$) this Ca^{2+} activation effect is significantly prevented as Mg^{2+} competes with Ca^{2+} , albeit with a much lower affinity, for the same binding site (Meissner et al., 1986). It is thought that Ca^{2+} binds also to a low affinity inhibitory site ($K_D \sim 0.1\text{mM}$) on the Ca^{2+} release channel (see Figure 1.5). Mg^{2+} also competes with Ca^{2+} as both Ca^{2+} and Mg^{2+} bind with a similar affinity to this relatively non-specific divalent cation site (Lamb, 1993). Under physiological conditions where the myoplasmic free $[\text{Mg}^{2+}]$ ($\sim 1\text{mM}$) is much higher than the resting $[\text{Ca}^{2+}]$ ($\sim 0.1\mu\text{M}$), this site would be almost fully saturated by Mg^{2+} and thus unavailable for Ca^{2+} binding and activation. As such, Lamb (1993) has proposed that this site should be referred to as a Mg^{2+} -inhibitory site rather than a Ca^{2+} -inhibitory site. Therefore in a resting muscle fibre the Ca^{2+} release channels remain closed due to the potent inhibitory action of Mg^{2+} at this inactivation site.

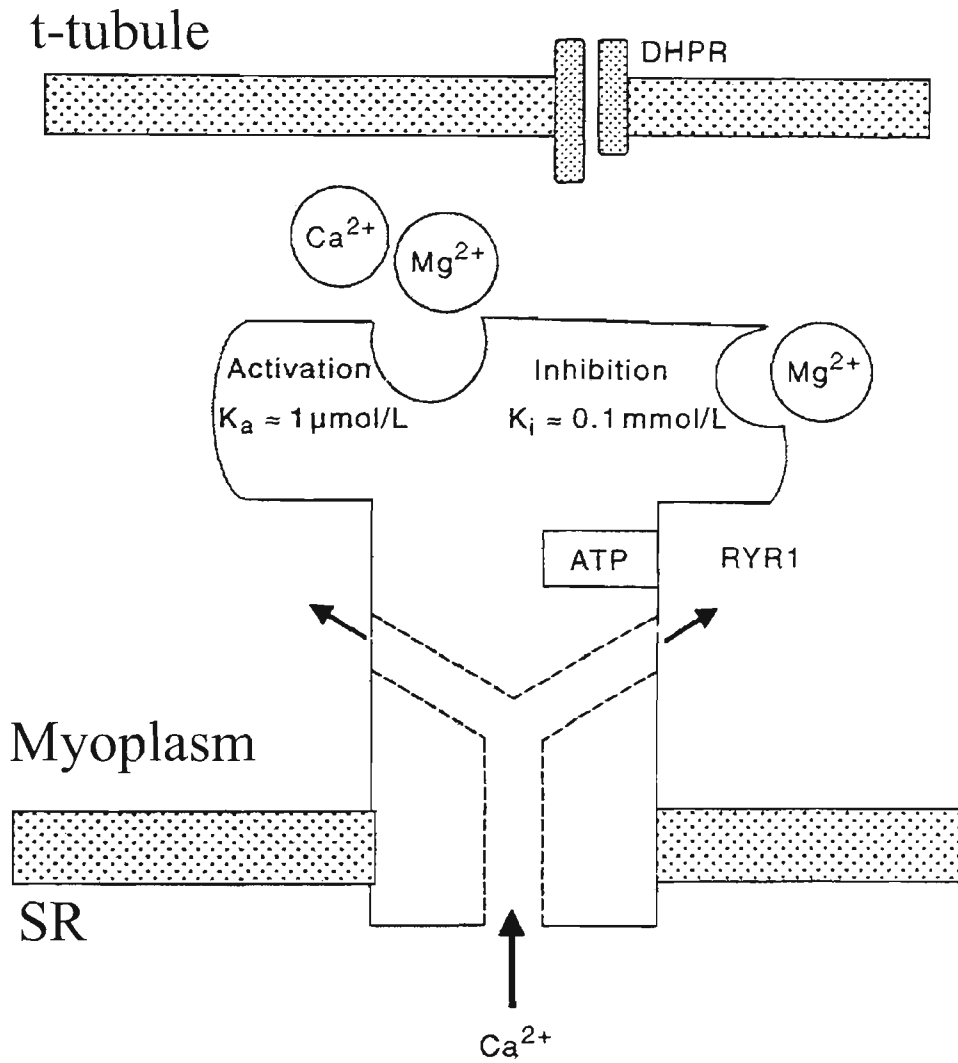


Figure 1.5 RyR/Ca²⁺ release channel regulation.

Diagram showing the major endogenous regulators (Mg²⁺, Ca²⁺ & ATP) of the SR

RyR/Ca²⁺ release channel. (Modified from Lamb, 2000)

(Figure 1.5). It has been proposed that upon depolarization, the T-system DHPR/voltage sensor lowers the affinity of the Mg^{2+} inhibitory site causing Mg^{2+} to dissociate and allowing Ca^{2+} release. The released Ca^{2+} displaces Mg^{2+} from the Ca^{2+} activation site giving maximum open probability of the RyR (Melzer, 1995 and Lamb, 2002b).

ATP

ATP is present in the muscle cell at a concentration of between 6 – 8 mM. Studies utilizing single release channels, SR vesicles and skinned fibres have shown that ATP in the millimolar range stimulates Ca^{2+} release from the RyR (Lamb, 2002b). ATP binds to a stimulatory site on the release channel ($K_D \sim 1$ mM) (see Figure 1.5) and its stimulatory effect does not involve ATP hydrolysis or protein phosphorylation (Lamb, 2002b).

Calmodulin

Calmodulin (CaM) is a ubiquitously expressed 17 kDa protein made up of a single 148 amino acid polypeptide and containing four E-F hand motifs capable of binding Ca^{2+} (Tang *et al.*, 2002). CaM can bind to proteins in both a Ca^{2+} -dependent and Ca^{2+} -independent manner. In the case of the RyR1/ Ca^{2+} release channel, the biphasic dependence of release channel activity on Ca^{2+} is altered by CaM binding in such a way that activation and inhibition take place at lower Ca^{2+} concentrations (Hamilton *et al.*, 2000). The Ca^{2+} free form of CaM (apoCaM) activates while the Ca^{2+} -CaM complex inhibits release channel activity (Rodney *et al.*, 2000). The exact role played by CaM in E-C coupling in vivo is at this stage unclear, but may involve protection of the RyR from various forms of oxidation at critical sites (Tang *et al.*, 2002).

Other triadic proteins

FKBP12

The FK binding protein 12 (FKBP12) is a small protein (12 kDa) bound to each RyR subunit with one homotetramer RyR containing four FKBP12s (see Figure 1.4). The number 12 is related to the particular isoform found in skeletal muscle. The FKBP12 is known to dissociate from the RyR in the presence of the immunosuppressant drugs FK-506 or rapamycin. Data on the function of this protein are at this stage conflicting. Many studies have found that when the FKBP12 is dissociated from isolated single RyR channels the channels are activated (Fill & Copello, 2002). However in the skinned fibre preparation where the RyR is under control of the DHPR, dissociation of the FKBP12 results in reduced Ca^{2+} release as it effectively uncouples the release channel from the voltage sensor (Lamb & Stephenson, 1996).

Triadin

Triadin is a 95 kDa intrinsic membrane glycoprotein located predominantly in the junctional SR. (Coronado *et al.*, 1994). It contains a single transmembrane domain with a relatively short myoplasmic N-terminal and a long luminal C-terminal. The C-terminal end has the ability to interact with calsequestrin while both the N-terminal and C-terminal ends have been proposed as candidates to interact with the RyR (Figure 1.4) (Franzini-Armstrong & Protasi, 1997). The exact function of triadin remains unclear but two proposals are that it provides a link between the RyR and calsequestrin or between the RyR and DHPR (Coronado *et al.*, 1994 and Franzini-Armstrong & Protasi, 1997).

Junctin

Junctin is a 26 kDa calsequestrin binding protein that is proposed to provide an anchor for calsequestrin to the junctional SR membrane (Franzini-Armstrong & Protasi, 1997).

SR Ca²⁺ ATPase/SR Ca²⁺ pump

The Ca²⁺ pump/ATPase, predominantly located in the longitudinal SR, is a 100 -110 kDa protein with ten membrane spanning α helices, three myoplasmic globular shaped domains and small luminal side loops (Lee, 2002). The myoplasmic portion of the pump contains an enzymatic binding site for one Mg-ATP molecule and two high affinity ($K_D \sim 0.3 \mu\text{M}$), high specificity binding sites for Ca²⁺ (Gillis, 1985). The process of Ca²⁺ transport involves the hydrolysis of ATP and Ca²⁺ translocation through the SR membrane. During translocation, the ATPase undergoes a dramatic loss of affinity for Ca²⁺ enabling it to be discharged on the luminal side of the SR membrane (Gillis, 1985). The Ca²⁺ pump is capable of lowering the myoplasmic free Ca²⁺ concentration to $\sim 10^{-8}$ M and generating a 1000 fold transmembrane Ca²⁺ gradient. Once Ca²⁺ has entered the SR lumen much of it will be sequestered by calsequestrin to keep free Ca²⁺ low and prevent feedback inhibition of pump activity (Gillis, 1985).

Two genes, known as SERCA1 and SERCA2 encode the Ca²⁺ ATPase proteins for skeletal muscle. SERCA1 produces two splice variants; (i) SERCA1a found in adult fast twitch skeletal muscle and (ii) SERCA1b found in neonatal skeletal. The SERCA2 produces one isoform (SERCA2a) expressed predominantly in adult slow

twitch, cardiac and neonatal skeletal muscle (Martonosi, 1994) (see Table 1.1, page 29).

In skeletal slow twitch and cardiac muscle, Ca^{2+} pump activity is enhanced by the presence of a pentameric, 22 – 25 kDa protein known as phospholamban.

Phospholamban is phosphorylated by either cAMP-dependent, calmodulin-dependent or phospholipid-dependent protein kinases (Dux, 1993). Once phosphorylated, phospholamban dissociates from the ATPase causing an increase in Ca^{2+} affinity and a two-fold increase in Ca^{2+} transport. Although detected in many mammalian species, phospholamban has not been detected in rat slow twitch skeletal muscle (Damiani *et al.*, 1999).

The contractile apparatus

Thin filament structure at rest

Actin filaments are predominantly polymers of the globular protein called G-actin, but also contain four regulatory proteins, Tropomyosin (Tm), TnC, Troponin T (TnT) and Troponin I (TnI). G-actin polymerizes to form a double helical strand known as F-actin (Craig, 1994). The regulatory protein Tm (MW ~ 35 kDa) is a 2 chain α -helix that extends over every seven G-actin molecules and is located in the groove between the two F-actin helical strands (see Figure. 1.6) (Craig, 1994).

To each Tm is bound one troponin (Tn) complex (see Figure. 1.6). The Tn complex comprises three subunits; TnC (MW ~ 18 kDa), TnI (MW~21 kDa) and TnT (MW~30 kDa) (Bagshaw, 1993). TnC interacts with TnI and TnT and binds Ca^{2+} causing a signal to be transmitted to the thin filament. TnC is dumbbell shaped with

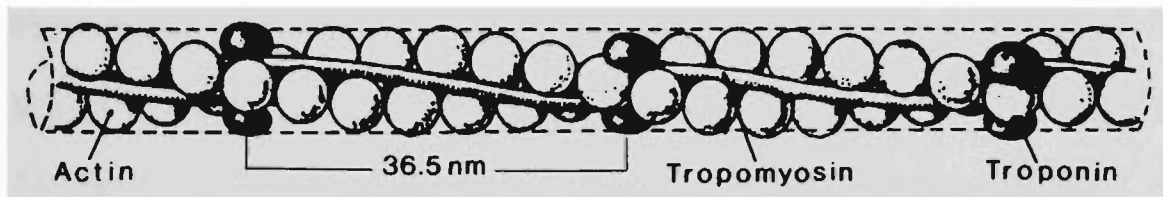


Figure 1.6. The ultrastructure of the thin filament in vertebrate skeletal muscle. The actin filament is made up of G-actin monomers and the associated troponin (Tn) complex and tropomyosin (Tm). (Reproduced from Lüttgau & Stephenson, 1986)

two divalent metal binding sites formed by helix-loop-helix EF hand motifs at each end (Squire & Morris, 1998). According to the current dogma, the two binding sites (sites I & II) located at the N-terminal which bind Ca^{2+} with a low affinity, are responsible for signal transmission (Squire & Morris, 1998) and therefore are referred to as regulatory sites. The other two binding sites (III & IV) at the C-terminal end can bind both Ca^{2+} and Mg^{2+} , however under physiological conditions (i.e. 1 mM free Mg^{2+}) these sites are most likely occupied by Mg^{2+} (Szczesna & Potter, 2002). TnI interacts with both TnC and TnT and when bound to actin is able to inhibit actin-myosin interaction (Craig, 1994). TnT interacts with both troponins I and C and with Tm (Bagshaw, 1993). Its exact role is unclear but what is known is that Tn-T is involved in attaching the Tn complex to Tm (Squire & Morris, 1998).

Thin filament activation and muscle contraction

At resting levels of cytoplasmic Ca^{2+} , Tm effectively blocks the attachment of myosin cross bridges to actin and hence the production of force. When Ca^{2+} levels rise due to the release of Ca^{2+} from the SR, Ca^{2+} binds to TnC which strengthens the binding of TnC to TnI and breaks the interaction between TnI and actin (Gordon *et al.*, 2000 & 2001). The detachment of TnI from actin allows Tm to move over the surface of the thin filament, in a back and forth motion, causing a large increase in the average number of weak binding sites for the myosin S1 head and a smaller increase in the average strong myosin binding sites (Gordon *et al.*, 2000 & 2001). As myosin cross bridges attach to the strong binding sites on actin, Tm is stabilized in such a position that strong myosin binding sites are on average exposed for a longer duration allowing even more myosin cross bridges to strongly attach (Gordon *et al.*, 2000 & 2001).

Thus, Ca^{2+} and strongly bound cross bridges act co-operatively to activate the thin filament and allow the production of force.

Thick filament structure

The thick filament is made up mostly of myosin hexamers that consist of two MHCs (MW~220 kDa) and four myosin light chains (MLC; MW~16 – 30 kDa). The two myosin heavy chains coil in a helical manner similar to two intertwined golf clubs (see Figure 1.7).

The MHC is an α -helix with most of the C-terminal half comprising a long tail and the N-terminal half folding into a globular head (Craig, 1994). Studies using controlled enzymatic digestion have produced two fragments known as light meromyosin (LMM), which makes up most of the tail, and heavy meromyosin (HMM) which makes up the globular head and the remainder of the tail (Figure. 1.7) (Craig, 1994). The HMM portion is able to bind to actin and hydrolyze ATP.

Alternative enzymatic digestion of MHC produces a rod fragment that makes up the whole tail and a sub fragment 1 (S1) that retains the ability to bind actin and to hydrolyze ATP. The rod portion can be further digested to produce LMM and an S2 sub fragment (Craig, 1994). Each S1 head also has attached two MLCs. MLCs are divided into two distinct classes known as essential or alkali and regulatory or phosphorylatable (Talmadge *et al.*, 1993).

Isoforms of the contractile and regulatory proteins of the thin and thick filaments

With the exception of actin, all the proteins associated with the contractile apparatus described thus far (TnC, TnI, TnT, Tm, MLC and MHC) exist as different isoforms.

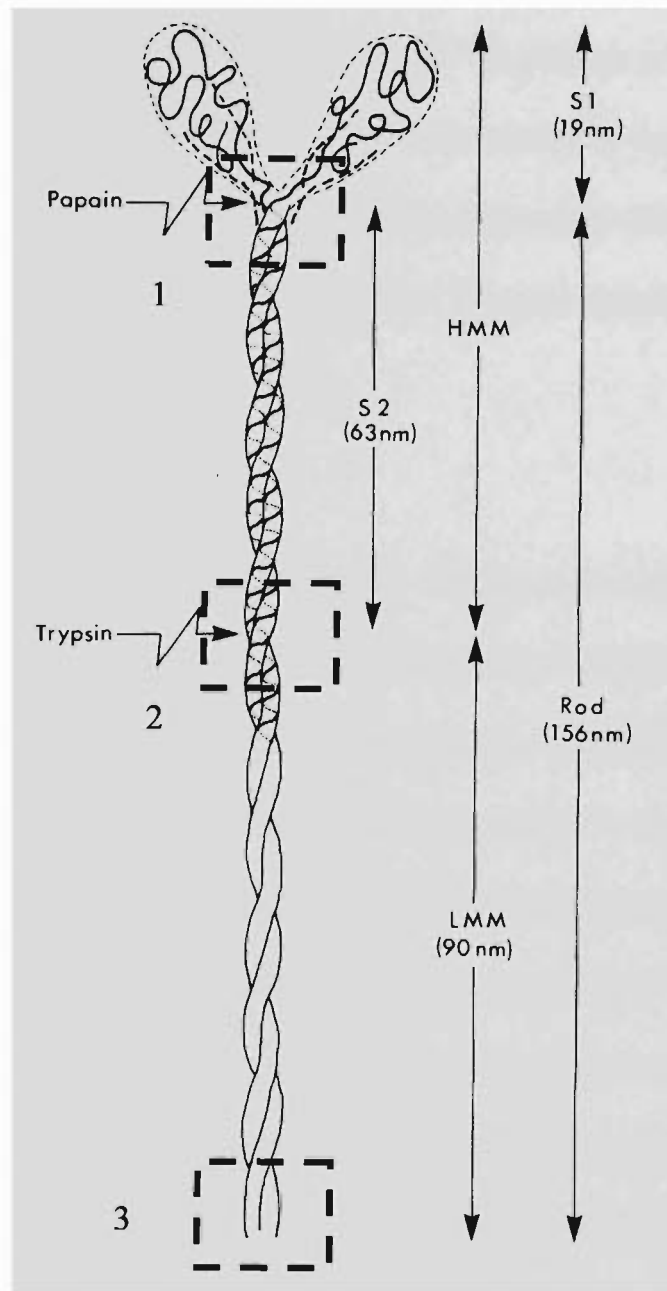


Figure 1.7 Myosin heavy chain. Diagram of two myosin heavy chains coiled together in a helical manner and the different sub fragments produced by the use of selective enzymatic digestion. (Reproduced from Craig, 1994). Boxed areas highlight proposed regions of amino acid sequence divergence that account for different MHC isoforms; (1) the α -helical neck region, (2) the hinge region between the LMM and S2 sub fragment and (3) the C-terminal (Schiaffino & Reggiani, 1996).

which are the products of either multiple genes or alternative splicing of a single mRNA transcript. A detailed description of the protein isoforms associated with the thin filament (TnC, TnI, TnT & Tm) or the MLC isoforms of the thick filament is beyond the scope of this literature review and beyond the purpose of this thesis. Comprehensive reviews regarding the expression and function of these proteins have previously been published by Pette & Staron, (1990), Moss et al. (1995) and Schiaffino & Reggiani (1996). Isoforms of the thick filament myosin heavy chain will however be reviewed in the next section.

Myosin heavy chain isoforms

Based on protein and mRNA analyses, mammalian extrafusal skeletal muscle contains eleven MHC isoforms encoded by multigene families (Weiss & Leinwand, 1996; Pette & Staron, 2000). Some MHC isoforms are expressed at different stages of muscle development, while in adult skeletal muscle some MHC isoforms are either expressed in a muscle specific manner or are distributed widely through out the musculature (Pette & Staron, 2000). The amino acid sequences of these MHC isoforms are highly homologous with the main regions of sequence divergence occurring at the C-terminal, the hinge region between the LMM and S2 subfragment and the α -helical neck region (Figure. 1.7) (Schiaffino & Reggiani, 1996). Note that the nomenclature used in this thesis for MHC isoform and fibre type is that of Pette & Staron (1997 & 2000) who use a Roman numeral and a lower case letter (e.g. IIa isoform) to identify the MHC isoform, and a Roman numeral and capital letter (e.g. IIA fibre) to identify muscle fibre type.

The mammalian MHC isoforms include:

- An embryonic (MHC_{emb}) and neonatal (MHC_{neo}) MHC isoform found in embryonic and early postnatal developing muscle, respectively. These isoforms are also found in adult extraocular and jaw muscles, and in muscle regenerating after some form of injury or damage.
- One slow-tonic MHC isoform ($MHCI_{ton}$) found in extraocular, laryngeal and inner ear muscle.
- Three slow-twitch MHC isoforms ($MHCI_a$, $MHCI_\alpha$ and $MHCI_\beta$). The $MHCI_a$ isoform is found in muscles such as plantaris, soleus and in fibres transforming from slow- to fast phenotype (Galler *et al.*, 1997). The $MHCI_\alpha$ isoform is found in the diaphragm, extraocular and jaw muscles and also in fibres transforming from slow- to fast phenotype. The $MHCI_\beta$ isoform is found in type I fibres and in IC and IIC hybrid fibres.
- Two super-fast MHC isoforms (MHC_{eom} and $MHCII_m$). The MHC_{eom} isoform is found in extraocular and laryngeal muscles while the $MHCII_m$ isoform is found in masticatory muscles.
- Three adult fast-twitch MHC isoforms ($MHCII_a$, $MHCII_d$ and $MHCII_b$). These MHC isoforms are found throughout the adult musculature (Pette & Staron, 1997 & 2000).

Ca²⁺ uptake by the SR calcium ATPase/Pump

As already stated at the beginning of this Introduction, relaxation of a muscle occurs following the deactivation of the DHPR/voltage receptors, closure of the RyR/Ca²⁺ release channels and the dissociation of Ca²⁺ from TnC on the contractile apparatus. The myoplasmic Ca²⁺ is buffered by Ca²⁺ binding protein parvalbumin and is also

actively pumped back into the SR lumen by the SR/ER Ca^{2+} ATPase (SERCA) or Ca^{2+} pump.

Signal transduction between the DHPR and the RyR

Three main hypotheses have been proposed to explain the mechanism of signal transduction from the t-tubule voltage sensors to the SR Ca^{2+} release channels.

Protein-protein interaction

The discovery by Schneider & Chandler (1973) of the intramembrane charge movement occurring within the T-system upon depolarization led to the hypothesis that there is a protein-protein interaction between the DHPR/voltage sensor and the RyR/ Ca^{2+} release channel. According to this model, the t-tubule voltage sensor is attached to a mechanical plunger-like structure such that at rest the plunger blocks the release channel opening and inhibits Ca^{2+} release (Chandler *et al.*, 1976). The t-tubule depolarization, which is detected by the voltage sensor (now known to be the positively charged S4 membrane spanning segment of the DHPR; see Dihydropyridine receptor/voltage sensor section, page 5), induces a conformational change in the plunger causing the RyR release channel pore to be unblocked thereby allowing Ca^{2+} to diffuse out (Csernoch, 1999).

Evidence suggesting a protein-protein interaction or conformational coupling (Dulhunty & Pouliquin, 2003) comes from morphological studies using electron microscopy. These studies showed evidence of ordered arrangement and close proximity of the electron dense ‘feet’ structures and the t-tubule DHPR tetrads thereby indicating a possible interaction between these two proteins (see Figure 1.1) (Franzini-Armstrong, 1970). Recently, it has been proposed that the II-III myoplasmic

loop between the 2nd and 3rd repeats of the DHPR α_{1S} subunit (see Figure 1.2) may directly interact with the RyR conferring skeletal muscle type E-C coupling. More specifically, the region of the DHPR II-III loop containing amino acid residues 724-760 and amino acid residues 1635-2635 on the RyR1 are being investigated as potential regions of interaction between the two proteins (for reviews see Mackrill, 1999; Dulhunty et al., 2002; Dulhunty & Pouliquin, 2003). Due to the large size of both the DHPR and RyR it is quite possible that there is more than one region of interaction between these proteins (Dulhunty & Pouliquin, 2003).

It appears that as well as the traditional communication from the DHPR to the RyR, known as orthograde coupling, the RyR can strongly influence the activity of the DHPR in a retrograde coupling action (for review see Dirksen, 2002). In this case, muscle cells expressing normal amounts of DHPR, but lacking skeletal RyR1, displayed a very small slow Ca^{2+} current through the L-type Ca^{2+} channel upon depolarization. When the RyR1 protein is expressed after injection of RyR cDNA into these cells, normal Ca^{2+} current is restored.

IP₃ mediated coupling

IP₃ or inositol trisphosphate, the product of the membrane phospholipid phosphatidylinositol 4,5-bisphosphate (PIP₂) hydrolysis by phospholipase C, has been considered as a candidate for transmitting the depolarization signal from the DHPR to the RyR due to its established role in Ca^{2+} release in smooth muscle and other non-muscle cells (Schneider, 1994). The idea was that IP₃ would be released from the t-tubular membrane following voltage dependent activation of phospholipase C and subsequently activate the RyR/ Ca^{2+} release channel (Schneider, 1994). There is now

however reasonable evidence to suggest that IP_3 would play a very minor role, if any, in the skeletal muscle signal transduction process. Thus, Walker *et al.* (1987) demonstrated that the photolytic liberation of IP_3 caused a very slow SR Ca^{2+} release, far too slow to be the main release activator. Also, Hannon *et al.* (1992) showed that there was no contractile activation when IP_3 was microinjected into fully polarized intact fibres. These later authors found only a small effect in fibres that were already partially depolarized. Evidence that these small responses were abolished in fully depolarized fibres or in nifedipine (blocker of the DHPR) treated fibres indicates that IP_3 has a minor effect on the t-tubule membrane which is then transmitted to the DHPR and subsequently to the RyR (Hannon *et al.*, 1992).

Ca²⁺ mediated coupling

Early work with skinned fibres showing that a rise in the intracellular $[Ca^{2+}]$ induces SR Ca^{2+} release, led to the proposal that in skeletal muscle SR Ca^{2+} release may be triggered by the process of Ca^{2+} -induced Ca^{2+} release (CICR) similar to cardiac muscle (Endo, 1977). More recent work however has shown that the influx of extracellular Ca^{2+} through the DHPR L-type Ca^{2+} channel following a depolarizing stimulus is too small and too slow to be responsible for the fast activation of SR Ca^{2+} release (Brum *et al.*, 1987). Furthermore, when external Ca^{2+} is removed or blocked from entering the cell, fibres retain their ability to contract. Taken together, these data rule out a cardiac style CICR as the major mechanism for inducing Ca^{2+} release in skeletal muscle (Csernoch, 1999).

It is worth considering that CICR could still play a secondary role in SR Ca^{2+} release, where Ca^{2+} released from RyRs directly apposed to DHPR/voltage sensor tetrads

activate neighboring RyRs not linked with a DHPR (see Figure 1.4A) causing a regenerative release of Ca^{2+} (for review see Melzer, 1995). Experiments where high concentrations (millimolar range) of strong Ca^{2+} buffers such as BAPTA or Fura 2 were injected into fibres have shown that when the voltage sensor mediated increase in intracellular Ca^{2+} was reduced to less than $0.1 \mu\text{M}$ the SR Ca^{2+} release was attenuated (Jacquemond *et al.*, 1991). This would suggest that the voltage sensor controlled SR Ca^{2+} release is responsible for further CICR, possibly through the RyR release channels not facing a DHPR/voltage sensor, and has led to the proposal of *dual control* (Ca^{2+} -independent and Ca^{2+} -dependent) of SR Ca^{2+} release. To date much of this evidence has been obtained using amphibian muscle. The extent of the role (if any) of CICR in mammalian muscle, under physiological conditions, remains to be determined (Csernoch, 1999).

Skeletal muscle fibre diversity

Skeletal muscle is a heterogeneous tissue consisting of fibres that differ in their physiological, biochemical and morphological properties. Diversity among muscle fibres is due to ‘qualitative and quantitative mechanisms’ of gene regulation (Bottinelli & Reggiani, 2000; Bortolotto & Reggiani, 2002). The ‘qualitative mechanism’ of gene regulation refers to the presence of many similar but not identical muscle proteins known as isoforms. These isoforms may have different functional properties and therefore modify the functional phenotype of a muscle fibre. Isoforms can be derived from multiple gene families or from the same gene through alternative splicing. The ‘quantitative mechanism’ of gene regulation refers to the extent of expression of the same gene. This means that one gene within a given muscle fibre may be expressed more or less than another or that a specific gene in one muscle fibre

may be expressed more or less than the same gene in another fibre (Bottinelli & Reggiani, 2000; Bortolotto & Reggiani, 2002). This could result in a greater amount or density of specific proteins (e.g. DHPR or glycolytic enzymes) and/or a greater amount or relative volume of an internal membrane network (i.e. T-system or SR). Table 1.1 lists some of the reported differences between fast-twitch and slow-twitch muscles/muscle fibres from adult mammalian muscle with respect to cellular structures and molecular species involved in the transduction of the T-system depolarization signal to SR Ca^{2+} release (for reviews see Lamb, 1992, Rüegg 1992, Stephenson *et al.*, 1998). To date, no studies have attempted to examine if any differences in E-C coupling characteristics exist between single fibres that have been typed as either fast or slow twitch. This issue is specifically examined in Chapter 4 of this thesis.

Methods of classifying muscle fibre types

As long ago as 1678, skeletal muscles had been observed to have differing degrees of red coloration and as such were classified as red and white muscles (Loughlin, 1993). Some two hundred years later Ranvier (1873) demonstrated that ‘red’ muscles contracted and relaxed more slowly than ‘white’ muscles. Over the last fifty years more sophisticated techniques have been developed to differentiate individual muscle fibres with respect to: (i) twitch contractile properties of a fibre subjected to electrical stimulation or maximal Ca^{2+} activation (Close, 1972); (ii) the sensitivity to strontium (Sr^{2+}) of the contractile apparatus (Fink *et al.*, 1986); (iii) the lability of the myofibrillar ATPase enzyme to incubation in solutions of different pH (Brooke & Kaiser, 1970); (iv) glycolytic or oxidative metabolic enzyme activity determined

Table 1.1. Fibre type differences in structures and molecular species involved in the E-C-R cycle.

Structure	Difference	Reference
T-system (% fibre volume)	FT (0.27) higher than ST (0.14)	Rüegg 1992
DHPR	2-3 x higher amount in FT than in ST	Lamb, 1992
DHPR α_1 subunit isoforms	α_{1s} in FT, α_{1c} & some α_{1c} in ST	Froemming <i>et al.</i> , 2000
Total SR (% fibre volume)	higher in FT (4.59) than in ST (3.15)	Rüegg 1992
Junctional SR (% fibre volume)	higher in FT (1.62) than in ST (0.96)	Rüegg 1992
RyR density	higher in FT than in ST	Lee <i>et al.</i> , 1991
SR luminal [Ca^{2+}]	lower in FT than in ST	Fryer & Stephenson, 1996
Calsequestrin isoforms	1 isoform in FT, 2 isoforms in ST	Damiani & Margreth, 1994
SERCA density	higher in FT than in ST	Briggs <i>et al.</i> , 1977
SERCA isoforms	SERCA1a in FT, SERCA2b in ST	Martonosi, 1994

(FT = fast twitch & ST = slow twitch)

histochemically (Barnard *et al.*, 1971; Peter *et al.*, 1972) and (v) the myosin heavy chain (MHC) isoform expression as determined by sodium dodecyl sulfate-polyacrylamide gel electrophoresis (SDS-PAGE) or immunohistochemistry (Pette & Staron, 1997).

To date three major groups of muscle fibres have been identified. Type I fibres typically rely heavily on oxidative metabolism, have slow contraction and relaxation times, and contain type I MHC (MHC I) isoforms. Type IIB fibres rely predominantly on glycolytic metabolism, have fast contraction and relaxation times, and contain type IIB MHC (MHC IIB) isoform. Type IIA fibres are generally intermediate with respect to oxidative and glycolytic metabolism, have fast contraction times but contain type IIA MHC (MHC IIA) isoform (for review see Pette & Staron, 1990 & 1997). A fourth MHC isoform (type IIX/IID) subsequently identified in rat skeletal by Bar and Pette (1988) and later confirmed by other groups (Schiaffino *et al.*, 1989; Gorza, 1990) has been confirmed to have properties intermediate to the IIA and IIB MHC isoforms (for review see Schiaffino & Reggiani, 1994). In adult skeletal muscle the MHC isoform composition of muscle fibres is not always exclusively homogeneous. Instead there seems to be a muscle-specific percentage of fibres that contain a mixture of MHC isoforms (Talmadge, 2000; Stephenson, 2001). Fibres containing different proportions of the different MHC isoforms are known as hybrid fibres while fibres containing only one MHC isoform are called pure fibres (for review see Stephenson, 2001).

Because of the central role played by MHC in muscle contractile performance (being the protein associated with myosin-ATPase activity and the crossbridge responsible for the production of force and muscle shortening; Bagshaw, 1993; see also *Thin*

filament activation and muscle contraction, page 19) and due to their relative abundance (accounting for ~ 50 % of total myofibrillar protein; Pearson & Young, 1989), MHC isoform expression (as detected by high resolution polyacrylamide gel electrophoresis or by immunohistochemistry) has become the method of choice for classifying skeletal muscle fibre types into distinct functional groups (Bottinelli *et al.*, 1996; Moss *et al.*, 1995; Stephenson, 2001).

Immunohistochemical determination of MHC isoforms

Immunohistochemistry involves the use of a specific antigen-antibody reaction to identify a required tissue constituent *in situ* (Loughlin, 1993). More specifically, transverse serial (or longitudinal) sections of muscle fibres are exposed to a certain MHC antibody tagged with a microscopically visible label. The advantage of the immunohistochemical technique is that it allows the investigator to identify the location of specific MHC isoforms along the width and/or length of the muscle fibre (Schiaffino & Salviati, 1997). The disadvantage of this technique is that because MHC composition has been shown to vary along the length of a muscle fibre (e.g. Edman *et al.*, 1988) several serial transverse sections need to be taken to identify whether a particular fibre is a pure or hybrid fibre. This technique also, does not allow accurate quantitation of the relative proportions of MHC isoforms in hybrids muscle fibres (Stephenson, 2001).

Determination of MHC isoforms using SDS-PAGE

Sodium dodecyl sulphate polyacrylamide gel electrophoresis or SDS-PAGE allows the investigator to quantify the relative proportion of MHC isoforms in a given muscle sample. Analysis of MHC isoforms can be performed using whole muscle

homogenates, crude myosin extracts, purified myosin and single muscle fibre segments. Carraro & Catani (1983), using a slightly modified version of Laemmli's (1970) protocol, were the first to utilize this technique to separate skeletal muscle MHC isoforms. SDS-PAGE allows the separation of the MHC isoforms based on minor molecular weight differences that translate into differing migration distances of each MHC isoform protein band on the gel. These MHC bands can be visualized by staining the protein with either a silver or Coomassie blue stain. Confirmation of each protein band's identity can be achieved with western blotting and specific antibodies and/or by running a standard MHC marker of known MHC isoform composition. The most important advantage of this technique is that the relative proportion of MHC isoforms co-expressed in hybrid fibres can be accurately quantified (Pette *et al.*, 1999). SDS PAGE was utilized in the study described in Chapter 4 of this thesis in which the relationship between E-C coupling characteristics and MHC isoform composition was investigated.

Aspects of postnatal development of rat skeletal muscle relevant to the E-C-R cycle

Rat development is characterized by a 22 day embryonic period (UNSW Embryology website) followed by a postnatal life span of between 2 -3 years depending on the specific strain (Weihe, 1987). Full weaning occurs at around 6 -7 wks while sexual maturity is reportedly reached by age 6-10 wks (Weihe, 1987). A survey of the literature to date reveals that there is a general lack of concensus regarding the age range of the 'adult' rat. For example, SR/t-tubule triads appear to reach 'adult' status at 1.5 to 2 wks while muscle fibre diameter reaches 'adult' dimensions by 27 wks.

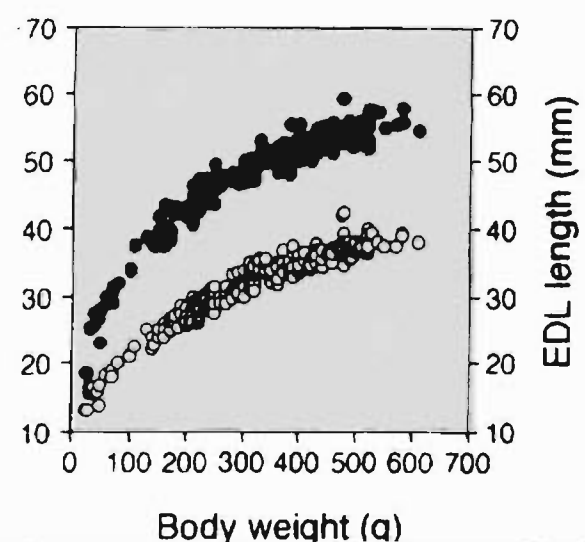
Growth of whole muscle and individual fibres

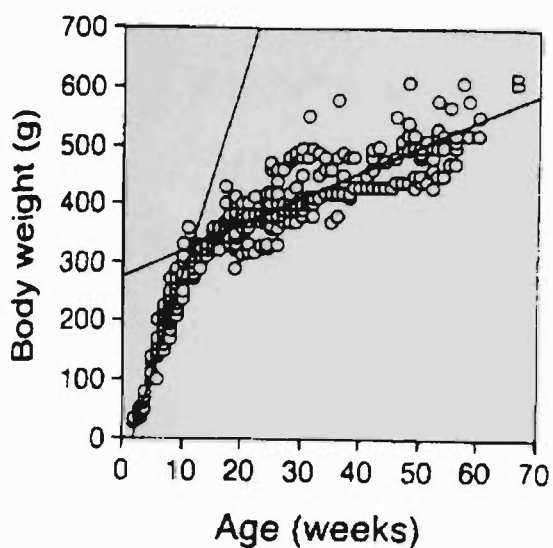
Baldwin (1984) categorized mammalian skeletal muscle growth and development processes into two phases. Phase one, or the differentiation phase, is characterized by the neonatal muscle undergoing rapid qualitative and quantitative alterations in structural, physiological, biochemical and metabolic properties. In the rat, this differentiation phase lasts from 0 to 4 wks. Phase two, or the growth/maturation phase, lasting 4 to 16 wks, involves the continued increase in the physical size of the muscle (i.e. quantitative changes) despite most structural, physiological, biochemical and metabolic properties being fully established (Baldwin, 1984).

Tamaki & Uchiyama (1995) described rat muscle growth as consisting of a rapid 'self accelerating phase' lasting up to 10 wks and a slower 'adult phase' from 10 wks up to 60 - 70 wks (Figure 1.8A). As the body (bones) of the rat rapidly increases in length and mass, skeletal muscles also increase in length (Figure 1.8B), by the addition of new sarcomeres in series (Goldspink, 1980), and in diameter (girth) (Figure 1.8C) via hypertrophy of individual fibres and fibre hyperplasia (Tamaka & Uchiyama, 1995). During the slower adult phase, skeletal muscle growth is accomplished mostly through fibre hypertrophy and is accompanied by increases in the connective tissue and fat content. Individual rat EDL muscle fibres have been shown to continue to increase in diameter up to approximately 27 wks (Alnaqeeb & Goldspink, 1986).

A

B





C

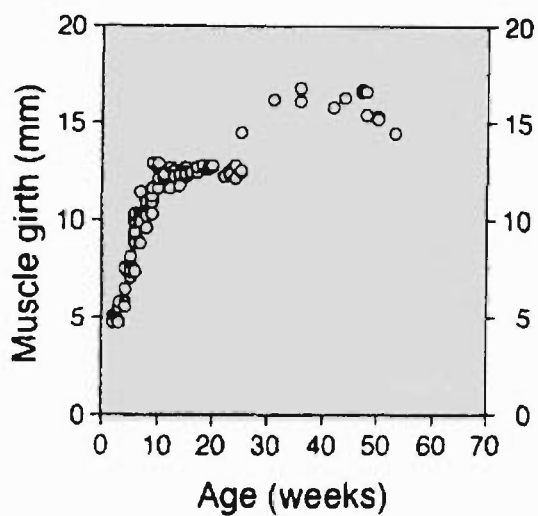


Figure 1.8 Changes in rat body mass, muscle length and muscle girth with age. A. Rat Body weight changes increasing with age. B. Rat EDL muscle length changes with increasing body weight. C. Rat skeletal muscle girth changes with age. (Reproduced from Tamaki & Uchiyama, 1995)

T-system and SR

At birth the SR in rat skeletal muscle is discontinuous around individual myofibrils at the level of the A band/I band junction (Schiaffino & Margreth, 1969). Triadic regions of SR and t-tubule are present at birth and when viewed by electron microscopy appear to be the same as those found in adult muscle, but are fewer in number and oriented longitudinally or obliquely instead of transversely (Schiaffino & Margreth, 1969; Edge, 1970). By 1.5 to 2 wks, triads achieve a transverse orientation typical of 'adult' rat skeletal muscle (Edge, 1970). The tubular-system of neonatal rat EDL muscle, when viewed under an electron microscope, displays extensive longitudinal tubules between all myofibrils and short transverse sections at the A and I band level that do not extend across consecutive parallel myofibrils (Kelly, 1980). Beam & Knudson (1988), using an indirect measure of relative T-system (linear capacitance/fibre surface area ratio) showed that the T-system of the rat fast twitch flexor digitorum brevis muscle continues to increase in area reaching adult levels by 5 to 6 wks of age.

DHPR/voltage sensors and RyR/calcium release channels

In terms of the two major protein complexes involved in E-C coupling, Kyselovic *et al.* (1994) reported a different time course of expression of the DHPR/voltage sensor and RyR/Ca²⁺ release channel in rat skeletal muscle. Dihydropyridine binding was shown to increase in a linear fashion from 1 week, reaching "adult" levels (5-6 wks) by 3 wks postnatal. In contrast, ryanodine binding remained relatively low from birth to 1-2 wks and then increased exponentially reaching adult levels by 4 to 5 wks (Kyselovic *et al.*, 1994). It should be noted that although very little research has been done on rat muscle, developing skeletal muscle from other species (e.g. mouse) has

been shown to contain two RyR/Ca²⁺ release channel isoforms (RyR 1 & RyR 3) (Flucher *et al.*, 1999). In mouse EDL, muscle RyR3 containing fibres account for 17 % of total at 2 wks, while there are no detectable RyR3 by 3.5 to 4 wks. The presence of two Ca²⁺ release channel isoforms in the immature muscle and only one in the adult muscle raises the possibility of differences in E-C coupling processes related to developmental age.

The presence of RyR3 isoforms in the early postnatal period correlates with finding that in the first two wks postnatal, E-C coupling in rat skeletal muscle relies on an inward flow of extracellular Ca²⁺ through the DHPR/voltage sensor (Pereon *et al.*, 1993). The increased expression of RyR/Ca²⁺ release channels after 2 wks coincides with the reported changes in triad orientation from longitudinal to transverse (Schiaffino & Margreth, 1969).

E-C coupling

The resting membrane potential (Em) of rat fast twitch skeletal muscle has been shown to increase from ~ -27 mV at birth (Pereon *et al.*, 1993), to ~ -51mV by one week (Conte Camerino *et al.*, 1989) and to ~ -68 mV by 3 to 4 wks (Hazlewood & Nichols, 1967; Conte Camerino *et al.*, 1989). Conte Camerino *et al.* (1989) reported that in rat EDL, Em did not reach adult levels (~ -75 mV) until 10 to 11 wks. It is worth noting that in this study no time points were examined between 4 and 10 wks, making it difficult to ascertain the time when Em reaches its adult level. Membrane conductance of chloride ions has been shown to increase to "adult" (10 -11 wks) levels by 4 wks postnatal (Conte Camerino *et al.*, 1989). Similarly, the number of active Na⁺/K⁺ pumps (as indicated by number of [³H] ouabain binding sites) was

reported to reach a peak value by approximately 4 wks postnatal in rat skeletal muscle (Clausen, 2003).

The calculated voltage required for activation of the DHPR/voltage sensor, as determined from potassium contracture experiments, is considerably less negative in newborns (~ -1.6 mV) than in adult (12 wks) rat EDL muscle with adult values (~ -19 mV) being reached by about 4 wks postnatal (Pereon *et al.*, 1993). The development of the membrane potential required for voltage sensor inactivation follows a slightly different time course than the activation potential. At birth the inactivation potential is ~ -20 mV, reaching adult values (~ -39 mV) by only 2 wks postnatal (Pereon *et al.*, 1993).

Pereon *et al.* (1993) also demonstrated that the twitch tension developed by immature (especially in the first week) rat EDL muscle is depressed or enhanced by the elimination or enhancement, respectively, of extracellular $[Ca^{2+}]$. This effect was still evident from 2 to 4 wks albeit to a much lesser extent. This indicates that an inflow of Ca^{2+} through the t-tubular L-type Ca^{2+} channel/voltage sensor is required for E-C coupling in the first few wks postnatal, which may be related to an under developed SR (Pereon *et al.*, 1993). The dependence of E-C coupling on extracellular Ca^{2+} could in part be due to the presence of RyR3/ Ca^{2+} release channel isoforms. As already mentioned, in mouse EDL muscle, the RyR3 isoform accounts for 100 % of Ca^{2+} release channels in the late embryonic stage of development decreasing to zero by 3.5 to 4 wks (Flucher *et al.*, 1999). RyR3 knockout studies have shown that this isoform is required for efficient transduction of an electrical signal to force generation. More specifically, the presence of the RyR3 isoform may amplify Ca^{2+} release in response

to an electrical stimulus via a Ca^{2+} induced Ca^{2+} release (CICR) mechanism (Bertocchini *et al.*, 1997). A CICR mechanism may allow more efficient E-C coupling at a time when triad structure and orientation, and functional coupling between T-tubule voltage sensors and SR RyR1/ Ca^{2+} release channels is yet to be fully established (Bertocchini, *et al.*, 1997).

Chaplin *et al.* (1970) examined excitation-contraction latencies (defined as the time taken for action potential conduction along the sarcolemma and into the T-tubules, Ca^{2+} release from the SR and subsequent contractile apparatus activation) in immature rat EDL muscles and found that the latency time decreased from ~ 6 milliseconds at birth, to 2.8 milliseconds by 2 wks and reached 'adult' values (2.5 milliseconds) by 3 wks postnatal.

Myosin heavy chain isoforms

At birth, fast twitch rat skeletal muscles predominantly express the embryonic (MHC_{emb}) and neonatal (MHC_{neo}) MHC isoforms. Adams *et al.* (1999), using gel electrophoresis and western blotting, showed that in the presence of normal innervation and thyroid status, 1 week old rat fast twitch plantaris muscle is composed of 61.5 % MHC_{neo} , 24.3 % MHC_{emb} , 5.6 % MHC I, 6.0 % MHC IIa and 3.6 % MHCIIb. By 3 - 4 wks, both rat plantaris (Adams *et al.*, 1999) and EDL (Albis *et al.*, 1989) muscles have been shown, using gel electrophoresis, to be composed of only adult MHC isoforms. Likewise, La Framboise *et al.* (1990) could not detect any MHC_{emb} or MHC_{neo} isoforms by electrophoresis in 3 week rat EDL muscles but when using immunohistochemistry was able to detect a positive reaction to MHC_{neo} in 24 % of fibres. This positive reaction was absent by postnatal wks 8-9.

Contractile properties

Close (1964) has shown that rat EDL isometric contraction time and half relaxation time reached a minimum by 5 wks and then increased slowly over the next 9 wks. In this study, Close (1964) also showed that the optimum frequency for tetanic stimulation reached its highest value by 5 wks, while isotonic speed of shortening (at one tenth of maximum tetanic tension) did not reach its maximum value until 7 to 8 wks. Later, Drachman & Johnston (1973) reported that isometric contraction time and half relaxation time decrease rapidly in rat EDL muscle, being half as fast as the adult muscle by the third day postnatal, and that 'adult' values could be reached as early as 3 wks. Although slightly different to the data of Close (1964), the decrease in relaxation time was consistent with an increase in the SR Ca^{2+} uptake which reached 85 % of adult levels by 3 wks postnatal (Drachman & Johnston, 1973).

Concluding remarks

The data reviewed above (and summarized in Table 1.2) suggest that, in the rat, a muscle reaches the 'adult' stage at different times during postnatal development, depending on the parameter under consideration. Thus, by 3-4 wks postnatal most of the molecular structures involved in the E-C-R cycle and the few physiological processes measured to date are similar to those found in 'adult' rat fast twitch muscle. Exceptions however include the number of RyR/ Ca^{2+} release channels which reach adult values by 4-5 wks, the relative volume of T-system and number of

Table 1.2. Summarized information on the time taken by various structures and processes involved in the E-C-R cycle to reach adult values.

	1	2	3	4	5	6	7	8	9	10	11	27	Reference
Weaning													Weihe, 1987
Reproductive maturity													Weihe, 1987
Relative T-system													Beam & Knudson, 1988
DHPR number													Kyselovic <i>et al.</i> , 1994
RyR number													Kyselovic <i>et al.</i> , 1994
Triad orientation													Edge, 1970
DHPR activation voltage													Pereon <i>et al.</i> , 1993
DHPR inactivation voltage													Pereon <i>et al.</i> , 1993
Membrane Cl ⁻ conductance													Conte Camerino <i>et al.</i> , 1989
Na ⁺ /K ⁺ ATPase number													Clausen, 2003
Resting membrane potential													Conte Camerino <i>et al.</i> , 1989
Excitation-contraction latency													Chaplin <i>et al.</i> , 1970
Myosin heavy chain													Albis <i>et al.</i> , 1989; La Framboise <i>et al.</i> 1990
Isometric contraction time													Drachman & Johnston, 1973; Close 1964
Isometric half relaxation time													Drachman & Johnston, 1973; Close 1964
Isotonic speed of shortening													Close, 1964
Muscle fibre diameter													Alnaqeeb & Goldspink, 1986

Note: The data were obtained for rat fast twitch skeletal muscle.

DHPR/voltage sensors which continue to increase until 5 -6 wks postnatal, and isotonic speed of shortening which reaches adult values by 7-8 wks. Due to study design limitations it is difficult to say with any certainty the age at which the resting membrane potential reaches adult values. The current data suggest a broad time period of between 4 and 10 wks postnatal [as indicated by the question marks (?) in Table 1.2] in which an 'adult' resting membrane potential is attained. Interestingly, muscle fibre diameter (a morphological parameter) continue to increase up to 27 wks of age.

An important question arising from these data is, at what age does rat fast twitch skeletal muscle reach a truly 'adult' status? Should fast twitch rat muscle be considered 'adult' at 3-4 wks, a time when most E-C-R cycle parameters stabilize, or should it be referred to as 'adult' only at ~27 wks when muscle fibre diameters plateau? Also, from the data reviewed here it is clear that, despite some focus on individual components of the E-C-R cycle, there exists very little information regarding functional characteristics of the E-C-R cycle over a broad range of postnatal ages in rat fast twitch skeletal muscle. In Chapter 3 of this thesis, responsiveness to T-system depolarization of mechanically skinned fibre preparations (a functional parameter of E-C coupling, Lamb & Stephenson, 1990a; see also Parameters describing skinned fibre responsiveness to T-system depolarization, page 67) has been determined over a broad range of rat ages (4 – 21 wks).

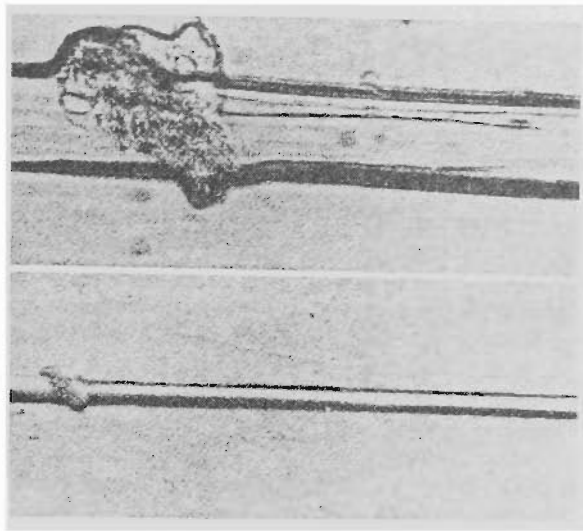
Use of skinned fibres for studying E-C coupling

Skinned fibres is a term used to describe individual muscle fibres that have had their sarcolemma either disrupted or removed chemically or mechanically. Chemical skinning involves incubating a single fibre or a bundle of muscle fibres in one or a

combination of skinning solutions for varying lengths of time. These solutions may contain compounds such as glycerol (Szent-Gyorgyi, 1949), EDTA (ethylenediaminetetraacetic acid; Winegrad, 1971), EGTA (ethyleneglycol-bis(β -aminoethylether)-N,N'-tetraacetic acid; Wood *et al.*, 1975), saponin (Launikonis & Stephenson, 1999), β -escin (Launikonis & Stephenson, 1999) or Triton-X (Brenner, 1998). The above skinning agents have a similar effect in removing or disrupting the sarcolemma but have differential effects of the SR membrane, which makes them less than suitable for examining E-C coupling. Another disadvantage of the chemically skinned fibre is the potential loss of soluble proteins during the prolonged skinning and storage periods.

The mechanically skinned fibre preparation was first demonstrated by Natori (1949) (Figure 1.9A) and has since continued to be used by several groups (Stephenson, 1981; Donaldson, 1985; Fill & Best, 1988; Lamb & Stephenson, 1990a; Bakker & Berg, 2002; Plant *et al.* 2002). Mechanical skinning involves the manual removal of the sarcolemma using either a pair of fine needles or forceps (Figure 1.9B). Once the sarcolemma has been removed from the fibre it has been shown that the t-tubular membrane reseals (Lamb *et al.*, 1995; Launikonis & Stephenson, 2001) essentially becoming an electrically and chemically isolated compartment (Schneider, 1994). When the mechanically skinned fibre is placed in a high K^+ solution with a small amount of Na^+ , the t-tubular Na^+/K^+ ATPase/pump re-establishes ion concentration

A



B

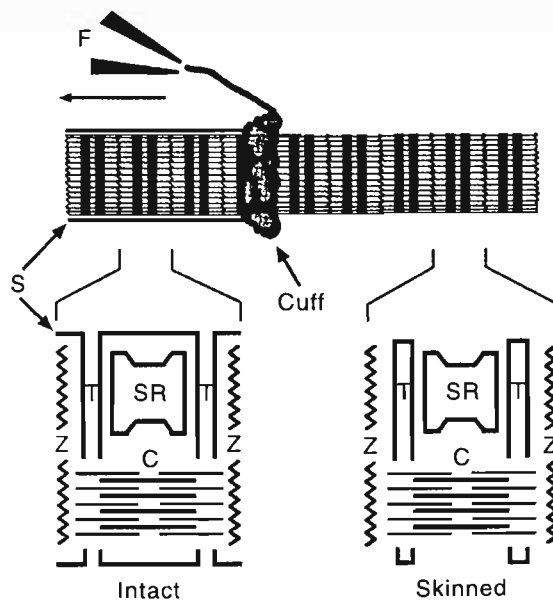


Figure 1.9 The mechanically skinned muscle fibre.

A. Photographs of a Natori single mechanically skinned fibre. The sarcolemma has been peeled back towards the left of the picture. (Reproduced from Umazume, 1991)

B. Diagram showing the mechanical skinning procedure. The sarcolemma is peeled back with the aid of forceps leaving a sealed T-system and intact E-C coupling.

(Reproduced from Posterino, 2001).

differences across the t-tubular membrane similar to those found *in vivo* (i.e. the t-tubular environment relatively more positive than the myoplasm) (Lamb & Stephenson, 1990a; Coonan & Lamb, 1998).

Advantages of the mechanically skinned fibre preparation

The major advantage of the mechanically skinned fibre is that it allows experimental manipulation of the myoplasmic environment while retaining the all essential elements of the E-C-R cycle (Lamb, 2002a & b; Posterino, 2001). In this preparation, contractile activation can be achieved either by the normal sequence of events starting with the depolarization of the sealed t-system and activation of the voltage sensors (Lamb & Stephenson, 1990 a & b; Launikonis & Stephenson, 2001), by direct activation of the ryanodine receptors (RyRs)/sarcoplasmic reticulum (SR) Ca^{2+} release channels (Lamb & Stephenson, 1990b; Endo & Iino, 1980; Fink & Stephenson, 1987) thus by-passing the voltage sensor activation, or by direct activation of the contractile machinery in strongly Ca^{2+} -buffered solutions (Fink *et al.*, 1986). Thus the mechanically skinned fibre allows the functional probing of the voltage dependent Ca^{2+} release (E-C coupling), SR properties (SR Ca^{2+} uptake and release) and Ca^{2+} -induced activation of the contractile apparatus. In addition, the skinned fibre allows the 'endogenous' SR Ca^{2+} content to be maintained or varied over a wide range (Lamb, 2002a & b). T-system depolarization can be achieved by rapidly lowering the myoplasmic K^+ concentration (substituted with equimolar amounts of Na^+) which reverses the t-tubular membrane potential (Lamb & Stephenson, 1990a).

Alternatively, mechanically skinned fibres can be electrically stimulated to produce action potentials that spread through the transverse and longitudinal tubular systems and trigger SR Ca^{2+} release (Posterino *et al.*, 2000; Posterino, 2001). Based on these

features, studies using the skinned fibre preparation fill the gap between whole muscle or intact fibre studies, and studies utilizing isolated SR and/or isolated contractile or channel proteins (Lamb, 2002b).

Disadvantages of the mechanically skinned fibre preparation

There are, however, some limitations to the mechanically skinned fibre preparation which include: (i) inability to accurately determine or control the T-system membrane potential as the t-tubule is too small to use the patch clamp or microelectrode techniques (Schneider, 1994; Melzer, 1995) and (ii) important soluble and diffusible intracellular components (such as some of the proteins participating in the E-C-R cycle, enzymes and some glycogen) may be lost from the preparation to the bathing solution.

Skeletal muscle glycogen

Glycogen enables muscle cells (as well as other cells) to store glucose in a form which has very little influence on the intracellular osmotic pressure (De Barsey & Hers, 1990). Skeletal muscle glycogen can reach up to 1% of total muscle wet weight and is the major form of stored energy for muscular work.

Glycogen particle structure

Glycogen, as viewed by electron microscopy, exists as spherical shaped β -particles (Geddes, 1986). The β -particle is not solely a chemically homogenous structure of stored glucose as it also contains a covalently bound protein core (glycogenin; see below), non-covalently bound enzymes responsible for glycogen metabolism and minor inorganic constituents such as phosphate (Roach, 2002). Figure 1.10 shows a

theoretical diagram highlighting the potential interaction between the molecular species associated with the glycogen particle that are responsible for its metabolism. Because of the presence of the enzymes required for glycogen metabolism and the constant turnover of glucose units, β -particles are considered to be independent organelles called glycosomes (Rybicka, 1996).

Glycogen particles are composed of D-glucose monomers that are covalently linked by α 1,4-glucosidic bonds (formed by the enzyme glycogen synthase). Branching occurs approximately every four to ten residues with glucose units linked by a α 1,6-glucosidic bond (formed by branching enzyme) (Illingworth et al., 1952; Smythe & Cohen, 1991). It is estimated that 93 % of glucose residues are linked by α 1,4 bonds and 7 % by α 1,6 bonds (Newsholme and Leech, 1995). The average glucose chain length within a glycogen molecule is approximately 12 - 17 residues (Illingworth et al., 1952). This highly branched nature of glycogen results in overall structure being tree or bush like with successive tiers of branches (see Figure 1.11). (Larner et al., 1952). A full sized glycogen β -particle has been estimated to contain \sim 55, 000 glucose residues in a maximum of 12 tiers (Melendez et al., 1997). Mathematical modeling suggests that a 13th tier, although theoretically possible, would limit the interaction between glycogen and the enzymes glycogen phosphorylase and glycogen synthase (Melendez et al., 1997; Melendez et al., 1998). As the glycogen particle is reduced in size each outer tier contains fewer absolute numbers of glucose residues but always contains 34.6 % of the total residues (Shearer & Graham, 2002).

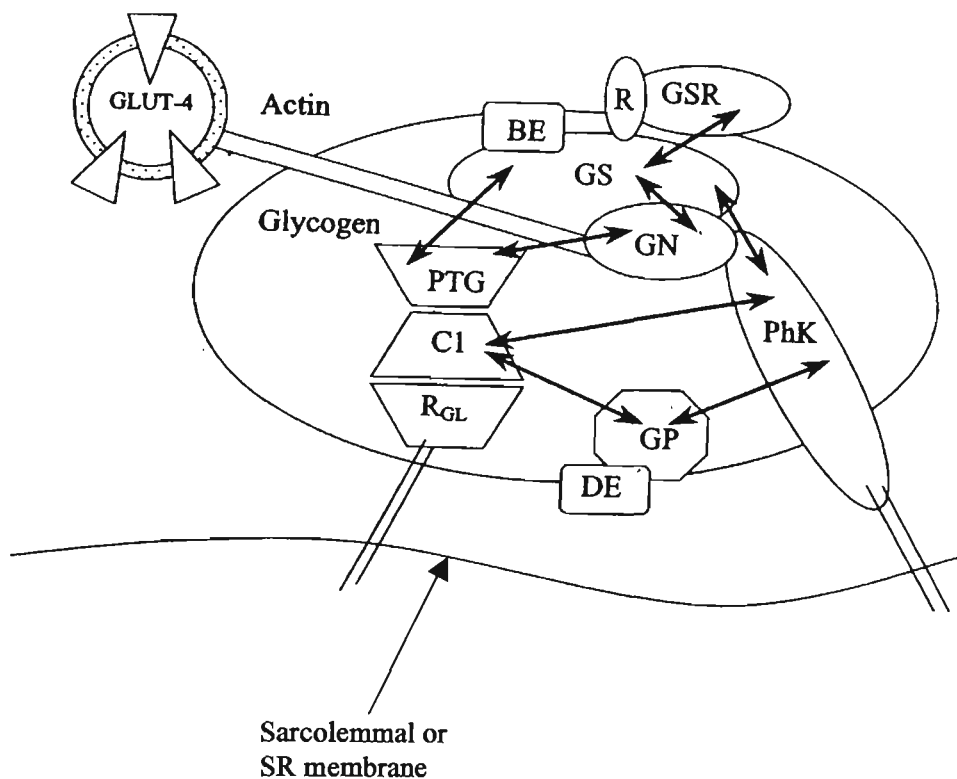


Figure 1.10 The glycosome.

This diagram shows a hypothetical arrangement of the glycogen particle, its associated enzymes and other neighboring structures. (GP, glycogen phosphorylase; GS, glycogen synthase; BE, branching enzyme; DE, debranching enzyme; PhK, phosphorylase kinase; GN, glycogenin; PTG, Protein targeting to glycogen; GSR, glycogen synthase kinase regulatory subunit; R_{GL}, glycogen targeting subunit; C1, type 1 phosphatase catalytic subunit; R, kinase targeting subunit) (Modified from Shearer & Graham, 2002).

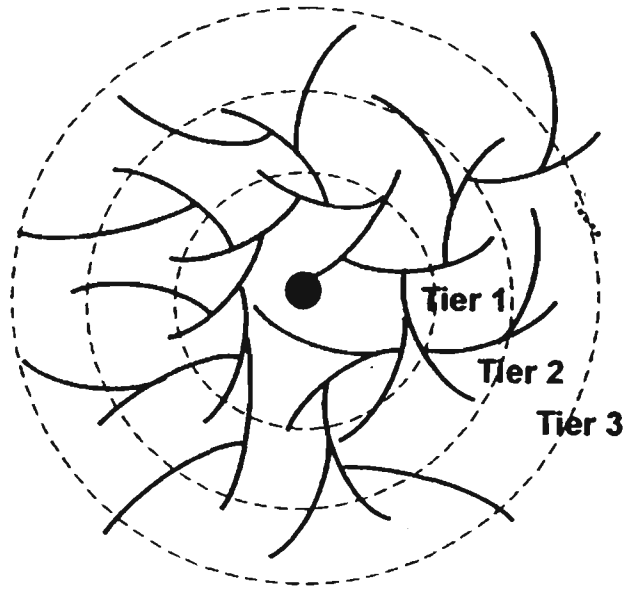


Figure 1.11 The molecular structure of a glycogen particle.

This diagram shows the first three inner tiers of the glycogen particle with glycogenin at the core. (Reproduced from Shearer & Graham, 2002)

Location of skeletal muscle glycogen and glycogenolytic enzymes

Skeletal muscle glycogen is heterogeneously distributed throughout the cell (Sjostrom *et al.*, 1982; Friden *et al.*, 1985 & 1989; Marchand *et al.*, 2002). Friden *et al.* (1989), using electron microscopy, revealed several locations of glycogen deposits within human skeletal muscle. These locations included the subsarcolemmal space especially in the near vicinity of subsarcolemmal mitochondria, the intermyofibrillar space particularly around the region of the I-band and as intramyofibrillar longitudinal rows between actin filaments on either side of the Z-line. More recently, Marchand *et al.* (2002) showed that the largest intracellular pool of glycogen was located in the intermyofibrillar space although the subsarcolemmal space was more densely packed with smaller glycogen particles. Of the glycogen found in the inter- and intramyofibrillar spaces, particles present at the level of the sarcomeric I band are of particular interest to studies on E-C coupling as the I band corresponds, in mammalian skeletal muscles, to the location of the T-system and SR junction (triad).

It has long been known that glycogen is somehow associated with the SR membrane (Wanson & Drochman, 1968; Meyer, 1970; Wanson & Drochman, 1972). However, it is difficult to conclude from the literature what proportion of SR associated glycogen is in physical contact with or attached to the SR membrane, and how much is just located near the SR. Wanson & Drochman (1968) observed 'some' particles in contact with the SR, while Entman *et al.* (1980) suggested that SR glycogen represented a 'minority' of total muscle glycogen. This is in contrast to the large pool of glycogen that has been shown to exist in the vicinity of the sarcotubular triad region by Friden *et al.* (1989) and Marchand *et al.* (2002). The possibility of glycogen attaching to membranous structures is supported by data showing that glycogenin, by

virtue of the presence of a very hydrophobic amino acid sequence (Kennedy *et al.*, 1985), could bind to membranous structures like the SR membrane (Polishchuk *et al.*, 1995). Another mechanism by which glycogen could be attached to the SR membrane is via the R_{GL} glycogen targeting subunit of protein phosphatase-1 (see Figure 1.10) that also contains a hydrophobic sequence that has been postulated to allow for the localization of glycogen to membranous sites including the SR (Newgard *et al.*, 2000).

Polishchuk *et al.* (1995) proposed that glycogen is initially synthesized on the SR membrane until the particle reaches a critical size (~ 200 kDa) after which it is released into the myoplasm. This proposal is consistent with the earlier observation of Wanson & Drochman (1972) that the few glycogen particles actually in contact with the SR membrane are much smaller than average glycogen particle. Two studies have attempted to quantify the amount of glycogen associated with the SR with the results obtained using rat skeletal muscle being quite divergent (32 µg/mg SR protein, Cuenda *et al.*, 1994 vs 400 µg/mg SR protein, Lees *et al.*, 2001). It remains unclear if these figures represent true *in vivo* values. Despite the growing volume of information regarding the intracellular location of glycogen, the exact relationship between glycogen and the function of the neighboring subcellular compartments remains to be elucidated.

As mentioned earlier (see *Glycogen particle structure*, page 45) glycogen particles or glycosomes contain the various protein species required for glycogenolysis such as glycogen phosphorylase (GP), phosphorylase kinase (PhK) and debranching enzyme (Figure 1.10). Previous studies have also shown that GP and PhK (Wanson & Drochman, 1972; Entman *et al.*, 1980; Cuenda *et al.*, 1993, 1994, 1995; Polishchuk *et*

al., 1995; Lees *et al.*, 2001), along with many of the enzymes of the glycolytic pathway (Xu *et al.*, 1995; Xu & Becker, 1998), are located on the SR membrane. More recently, GP has been shown to be associated with the RyR1/Ca²⁺ release channel (Hirata *et al.*, 2003) and the Na⁺/K⁺-ATPase/pump α subunit (Takeyasu *et al.*, 2003).

Glycogenolysis

Muscle glycogen is broken down in a process known as glycogenolysis. This pathway is distinct from the glycogen synthesis pathway that involves different enzymes. Firstly, the enzyme GP in the presence of inorganic phosphate (Pi) phosphorolytically cleaves the α -1, 4 glucosidic bond joining the terminal non-reducing glucose residue and its neighbour resulting in the formation of glucose-1-phosphate (Stryer, 1995). The glucose-1-phosphate can then enter the glycolytic pathway to produce ATP, nicotinamide adenine dinucleotide (reduced form; NADH) and pyruvate. GP continues activate phosphorolysis of successive α -1, 4 bonds toward the centre of the β -particle until it reaches a glucose residue that is four residues away from an α -1, 6 branch point. At this point another enzyme known as debranching enzyme or amylo-1, 6-glucosidase catalyses a two step reaction to remove the branch point glucose residue, since the α -1, 6 glucosidic bond is not susceptible to cleavage by GP (Stryer, 1995). In the first step, the debranching enzyme acts as a transferase that removes three glucose residues and adds them to another side chain of α -1,4 residues which effectively exposes the α -1,6 connected residue. The second action of the debranching enzyme is then to hydrolyse the α -1. 6

bond and release a single glucose molecule (Brown, 1994). GP is then free to continue to cleave α -1, 4 linked residues until the next α -1, 6 branch point.

Glycogen phosphorylase

GP, the rate limiting enzyme of glycogenolysis, exists as a dimer with a molecular weight of 97.5 kDa (Johnson, 1992). GP can exist in either a less active T state or a more active R state (Newgard *et al.*, 1989), with the most active form having a K_m for glycogen of \sim 1-2 mM (Shearer & Graham, 2002). The activity state of GP is modulated by phosphorylation and/or the binding of various metabolites. Thus, phosphorylation at the Ser14 residue converts the unphosphorylated phosphorylase **b** (phos **b**) into the potentially more active phosphorylase **a** (phos **a**). Metabolic effectors including glycogen, Pi, glucose-1-phosphate, fructose-1-phosphate and uridine diphosphate glucose activate both phos **a** and phos **b** while AMP activates phos **b** only. Factors such as glucose and caffeine act as inhibitors for both phos **a** and phos **b**, while glucose-6-phosphate (G-6-P) and ATP act as inhibitors for phos **b** only (Newgard *et al.*, 1989). In this thesis, phos **a** and phos **b** activities have been examined as part of a study aimed to establish the stability of glycogen in rat (and toad) skeletal muscle stored for various lengths of time and at different temperatures (Chapter 5).

Phosphorylase kinase

PhK is responsible for the Ser14 phosphorylation of Phos **b** that leads to the transformation of GP into the more active **a** form. PhK is composed of 16 subunits: 4 x α , β , γ , δ . The α and β subunits contain cAMP phosphorylation sites, the γ subunit has the catalytic site while the δ subunit is the Ca^{2+} binding protein calmodulin

(Roach, 2002). Two isozymes of the α subunit exist with the α' isozyme, a splice variant of the PHKA1 gene, being expressed in red/slow skeletal muscle while the α isozyme, a splice variant of the PHKB gene, is expressed in white/fast skeletal muscle (Roach, 2002). The functional significance of these isozymes remains unknown. PhK can be activated by cAMP phosphorylation, elevated levels of ADP and by Ca^{2+} binding to the δ calmodulin subunit (Kruszynska *et al.*, 2001). Ca^{2+} released from the SR following membrane depolarization is sufficient to activate PhK which in turn phosphorylates and activates GP leading to increased glycogenolysis (Ebashi & Endo, 1968). So far, most studies concerned with the regulation of phosphorylase kinase and other glycogenolytic enzymes have involved the use of whole muscle preparations that do not allow an insight into the inter-fibre differences with respect to these issues. The findings presented in Chapter 6 together with the results of Stephenson *et al.* (1999) strongly suggest that the mechanically skinned fibre preparation can be used in studies of skeletal muscle glycogen.

Glycogen and muscle fatigue

Muscular fatigue, defined as the inability of a muscle to maintain a required force output with respect to time (Fitts, 1994 ; Asmussen, 1979 for reviews), is a multifactorial phenomenon and is largely task dependent (Fitts, 1994 ; Enoka, 1995 for reviews). The actual site(s) of fatigue within the muscle cell are still speculative but much attention has been focused recently on factors that influence the E-C coupling mechanism and more specifically, the release of Ca^{2+} from the SR. It is well established that Ca^{2+} is essential for removal of the inhibition of actin-myosin interaction which then enables the sliding of the protein filaments which in turn causes the muscle to shorten and produce force (Allen *et al.*, 1995 for review; also see

Thin filament activation and muscle contraction, page 19). A reduction in Ca^{2+} release would in theory result in reduced force generation by the contractile proteins.

Bergstrom *et al.* (1967) were the first to demonstrate that during moderate to heavy intensity exercise (65 - 90 % of maximal oxygen uptake; VO_2max) there is a high positive correlation ($r = 0.92$) between muscle glycogen depletion and muscular fatigue. This correlation however only holds true at this range of work intensities. At lower intensities (i.e. < 60 % VO_2max) fatty acid and blood glucose oxidation are capable of supplying sufficient energy as evidenced by high muscle glycogen levels after exercise (Fitts, 1994). Likewise, exercise at 90 % VO_2max or above results in rapid fatigue despite high remaining muscle glycogen levels (Fitts, 1994). At moderate to heavy work levels, fatigue is possibly related to an inability of the muscle to sustain the rate of flux through the glycolytic pathway; this would result in a reduction of the rate of ATP production needed to maintain the required level of work (for review see Green, 1991). Indeed, the data of Broberg & Sahlin (1989) showed a 10 % decrease in ATP and an increase in inosine monophosphate (an indicator of ATP degradation) with prolonged exercise at 60 - 70 % of VO_2 max. until exhaustion (Broberg & Sahlin, 1989). Whether this decrease in ATP is enough to reduce power output is still however questionable (Fitts, 1992).

Energy related role of glycogen in fatigue

Recently, Chin and Allen (1997) investigated the influence of muscle glycogen concentration on Ca^{2+} release and force production in single muscle fibres of the mouse. Using two fatiguing stimulation periods, separated by incubation of the fibre either with or without glucose, and comparing the Ca^{2+} release and force production

for each of the work periods, Chin and Allen (1997) have showed that both force and Ca^{2+} release are affected by the level of muscle glycogen. When fibres were incubated with glucose between stimulation periods, glycogen recovered and Ca^{2+} release increased from 47 % to 82 % at the end of the first stimulation period. However when the fibres were incubated without glucose, muscle glycogen remained low and Ca^{2+} release recovered to only 57 %. They concluded that 25 % (82 minus 57 %) of the Ca^{2+} release recovery was glycogen dependent.

Based on these findings the authors speculated that the repeated tetanic contractions reduced glycogen and creatine phosphate below a critical level causing a small localized decrease in [ATP] near the SR-T tubule triad (Han *et al.*, 1992; for review see Korge & Campbell, 1995). This in turn would have had an inhibitory effect on the release of Ca^{2+} through the Ca^{2+} release channels (see *Putative endogenous regulators of the skeletal muscle RyR1 isoform*, page 12) and/or a direct or indirect effect on the actin-myosin interaction and hence force production (Chin & Allen, 1997).

Non energy related role of glycogen in fatigue

There is evidence, produced mainly by studies on muscle fatigue, to suggest that glycogen function in the muscle is not strictly confined to its role as an energy store. Thus, Vøllestad *et al.* (1988) were unable to show any significant decrease in cellular ATP at the point of fatigue despite a large decrease in muscle glycogen. The study of Vøllestad *et al.* (1988) demonstrated that fatigue from prolonged muscular activity is unlikely to be due to depletion of ATP.

Recently, Stephenson *et al.* (1999) investigated the hypothesis that glycogen, as well as having a role in energy storage and supply, also plays a non-energy related protective role against fatigue. To test this hypothesis, these authors examined glycogen content in single mechanically skinned muscle fibres of the toad and fibre responsiveness to T-system depolarization in solutions containing excess ATP (8 mM) and creatine phosphate (10 mM). This strategy eliminates the possibility of low energy charge of the muscle cell causing reduced force output. As shown in Figure 1.12 a positive correlation ($r = 0.83$) was found between single fibre glycogen content and its ability to respond to depolarization of the T-system (Stephenson *et al.*, 1999). Therefore despite adequate ATP levels within the fibre, low muscle glycogen was associated with lower force responses to T-tubule depolarization indicating a possible function link between glycogen content and Ca^{2+} release from the SR. An examination of the relationship between glycogen content and mechanically skinned fibre responsiveness to T-system depolarization in rat skeletal muscle was carried out in the study presented in Chapter 6 using the depolarization/repolarization protocols of Stephenson *et al.* (1999).

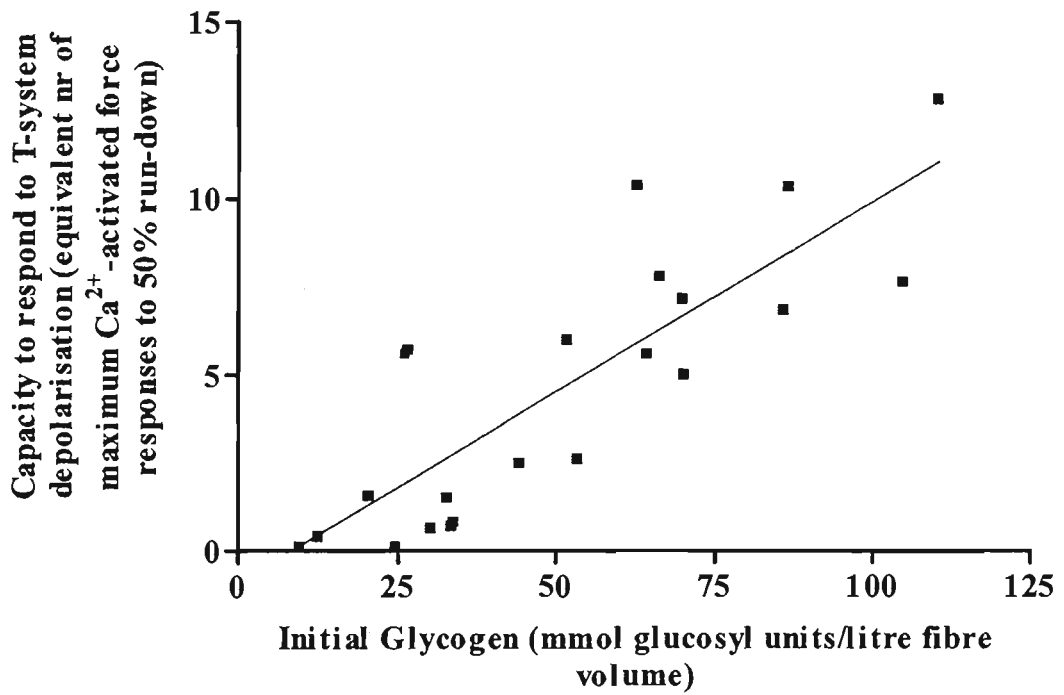


Figure 1.12. Correlation between toad fibre capacity to respond to T-system depolarization and initial fibre glycogen concentration.

Correlation factor (r) = 0.83. (Reproduced from Stephenson *et al.*, 1999)

Aims of this study

At the time when work for this thesis was started, the experimental approach employed in the majority of studies using the mechanically skinned fibre preparation to examine E-C-R cycle events in mammalian systems at the cellular level involved the use of muscles dissected from animals belonging to an age range of 12 to ~ 20 wks (e.g. Posterino & Fryer, 2000; Posterino *et al.*, 2001) which is smaller than the range of 4 – 21 wks commonly used in studies of adult skeletal muscle (see *Aspects of postnatal development of rat skeletal muscle relevant to the E-C-R cycle*, page 32). Furthermore, the fibres used in most of these studies were obtained from the rat extensor digitorum longus (EDL), a muscle that has a relatively homogeneous fast-twitch fibre type composition (Armstrong & Phelps, 1984). Finally, when examining the mechanisms underlying the effect of potential regulators of E-C-R cycle events, experimenters typically used the test fibre as its own control. Thus, little was known about differences in rat skinned fibre responsiveness to T-system depolarization between (i) fibres from animals belonging to the whole "adult" age range, (ii) fibres containing different MHC isoforms and (iii) fibres containing different glycogen concentrations. Therefore the aim of this study was to examine the relationship between mechanically skinned fibre excitability and the developmental age of the rat, in the range of 4 to 21 wks (*Chapter 3*), MHC isoform composition, muscle of origin (*Chapter 4*) and glycogen content (*Chapter 6*). Prior to examining the relationship between glycogen content and skinned fibre excitability in rat EDL muscle, the stability of glycogen in EDL (and soleus; SOL) muscle stored for various lengths of time and at different temperatures was established and compared to that in toad iliofibularis (IF) muscle (*Chapter 5*).

Chapter 2

GENERAL MATERIALS AND METHODS

Animals

The animals used in this study were male rats (*Rattus norvegicus*) aged between 4 and 21 weeks and male and female cane toads (*Bufo marinus*). Rats were housed at room temperature (20 – 25°C) with normal light and dark cycle and access to food and water *ad libitum*. Cane toads were kept unfed in a dark environment at room temperature. Rats were killed by deep inhalation of the volatile anaesthetic halothane (Zeneca) while toads were double pithed. All animal related procedures described in this thesis were carried out in accordance with the guidelines of the Victoria University Animal Experimentation Ethics Committee.

Muscle dissection

Immediately after animal death, the muscle required, EDL, soleus (SOL) or sternomastoid (SM) from the rat or iliofibularis (IF) from the toad were dissected from the body taking care not to cut or excessively stretch the muscle. The muscle was subsequently blotted dry on Whatman No 1 filter paper to remove any excess interstitial fluid or blood. Each muscle was then placed into a Petri dish layered with a bed of Sylgard 184 transparent resin (Dow Corning Chemicals, USA) and covered with paraffin oil (Ajax Chemicals, Australia). In studies of mechanically skinned fibres, paraffin oil is used in the Petri dish for the following reasons: (i) it facilitates the visualization of the single muscle fibres by having a different refractive index; (ii) it prevents muscle fibre gaining or losing water while the fibre is being prepared; and

(iii) it helps to confer the fibre a quasicircular cross-sectional area through the surface tension exerted on the fibre at the fibre/oil interface (Bortolotto *et al.*, 1999). Each muscle was pinned through the tendons to the Sylgard resin bed with entomological pins at approximate resting length. Unless stated otherwise, when not being used for single fibre dissection, the muscles were kept refrigerated at 4°C.

Single muscle fibre dissection

Single muscle fibres were dissected from muscles with the aid of No. 5 jewellers forceps (Dupont, Switzerland), iris scissors (Vannas, Germany) and an Olympus dissecting microscope (magnification range- 6.4x – 40x) (see Figure 2.1). To begin, a small incision was made through the epimysium, then while holding a small bundle of 5 – 10 fibres, another incision was made parallel to the muscle fibre's long axis and the bundle carefully pulled away to about 1 – 1.5 cm from the muscle. Then using the forceps, this larger bundle was then continuously halved until a single fibre remained.

Mechanical skinning

Taking the free end of the dissected fibre with one pair of forceps, the other forceps was used to pinch a small portion of sarcolemma and peel the membrane up the fibre towards the muscle belly (See Figure 1.9, Chapter 1). Caution was taken to not excessively stretch the fibre during this procedure. The presence of a 'cuff' as the membrane was peeled back indicated that the fibre was being skinned properly and not split into two pieces.

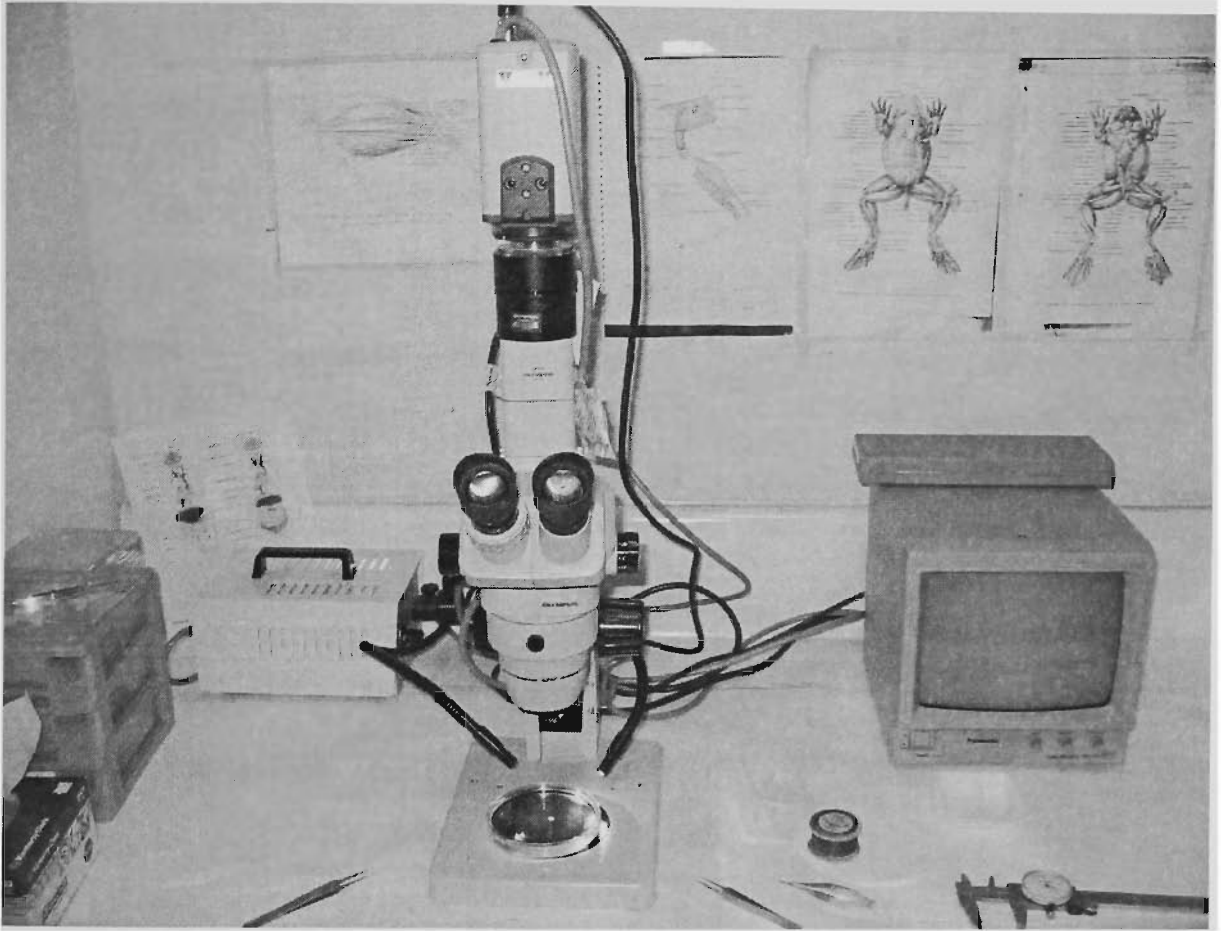


Figure 2.1 Dissecting microscope with video monitor system used for dissection, skinning and measuring single muscle fibres.

Measurement of muscle fibre dimensions

A video camera-monitor system (Olympus; see Figure 2.1) and a pair of callipers (Mitutoyo, Japan) were used to measure the length (l) and width ($w \cong d$) of each skinned muscle fibre segment under paraffin oil at 6.4 x and 40 x magnification respectively. Muscle fibre width was measured in 2 – 3 places along the length of the fibre and a mean calculated. Dimensions measured on the monitor screen were converted to actual fibre dimensions (expressed in mm) using conversion factors obtained from calibration with a graticule. Assuming the fibre to be cylindrical, fibre volume (V) was calculated using the following equation:

$$V = \pi d^2 l / 4 \quad (\text{Eq 1})$$

Mounting the skinned muscle fibre preparation to the force measuring system

While still under oil and using finely braided surgical silk (Deknatel, No 10), a single knot was tied to the free end of the skinned muscle fibre. The Petri dish with fibre preparation was then positioned under the force measuring apparatus. With the aid of an inverted microscope (Olympus; see Figure 2.2A), the single fibre segment was then attached to a stainless steel pin (connected with shellac to a force transducer) with a surgeon's double knot (see Figure 2.2B). Once tied, the other end of the fibre was clamped between the tips of a pair of fine forceps attached to a micromanipulator. The fibre was freed from the whole muscle by cutting it with microscissors, between the muscle and forceps, as close as possible to the edge of the forceps. Resting length was obtained by slightly stretching the fibre so that force was just detectable on the chart recorder and then releasing the tension until no measurable force could be detected. This length was measured with the aid of an eye piece graticule in the

A



M

CR

LJ

PT & PC

B

MM

T

F

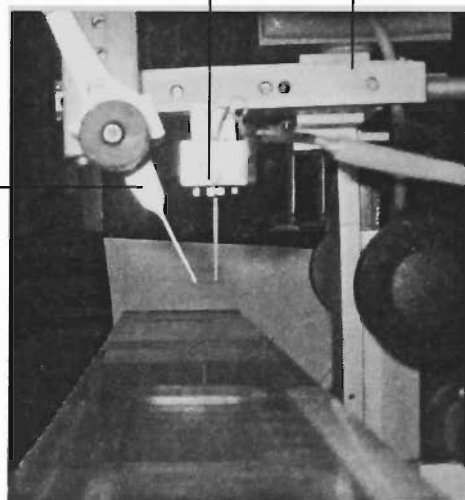


Figure 2.2 Force measurement and recording apparatus. A) Microscope (M), chart recorder (CR), laboratory jack (LJ), Perspex tray (PT) and Perspex cover (PC). (power supply and Wheatstone bridge not shown). **B)** Enlarged photo of micromanipulator (MM), forceps (F) and transducer (T) with steel pin attached.

inverted microscope. The fibre was then stretched to 120 % of its resting length resulting in an approximate sarcomere length of 2.8 – 3.0 μm for rat skeletal muscle fibres. The sarcomere length adjustment was performed based on compelling evidence that: (i) the plateau region for isometric force production in rat skeletal muscle occurs at longer sarcomere lengths (2.4 - 2.9 μm) (Stephenson & Williams, 1982), a characteristic which has been related to longer thin filaments (Close, 1972), and (ii) in vertebrate skeletal muscle, an increase in the sarcomere length is accompanied by an increase in the sensitivity of the contractile apparatus to Ca^{2+} (Rassier *et al.*, 1999). At sarcomere lengths of 2.8 - 3.0 μm , rat EDL muscle fibres produce close to maximum force. With the activation procedures used in this study, both the sarcomere pattern and sarcomere homogeneity in small vertebrate skeletal muscle fibre segments are well preserved during sub-maximal activation (Stephenson & Williams, 1982). Finally, the Petri dish was removed and the fibre was lowered into a 2 ml Perspex bath containing a K^+ -HDTA based Polarizing solution, where it was allowed to equilibrate for 2 mins before the commencement of depolarization experiments.

Force measurement and recording apparatus

As shown in Figure 2.2 A & B, the apparatus used for measuring the force output of a single skinned muscle fibre consisted of a micromanipulator (Prior, UK), a pair of fine forceps, a piezzo-resistive force transducer (AME801, Sensoror, Norway) with a stainless steel pin secured to it with shellac, a chart recorder (Linear), a Wheatstone bridge (see Figure 2.3), preamplifier, power supply and laboratory jack.

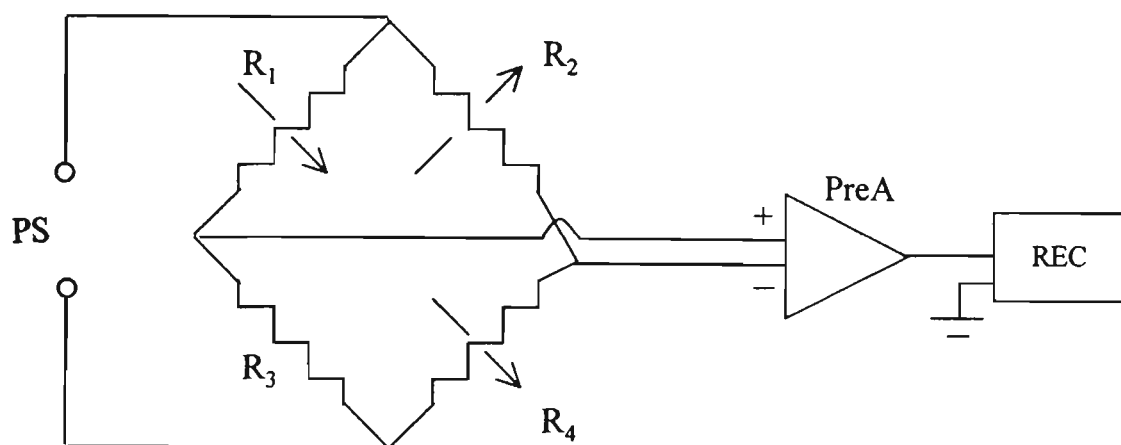


Figure 2.3 Circuit diagram of the Wheatstone bridge.

R_1 and R_2 , strain sensitive resistors (1 kohm) associated with the force transducer; R_3 , fixed resistor (1 kohm); R_4 adjustable resistor for balancing the bridge; PS, 10V DC power supply; PreA, preamplifier; REC, chart recorder.

Force transducer calibration

To calibrate the force transducer, the micromanipulator was laid on its side so that the transducer and attached steel pin were in a horizontal position. Small weights, ranging from 6.9 mg (35.3 μN) to 93.5 mg (919.2 μN), were then placed on the end of the pin where a fibre would normally be tied. The resulting force signals were recorded on the chart recorder at different sensitivities (2, 5 & 10 mV) and subsequently plotted to create a calibration curve of chart recorder pen displacement (mm) versus weight (mg or μN) (See Figure 2.4).

Protocol for T-system depolarization induced activation in mechanically skinned fibres

Immediately after a fibre is mechanically skinned, it is placed in a high K^+ solution (Polarizing solution; the chemical composition of this and all other solutions mentioned below are given in detail in Chapter 2) for 2 mins to allow the t-tubule membrane to repolarize. Once repolarized, depolarization of the t-tubules, which triggers a force response (depolarization-induced force response; DIFR) via the normal E-C coupling pathway, is achieved by placing the fibre into a Depolarizing solution in which the K^+ has been replaced with sodium (Na^+) (Lamb & Stephenson, 1990a). Each depolarization typically lasts for approximately 3 – 5 seconds after which the fibre is returned to the Polarizing solution to repolarize the T-system membrane and reprime the voltage sensor, for 1 min before the next depolarization. The typical pattern of DIFRs produced by a fibre subjected to this protocol includes: (i) an initial 'work-up' period where the force generated gradually increases to a maximum value (Coonan & Lamb, 1998) and (ii) a 'run-down' period where the force responses decrease until no more force responses can be elicited (Lamb &

Stephenson, 1990a). The amplitude of the force response reached at the end of the work-up period may begin to decrease rapidly or may be maintained for several depolarization/repolarization cycles.

In the studies described in this thesis, depolarizations were continued until the force response had run-down by a value of 75 % of the largest depolarization-induced force response. After the last DIFR, the fibre was placed back into the Polarizing solution. Then, to check if the run-down was due to depleted SR Ca^{2+} levels or to dysfunction of the Ca^{2+} release channels, each fibre was placed in a low (0.015 mM) $[\text{Mg}^{2+}]$ (Low Mg^{2+}) solution to release endogenous SR Ca^{2+} . From the Low Mg^{2+} solution the fibre was then placed into a Relaxing solution before the maximum Ca^{2+} -activated force (maxCaF) was obtained in a high Ca^{2+} (pCa 4.5; Maximum Ca^{2+} Activation) solution.

Parameters describing skinned fibre responsiveness to T-system depolarization

The two most commonly used descriptors of skinned fibre responsiveness to T-system depolarization are the amplitude of the maximum DIFR (maxDIFR), normalized to maxCaF in the same fibre and the number of DIFRs produced by the fibre until the force response decreasing by a certain percentage of the maxDIFR . As mentioned above, in this thesis, this percentage was 75% and the corresponding parameter is referred to as $75\%R-D$. Other parameters particular to each study are defined in the Methods section of individual chapters.

In mechanically skinned muscle fibre preparations, the maxDIFR is ultimately determined by the amount of Ca^{2+} released from the SR, the rate of Ca^{2+} release/uptake and the sensitivity to Ca^{2+} of the contractile apparatus. As shown in

Table 2.1, several non-experimenter-related events involving the T-system and SR can impact on the amount of Ca^{2+} released and on the rate of Ca^{2+} release/uptake by the SR compartment. Generally, the size of a DIFR is influenced by the number of voltage sensors activated by the depolarizing stimulus, the number of SR Ca^{2+} release channels opened as the result of the cross-talk between voltage sensors and the SR channels, and by the SR luminal $[\text{Ca}^{2+}]$. It is assumed that, if Ca^{2+} loss from the intra-myofibrillar space into the aqueous bathing solution is minimal (Lamb & Stephenson, 1990a), full coupling of the two compartments will result in enough Ca^{2+} being released from the SR to elicit a near maximal contractile response as compared to the maximum Ca^{2+} activated force response (Lamb & Stephenson, 1990a).

The determinants of the second parameter, $75\%R-D$, are as yet unknown. According to Lamb & Stephenson (1990a), the run-down phenomenon is not related to the length of time that a fibre is exposed to aqueous solutions, nor to the depletion of SR Ca^{2+} content, as exposure to low $[\text{Mg}^{2+}]$ (0.015 mM), produces relatively large force responses in run-down fibres indicative of adequate SR free Ca^{2+} and functional RyR/ Ca^{2+} release channels (Lamb & Stephenson, 1994). Run-down in mechanically skinned muscle fibres is unlikely to be related to energy depletion as experiments are carried out in the presence of high $[\text{ATP}]$ (8 mM) and $[\text{CP}]$ (10 mM) which maintain the energetic potential of the fibre. One possibility is that the decrease in DIFRs in mechanically skinned fibre preparations is related to a use-dependent loss of some factor such as glycogen located near the triad region (Stephenson *et al.*, 1999; see *Non Energy Related Role of Glycogen in Fatigue*, page 55). Ca^{2+} -dependent or phosphorylation/dephosphorylation-dependent processes leading to a gradual inactivation of t-tubule voltage sensors or disruption of the coupling between the

Table 2.1. Essential positive contributors to the upstroke and downstroke of T-system depolarization induced force responses in mechanically skinned fibre preparations.

Upstroke	Downstroke
<i>experimenter/protocol related</i>	
<ul style="list-style-type: none"> • effective sealing of the T-system after mechanical skinning. • optimum conditions (composition of solutions, incubation times) for repolarization and depolarization of the sealed T-system in the skinned fibre preparation. 	
<i>T-system related (assumption: $P_K \gg P_{Na}$)</i>	
<ul style="list-style-type: none"> • effective polarization of the sealed t-tubule membrane (dependent on Na,K ATPase/pump & $[K^+]$ on both sides of the t-tubule membrane). • effective depolarization of the t-tubule membrane in low $[K^+]$ solution • effective activation of the voltage sensors associated with the DHP receptors. • effective signal transmission between the DHPR/voltage sensors and RyR/Ca^{2+} release channels. 	<ul style="list-style-type: none"> • effective depolarization induced inactivation of the DHPR/voltage sensors.
<i>sarcoplasmic reticulum related</i>	
<ul style="list-style-type: none"> • effective signal reception by the SR RyR/Ca^{2+}-release channels and opening of the channels • amount and rate of Ca^{2+} released from the SR following depolarization (dependent on the SR-Ca^{2+} content, the functional status of the SR RyR/Ca^{2+}-release channels and the number of SR RyR/Ca^{2+}-release channels functionally coupled to the DHPR/voltage sensors) • SR Ca^{2+} ATPase/pump activity 	<ul style="list-style-type: none"> • inactivation or closure of SR RyR/Ca^{2+} channels (use-dependent, Ca^{2+}-dependent) • SR Ca^{2+} ATPase/pump activity
<i>contractile apparatus related</i>	
<ul style="list-style-type: none"> • responsiveness to Ca^{2+} of the contractile apparatus (dependent on its sensitivity to Ca^{2+}) 	<ul style="list-style-type: none"> • diffusion-related loss of Ca^{2+} from the myofilament environment

DHPR/voltage sensor and RyR/Ca²⁺ release channel may also contribute to the run-down (for review see Stephenson *et al.*, 1995).

Force detection limit

Under our experimental conditions, accurate determination of the amplitude of the force response developed by a fibre was possible if the response was $\geq 12 \mu\text{N}$ (the detection limit for 5 mV/scale).

Solution composition

An important feature of the mechanically skinned fibre preparation is that the experimenter can control the myoplasmic milieu by exposing the fibre to various solutions (see *Advantages of the skinned fibre preparation* in Chapter 1, page 44). The solutions used in the T-system depolarization induced activation experiments (Polarizing, Depolarizing, Low Mg²⁺, Relaxing and Maximum Ca²⁺ Activation) contained the following important ingredients (see also Table 2.2):

Table 2.2. Solutions used in E-C coupling experiments.

Depolarization Solutions	K ⁺ (mM)	Na ⁺ (mM)	Free Ca ²⁺ (pCa)	EGTA (mM)	HDTA (mM)	Free Mg ²⁺ (mM)	Total Mg ²⁺ (mM)	ATP (mM)	CP (mM)	Azide (mM)	HEPES (mM)
Polarizing	126	37	6.8	0 or 0.05	50	1.0	8.5	8	10	1	90
Depolarizing	—	163	6.8	0 or 0.05	50	1.0	8.5	8	10	1	90
Low Mg ²⁺	126	37	6.8	0 or 0.05	50	0.015	1.1	8	10	1	90
Relaxing	126	37	> 9.0	50	—	1.0	10.3	8	10	1	90
Maximum Ca ²⁺ Activation	126	37	4.5	50	—	1.0	8.12	8	10	1	90

Note: [EGTA] in Polarizing, Depolarizing and Low Mg²⁺ solutions was dependent on the source of HDTA. HDTA purchased from Fluka required no EGTA to be added to bring free Ca²⁺ to ~ pCa 6.8 while HDTA from Sigma Aldrich required the addition of 50 μM EGTA. All other chemicals were from Sigma, except Mg²⁺ (Riedel-de Haen). All solutions were pH 7.10 ± 0.01.

1. All solutions, with the exception of the Depolarizing solution, contained 126 mM K^+ and 37 mM Na^+ . For the Depolarizing solution, all K^+ was substituted with Na^+ bringing the final Na^+ concentration to 163 mM.
2. In all solutions the total concentrations of ATP and CP were 8 mM and 10 mM, respectively, so that with the aid of the endogenous creatine kinase, structures and processes (such as the contractile apparatus, RyR/ Ca^{2+} release channel, SR Ca^{2+} ATPase/pump and T-tubular Na^+/K^+ ATPase/pump) would be kept in constant supply of ATP.
3. The major anion in the Polarizing, Depolarizing and Low Mg^{2+} solutions was $HDTA^{2-}$ (hexamethalenediamine N,N,N',N'-tetraacetic acid; 50mM) that does not diffuse through the SR or T-tubule membranes or significantly bind Ca^{2+} . In the Relaxing and Maximum Ca^{2+} Activation solutions $HDTA^{2-}$ was replaced with 50 mM of the Ca^{2+} chelator $EGTA^{2-}$.
4. With the exception of the Low Mg^{2+} solution, the *free* Mg^{2+} concentration in all other solutions was 1 mM, a concentration similar to that found at rest *in vivo*. The concentration of free Mg^{2+} in the Low Mg^{2+} solution (0.015 mM) was obtained by mixing two otherwise identical solutions containing 0.05 mM and 0.0 mM free Mg^{2+} at a 1:1 ratio. The total Mg^{2+} required to make up these levels of free Mg^{2+} was calculated using the apparent Mg^{2+} affinity constants of $6.9 \times 10^3 M^{-1}$ for ATP, $8 M^{-1}$ for $HDTA^{2-}$, $15 M^{-1}$ for CP and $5 \times 10^6 M^{-1}$ for EGTA (Moiescu & Thieleczek, 1978; Stephenson & Williams, 1981; Fink *et al.* 1986). The total concentration (mM) of Mg^{2+} in the Polarizing,

Depolarizing, Low Mg^{2+} , Relaxing, and Maximum Ca^{2+} Activation solutions was 8.5, 8.5, 1.1, 10.3, 8.12, respectively.

5. 1 mM Azide (NaN_3) was added to all solutions to prevent mitochondria from influencing Ca^{2+} transients.
6. The pH ($pH = -\log_{10}[H^+]$) was strongly buffered with 90 mM HEPES (N-2-hydroxyethyl-piper-azine-N'-2-ethylsulphonic acid) at 7.10 ± 0.01 . The pH of all solutions was measured with a digital pH meter (Orion).
7. The Maximum Ca^{2+} Activation solution contained 48.5 mM total $[Ca^{2+}]$ resulting in a free $[Ca^{2+}]$ of $\sim 31.6 \mu M$ (pCa 4.5). The Relaxing solution containing 50 mM EGTA²⁻ and no added Ca^{2+} had a free $[Ca^{2+}]$ of < 1.0 nM (pCa < 9.0).
8. The osmolality of all solutions was 290 mosmol/kg, similar to that found *in vivo*.

Free $[Ca^{2+}]$ in the Polarizing solution

An important feature of the mechanically skinned fibre preparation is that at the beginning of an experiment, it contains approximately the normal endogenous SR $[Ca^{2+}]$ (Owen *et al.*, 1997). This is because the fibre is skinned under paraffin oil, a procedure that prevents a loss or gain of SR Ca^{2+} . Lamb & Stephenson (1990a) showed that during each depolarization, a small amount of released Ca^{2+} ($\sim 10\%$) is lost to the bathing solution. This loss of SR Ca^{2+} is, however, offset by the SR Ca^{2+}

ATPase/pump slowly sequestering a small amount of contaminating Ca^{2+} from the solution during the subsequent 1 minute polarizing step (Owen *et al.*, 1997).

To qualitatively assess whether the free $[\text{Ca}^{2+}]$ in the Polarizing solution was sufficient to maintain approximate endogenous levels of SR Ca^{2+} after each depolarization, single fibres were tested using the Polarizing solution from a freshly made batch. If, during this preliminary testing, successive DIFRs became larger and progressively wider, this would indicate that the contaminating Ca^{2+} in the Polarizing solution was too high and the SR was artificially loading too much Ca^{2+} . If, however, the DIFRs became smaller and progressively thinner, this would indicate that the contaminating Ca^{2+} in the Polarizing solution was too low leading to progressive SR Ca^{2+} depletion. If a solution was deemed to have too little or too much free Ca^{2+} then a small amount of Ca^{2+} or the Ca^{2+} chelator EGTA, respectively, was added.

When DIFRs remained relatively constant (especially the width) it was judged that the approximate endogenous levels of SR Ca^{2+} were being maintained. Once established as appropriate to use for the following E-C coupling experiments, the free $[\text{Ca}^{2+}]$ was checked with a Ca^{2+} -sensitive electrode (Orion, model no. 9720), and found to be equivalent to a pCa of 6.8.

The freshly made Polarizing solutions were also compared to a reference Polarizing solution, i.e. an older solution that had previously been demonstrated to contain an adequate free $[\text{Ca}^{2+}]$.

Chapter 3

DEVELOPMENTAL AGE AND RESPONSIVENESS TO T-SYSTEM DEPOLARIZATION IN RAT MECHANICALLY SKINNED SKELETAL MUSCLE FIBRES

Introduction

So far, the method of Lamb and Stephenson (1990a) for determining responsiveness to T-system depolarization in mechanically skinned fibres, introduced in Chapter 1, has been employed in studies aimed at furthering the understanding of the cellular events involved in E-C coupling and identifying endogenous regulators which may act as potential fatiguing agents in normal vertebrate skeletal muscle (rat, toad and mouse) (for reviews see Lamb, 2002a & b; Posterino, 2001).

It is reasonable to expect that this method, which was developed for fast twitch muscle of disease-free rats aged 12-20 wks (Lamb and Stephenson, 1990a; Lamb and Stephenson, 1994), could also provide important insights into aspects of E-C coupling in muscles of rats used as experimental models of human disease at different stages of development of the disease, which often involve the use of animals aged between 4 and 20 wks (e.g. hypertension; Bortolotto *et al.*, 1999). An obvious prerequisite for such application is that T-system depolarization-induced activation of Ca^{2+} release is achievable in skinned fibre preparations from the animals used as controls for the pathological conditions under consideration. Thus far there have been no investigations on the impact of animal age within the full adult age range on the

applicability of the Lamb and Stephenson method to single fibres from rat skeletal muscle. Therefore, the aim of the present study was to systematically examine whether E-C coupling characteristics in mechanically skinned fibre preparations from rat fast-twitch skeletal muscle vary with age, within the 'adult' range.

Materials and methods

Note that the contractile apparatus experiments in this study were performed with the assistance of Dr R Blazev.

Animals

In this study, excitation-contraction (E-C) coupling characteristics were examined in mechanically skinned fibre segments of EDL muscle from Long Evans (LE) hooded rats aged 4-wks (4.0 to 4.4-wks), 8-wks (7.6 to 8.0-wks), 10-wks (10.1 to 10.6-wks), 15-wks (15.0 to 15.6-wks), and 21-wks (20.7 to 21.3-wks) postnatal.

Skinned fibre preparation

Mechanically skinned fibre segments were prepared and their dimensions measured as described in Chapter 2. All experiments were carried out at room temperature (20-25 °C).

Skinned fibre solutions

All solutions were as described in Chapter 2 with the exception of a Ca^{2+} load solution. This was identical to the Polarizing solution except that it contained 40 μM CaCl_2 and 25 μM EGTA. Unless otherwise stated, the 'Ca²⁺ loading strategy' involved exposure of a fibre to a Ca^{2+} load solution (see above) for 15-30 s to allow the SR to actively load extra Ca^{2+} .

T-system depolarization and E-C coupling parameters

In addition to the two commonly used E-C coupling parameters mentioned in Chapter 2 (see *Parameters describing skinned fibre responsiveness to T-system depolarization*, page 67), maxDIFR and $75\%R-D$, two new parameters were introduced in this study. These were (i) the number of responses taken to reach the maximum depolarization-induced response and (ii) the stability of the responsiveness to T-system depolarization expressed as the number of consecutive depolarization-induced force responses within the range 80 to 100% of the maximum depolarization-induced response ($\#DIFR_{80-100\%}$).

In this study, the force response developed in the low Mg^{2+} solution (LMgFR) was related to the DIFR produced by the fibre preceding its exposure to low Mg^{2+} ($R-D$ DIFR). More specifically, the SR in a run-down fibre was deemed to be functionally competent if the ratio of the two responses (LMgFR/ $R-D$ DIFR) was higher than 4, which is the value of the ratio between the maxDIFR and the DIFR produced by the fibre at 75% run-down.

Contractile apparatus experiments

The Ca^{2+} -sensitivity of the contractile apparatus in skinned fibres from 4- and 10-wk rats was determined using a procedure similar to that employed previously by Bortolotto *et al.* (1999 & 2000). It should be noted that, to be consistent with fibres used in the E-C coupling experiments (*Mounting the skinned muscle fibre preparation to the force measuring system* in Chapter 2, page 62), the fibres used in these experiments were stretched to 120% of resting length. To obtain solutions with the required free $[Ca^{2+}]$ (pCa) values, the Relaxing (high EGTA) and Maximum Ca^{2+}

Activation (high Ca-EGTA) solutions were mixed together in specific ratios. Prior to mixing these two solutions, the free [EGTA] of the heavily buffered high Ca-EGTA solution was determined using the pH titration method of Moisescu & Pusch (1975). Specific proportions of the Maximum Ca^{2+} Activation and Relaxing solutions were then mixed together (see Table 3.1) and the free [Ca^{2+}] (pCa) of these new solutions was determined using the following equation:

$$[\text{Ca}^{2+}]_{\text{free}} = [\text{CaEGTA}]/[\text{EGTA}]_{\text{free}} \times 1/K_{\text{app}},$$

where $[\text{CaEGTA}] = [\text{EGTA}]_{\text{total}} - [\text{EGTA}]_{\text{free}}$ and $K_{\text{app}} = 5 \times 10^6 \text{ M}^{-1}$ (Moisescu & Thieleczek, 1978; Fink *et al.*, 1986) at pH 7.1 and 1 mM free [Mg^{2+}].

As shown in the force trace of Figure 3.1, skinned fibres were exposed to a sequence of heavily buffered EGTA–CaEGTA solutions over a range of progressively higher free [Ca^{2+}] (pCa>9 to pCa<5), until the maximum Ca^{2+} -activated force was obtained. After the maximum Ca^{2+} - force was recorded, fibres were placed into the Relaxing solution.

The force produced at each [Ca^{2+}] was expressed as a percentage of the maximum Ca^{2+} -activated response and plotted as a function of pCa, using GraphPad Prism (GraphPad Software Inc., San Diego, CA, USA). Hill curves were fitted to the force–pCa data and the pCa₅₀ (pCa giving half-maximum force), pCa₁₀ value (pCa giving 10% maximum force) and Hill co-efficient (steepness of the force-pCa curve) were determined.

Table 3.1 Volumes of Relaxing (high EGTA) and Maximum Ca^{2+} -activation (high Ca-EGTA) solutions required to obtain Ca^{2+} -activation solutions used in force/pCa experiments.

Free Ca^{2+} (pCa)	Volume of Relaxing solution (high EGTA)	Volume of Maximum Ca^{2+} Activation solution (high Ca-EGTA)	Relaxing to Maximum Ca^{2+} Activation solution ratio
> 9.0	2.00 ml	0.0 ml	1:0
8.0	1.99 ml	0.01 ml	199:1
7.0	1.33 ml	0.67 ml	2:1
6.7	1.00 ml	1.00 ml	1:1
6.39	0.67 ml	1.33 ml	1:2
6.22	0.50 ml	1.50 ml	1:3
6.10	0.40 ml	1.60 ml	1:4
6.01	0.33 ml	1.66 ml	1:5
5.87	0.29 ml	1.71 ml	1:7
5.77	0.22 ml	1.78 ml	1:9
4.5	0.0 ml	2.00 ml	0:1

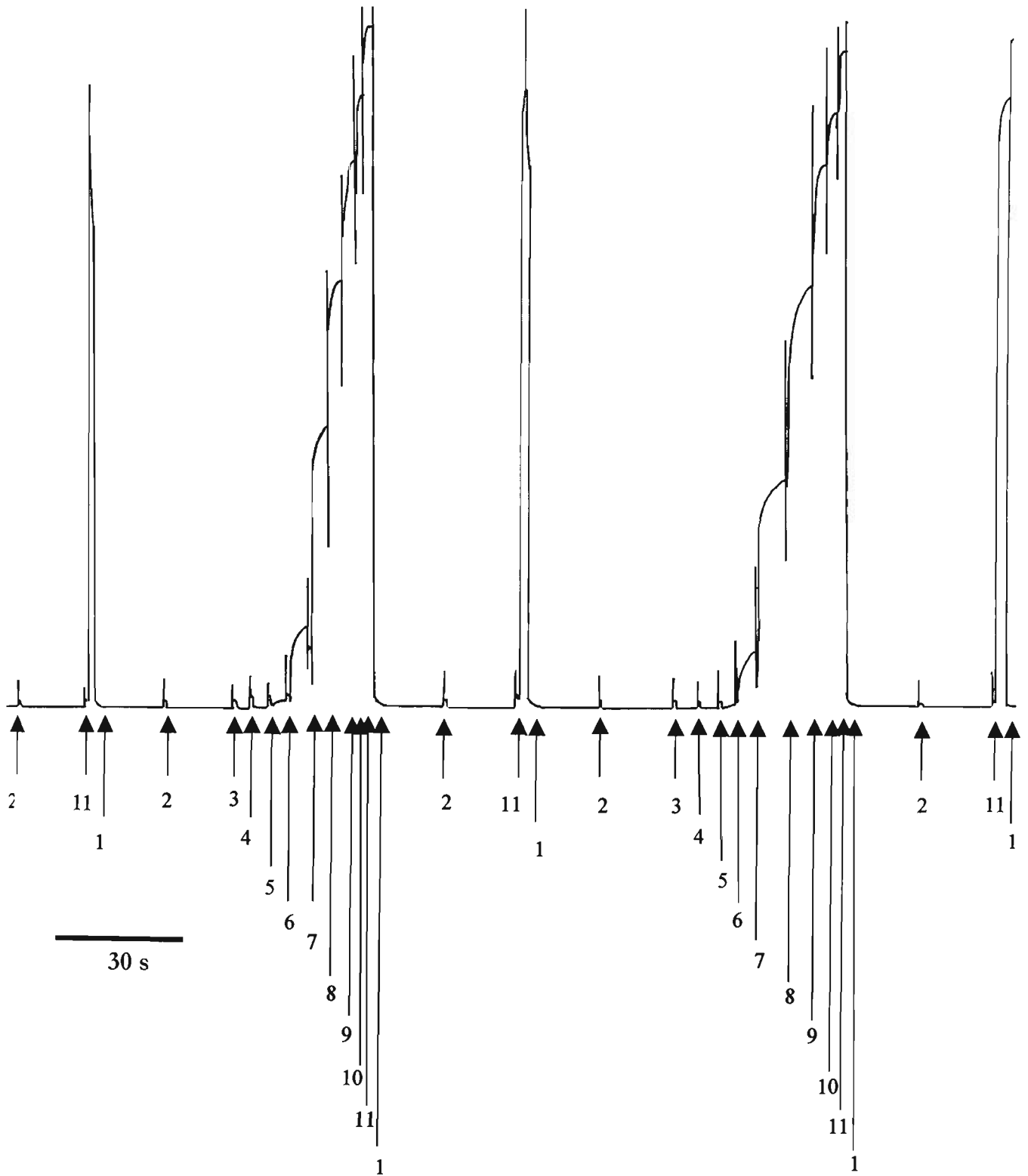


Figure 3.1. Representative chart recording of force response by a 10 week rat EDL fibre exposed to solutions with varying free Ca^{2+} concentrations.

Solutions 1-11 represent pCa values of: 9.0 (1), 8.0 (2), 7.0 (3), 6.7 (4), 6.39 (5), 6.22 (6), 6.10 (7), 6.01 (8), 5.87 (9), 5.77 (10) and 4.5 (11).

Data analyses and statistics

In the text, mean values are given \pm S.E.M. and unless indicated otherwise all statistical analyses were performed using a one-way ANOVA with a Bonferroni post-test. Statistical significance was accepted as $P < 0.05$. Sample size is denoted by n .

Results

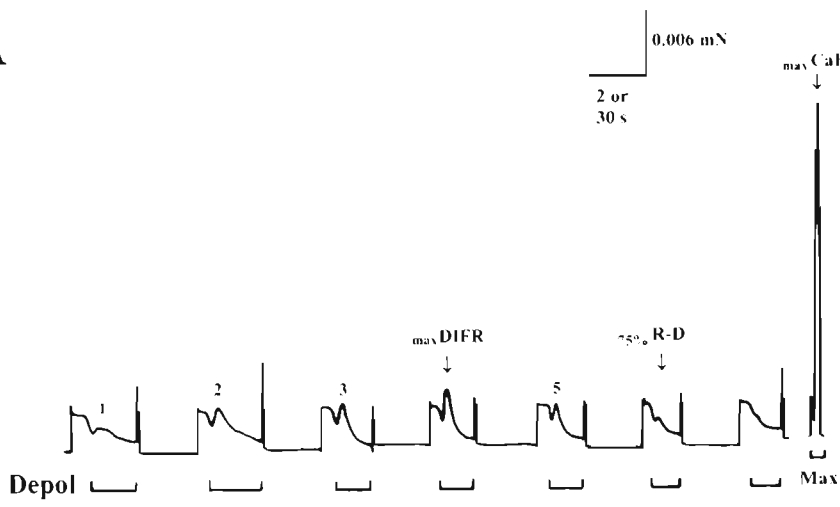
Age related differences in E-C coupling characteristics

Figure 3.2 shows a series of depolarization-induced force responses (DIFRs) produced by mechanically skinned EDL fibres from 4-wk (Figure. 3.2A), 10-wk (Figure. 3.2B), and 21-wk (Figure. 3.2C) rats. During the course of the experiments undertaken in this study, it was apparent that some fibres gave no detectable force in response to T-system depolarization within the first few depolarization challenges. The proportion of fibres that produced no force (*nF* fibres) was greatest in the fibre population isolated from 4-wk rats (10/30). By comparison, the proportion of *nF* fibres from 8-wk (1/26), 10-wk (1/22), 15-wk (3/26), and 21-wk (0/16) rats was substantially lower. With the ten *nF* fibres from 4-wk rats, subsequent loading of the SR with Ca^{2+} for a sufficiently long period (30 to 180 s) failed to induce any response to T-system depolarization. All *nF* fibres were excluded from data analyses.

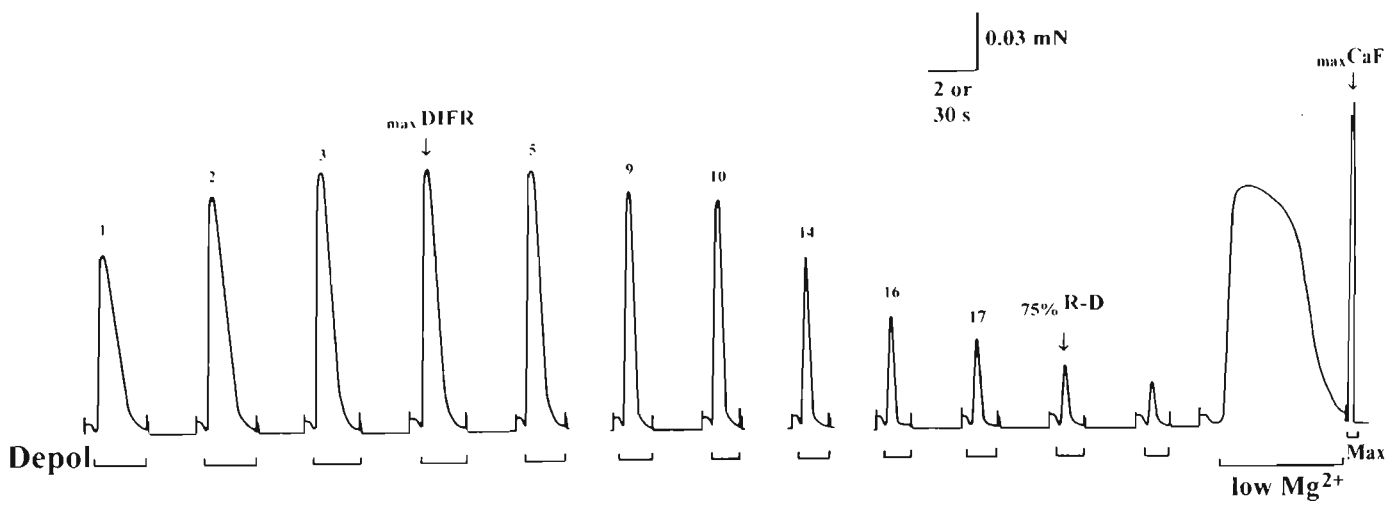
Maximum depolarization-induced force response.

As seen in the traces illustrated in Figure. 3.2, the profile of the DIFR was qualitatively similar (rapid transient type) in skinned fibres from 4-wk, 10-wk, and 21-wk rats. This was also the case for the other age groups examined in this study (8- and 15-wks) for which data are not shown. However, it is clear that the amplitude of the maxDIFR was smaller in the 4-wk fibre (Figure. 3.2A) than in the 10-wk fibre

A



B



C

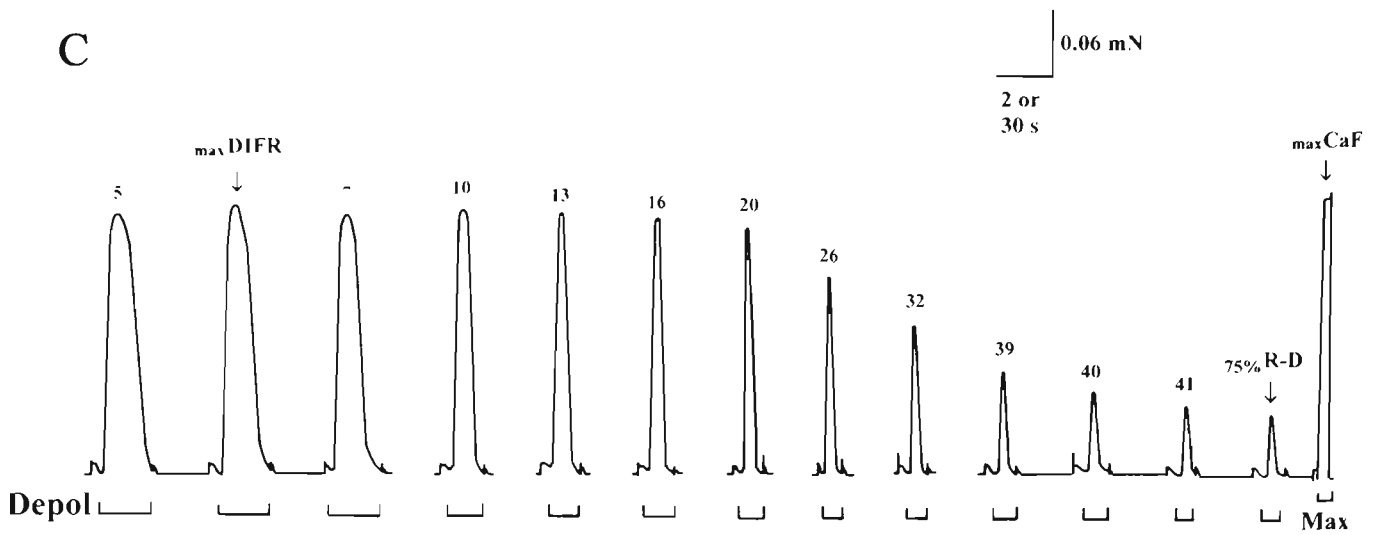


Figure 3.2 T-system depolarization-induced force responses elicited in single mechanically skinned EDL fibres from Long Evans rats of different ages.

Shown are representative chart recordings of force responses obtained in a 4-wk (A), 10-wk (B), and 21-wk (C) fibre segment. Numbers above responses to depolarization refer to response number. Brief artefacts just before and after depolarizations are related to the fibre being moved in between the solution–air interface. These artefacts are more prominent in the 4-wk fibre because the sensitivity of the recording system was increased in this fibre. maxDIFR , maximum depolarization-induced force response; $75\%R-D$, 75% run-down point (i.e. point at which the response to depolarization has decreased by 75% of the maxDIFR) (see text). Maximum Ca^{2+} -activated force (maxCaF) was determined by exposure to a solution with 50 mM CaEGTA (pCa 4.5) ('Max'). Time scale: 2 s during depolarizations and low (0.015 mM) Mg^{2+} exposure, and 30 s elsewhere.

(Figure 3.2B). Indeed, when this response was normalised to its respective maximum Ca^{2+} -activated response (labelled maxCaF in Figure. 3.2), the amplitude of the maxDIFR in the 4-wk fibre was 13% compared to 85% in the 10-wk fibre (compare $\text{maxDIFR}/\text{maxCaF}$ in Figure. 3.2A & B). The summarized data presented in Figure. 3.3A show significant differences with respect to this E-C coupling parameter between fibres from 4-wk rats and fibres from all the other age groups investigated, as well as significant differences between fibres from 8-wk rats and all other age groups. In contrast, there were no significant differences in the maxDIFR between fibres isolated from 10-wk, 15-wk, and 21-wk rats (Figure. 3.3A).

The significant difference found with respect to the maxDIFR , between fibres isolated from 4-wk rats and fibres isolated from 10- to 21-wk rats could be related to differences in the Ca^{2+} -sensitivity of contractile apparatus between these age groups. To investigate this possibility, the Ca^{2+} -activation properties of the contractile apparatus in 10-wk fibres (chosen because the maxDIFR for fibres from this group was not significantly different from that of fibres for 15- and 21-wk groups) was compared with fibres from 4-wk rats. These experiments (see Figure 3.4) showed that 10-wk fibres ($n=21$) had a significantly lower sensitivity to Ca^{2+} as compared to 4-wk fibres ($n=16$), with the pCa_{50} being on average lower by 0.07 ± 0.01 pCa units in 10-wk fibres (mean pCa_{50} in 10-wk and 4-wk fibres: 6.06 ± 0.01 and 6.13 ± 0.01 , respectively; $P < 0.05$, unpaired t-test). A similar result was also observed with the pCa_{10} values, where the mean pCa_{10} in 10-wk and 4-wk fibres was 6.28 ± 0.01 and 6.33 ± 0.01 , respectively (mean change in pCa_{10} : 0.05 ± 0.01 ; $P < 0.05$, unpaired t-test). No significant differences were observed between these two age groups with respect to

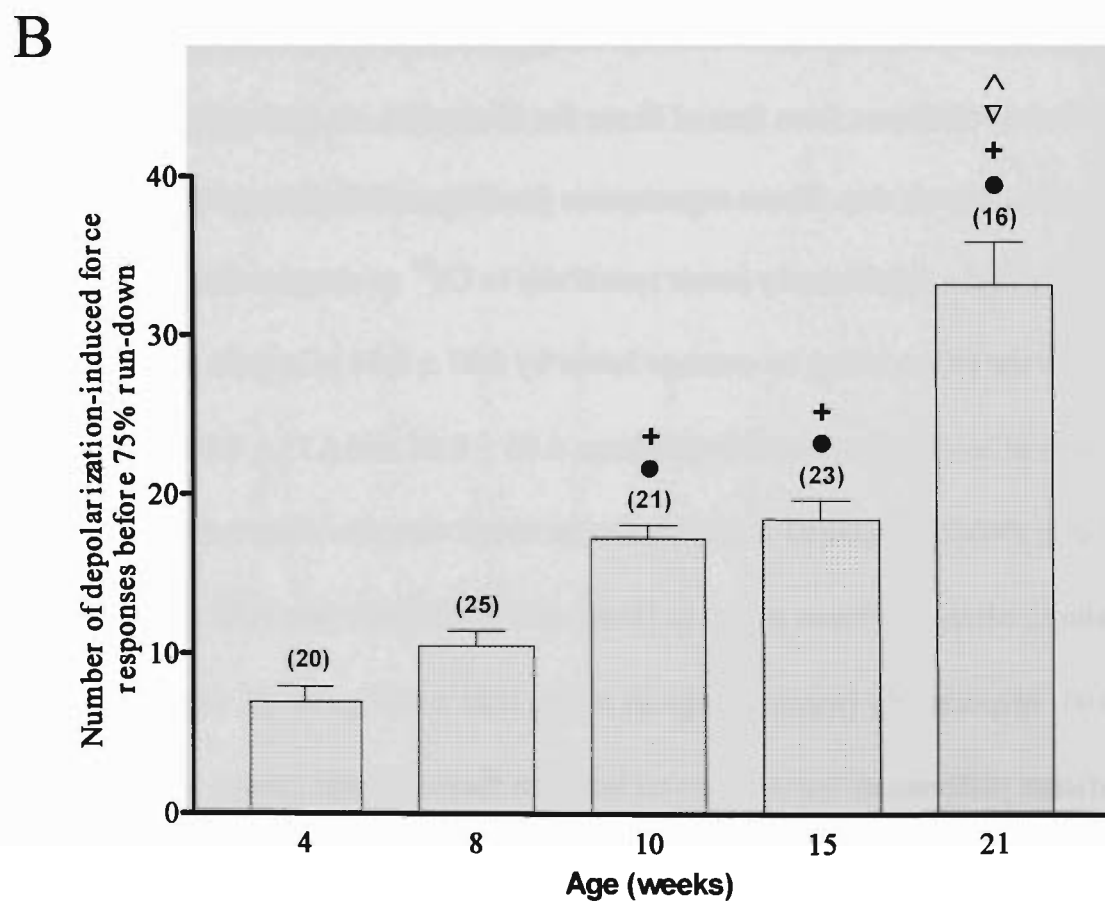
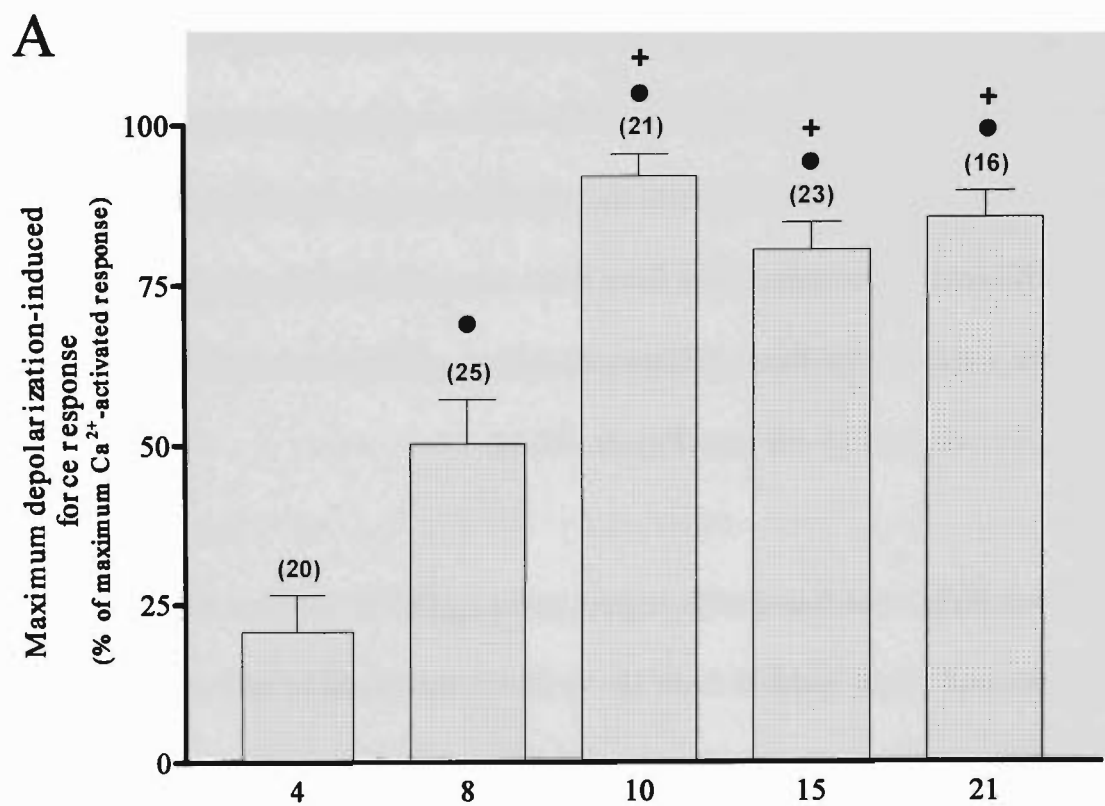


Figure 3.3 Summarized data for (A) the maximum depolarization-induced force response and (B) the number of responses to depolarization obtained before 75% run-down in skinned fibres from 4-wk, 8-wk, 10-wk, 15-wk, and 21-wk Long Evans rats. Bars show mean \pm S.E.M in 'n' fibres. Symbols indicate \bullet significantly different ($P < 0.05$) from 4-wks, $+$ significantly different ($P < 0.05$) from 8-wks, ∇ significantly different ($P < 0.05$) from 10-wks, \wedge significantly different ($P < 0.05$) from 15-wks, as determined by an ANOVA with Bonferroni post-test.

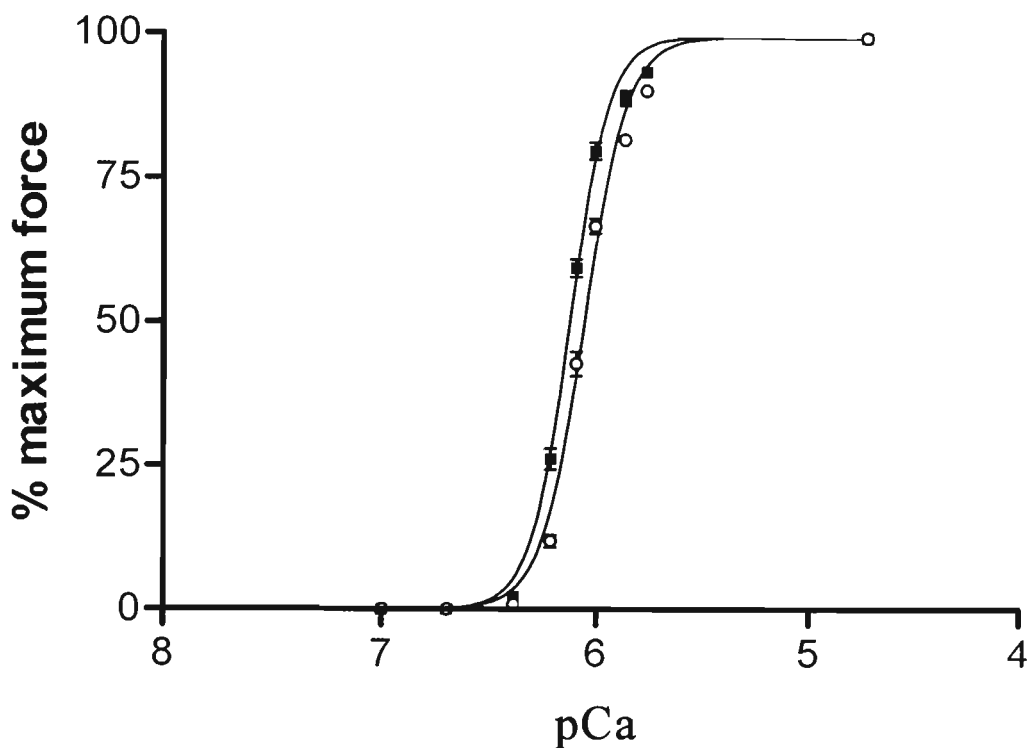


Figure 3.4. Averaged force/pCa curves for 4 week (■) and 10 week (○) EDL fibres.

All fibres were stretched to 120% of resting length. The mean pCa_{50} in 4-wk and 10-wk fibres: 6.13 ± 0.01 ($n = 16$) and 6.06 ± 0.01 ($n = 21$), respectively; $P < 0.05$, unpaired t-test). The mean pCa_{10} in 4-wk and 10-wk fibres was 6.33 ± 0.01 ($n = 16$) and 6.28 ± 0.01 ($n = 21$), respectively (mean change in pCa_{10} : 0.05 ± 0.01 ; $P < 0.05$, unpaired t-test). There was no significant difference in the Hill coefficient (4.87 ± 0.19 and 4.49 ± 0.10 for 4-wk and 10-wk fibres, respectively; $P > 0.05$, unpaired t-test) between these two age groups.

the Hill coefficient (4.49 ± 0.10 and 4.87 ± 0.19 for 10-wk and 4-wk fibres, respectively; $P > 0.05$, unpaired t-test). Thus, differences in Ca^{2+} - sensitivity of the contractile apparatus do not explain why fibres from 4-wk rats developed smaller DIFRs than fibres from rats aged 10-21 wk.

Closer inspection of the trace illustrated in Figure. 3.2B shows that the amplitude of the DIFR progressively increased before it reached a steady level. This phenomenon, referred to as 'work-up', is commonly seen in mechanically skinned fibre preparations where T-system depolarization is achieved by Na^+ substitution (Coonan & Lamb, 1998). As shown in Table 3.2, it took on average ~ 3 depolarizations before the maxDIFR was elicited in 4- and 8-wk fibres and on average ~ 6 depolarizations before this response was reached in 21-wk fibres. However, statistical analysis indicated that the longer 'work-up' period observed in fibres from 21-wk rats was not significantly different from that observed in the other fibre groups, with the exception of the 8-wk fibres.

75% Run-down.

The three representative traces illustrated in Figure. 3.2 of single skinned fibres from a 4-wk, 10-wk, and 21-wk rat, also reveal age related differences in the $75\% \mathbf{R-D}$ parameter. Only 5 responses to depolarization were elicited before 75% run-down in the 4-wk fibre shown in Figure. 3.2A, while a substantially greater number of responses could be obtained in the 10- and 21-wk fibres (17 and 41 responses, respectively) shown in Figure. 3.2 B & C.

The summarized data presented in Figure 3.3B show that significantly more depolarization-induced responses could be obtained before $75\%R-D$ in fibres from 10-wk rats as compared to fibres from 4-wk rats, and in fibres from 21-wk rats as compared to fibres from 10-wk rats (mean number of responses before $75\%R-D$: 7.0 ± 1.0 , 17.2 ± 0.81 and 33.1 ± 2.7 for 4-wk, 10-wk, and 21-wk fibres, respectively).

As explained in the Materials and Methods, the SR in a run-down fibre was deemed to be functionally competent if the ratio of the force response developed in the low Mg^{2+} solution and the depolarization-induced force response produced by the fibre preceding its exposure to low Mg^{2+} was ≥ 4 . The mean values for this ratio were 36.0 ± 7.9 (4-wk, n=12), 16.5 ± 4.4 (8-wk, n=24), 8.1 ± 0.8 (10-wk, n=19), 5.3 ± 0.5 (15-wk, n=22), and 6.9 ± 0.9 (21-wk, n=10). Based on these data, it is reasonable to suggest that the lower responsiveness to T-system depolarization observed in 4 and 8 wk fibres from the age study was more likely to be related to differences in the T-system and/or coupling mechanism than to SR dysfunction.

The summarized data of fibre cross-sectional area for the age groups investigated in this study are summarized in Table 3.2. The cross-sectional area of skinned fibres isolated from 10-wk rats was significantly larger than the cross-sectional area of skinned fibres isolated from 4-wk rats. Furthermore, the cross-sectional area of 21-wk skinned fibres was significantly greater than that for skinned fibres of all the other age groups examined in this study (i.e. 4-wks, 8-wks, 10-wks, and 15-wks). Because fibres of 21-wk rats also performed significantly better with respect to the $75\%R-D$ parameter than fibres of all the other age groups examined (see above & Figure 3.3B), the

Table 3.2 Mean summarized data for E-C coupling (and other) parameters examined in skinned fibres of different aged Long Evans rats.

PARAMETER	4-wks (n = 20)	8-wks (n = 25)	10-wks (n = 21)	15-wks (n = 23)	21-wks (n = 16)
<u>work up</u>					
mean \pm S.E.M. (range)	3.4 \pm 0.4 (1 - 8)	3.0 \pm 0.3 (1 - 6)	3.8 \pm 0.5 (1 - 9)	4.7 \pm 0.7 (1 - 12)	5.8 \pm 1.2 [†] (1 - 21)
<u>cross-sectional area</u> (μm^2)					
mean \pm S.E.M.	409 \pm 27	663 \pm 37 [*]	1097 \pm 90 ^{*†}	931 \pm 44 ^{*†}	1401 \pm 102 ^{*†∇}
<u>#DIFR_{80-100%}</u> mean \pm S.E.M. (range)	2.2 \pm 0.4 (1 - 8)	4.5 \pm 0.5 (1 - 10)	7.5 \pm 0.7 [*] (3 - 16)	7.1 \pm 0.8 [*] (1 - 17)	12.4 \pm 1.6 ^{*†∇} (4 - 24)

Note: Number of fibres is denoted by n. Symbols indicate that mean value is * significantly different ($P < 0.05$) from 4-wks, [†] significantly different ($P < 0.05$) from 8-wks, [∇] significantly different ($P < 0.05$) from 10-wks, and [^] significantly different ($P < 0.05$) from 15-wks, as determined by an ANOVA with Bonferroni post-test. Note: #DIFR_{80-100%} parameter refers to the stability of the responsiveness to T-system depolarization (see text).

relationship between fibre cross-sectional area and fibre run-down was investigated. Figure 3.5 shows a significant correlation ($r^2 = 0.51$, $P < 0.0001$) between fibre cross-sectional area and the number of responses to depolarization attained prior to 75%R-D, when the data for fibres from all age groups were pooled together.

Stability of responsiveness to T-system depolarization.

As part of the investigation into age related differences in E-C coupling characteristics, the stability of the responsiveness to T-system depolarization expressed as the number of consecutive DIFRs within the range 80 to 100% of the maxDIFR ($\#DIFR_{80-100\%}$) was examined. The summarized data presented in Table 3.2 show that fibres isolated from 21-wk rats were able to generate the greatest number of consecutive responses to depolarization that were larger than 80% of the maximum depolarization-induced response, and that there were significant differences with respect to the $\#DIFR_{80-100\%}$ parameter between fibres from 21-wk rats and fibres from all the other age groups examined (4, 8, 10 and 15-wks). Significant differences with respect to this parameter were also observed between both 4 and 10-wk fibres and 4 and 15-wk fibres (Table 3.2).

Discussion

Here, it is reported for the first time that the responsiveness of mechanically skinned fibre preparations from rat EDL muscle to T-system depolarization varies with the developmental age of the rat within the range commonly regarded as the 'adult' stage. In agreement with previous findings summarized in Table 1.2 (Chapter 1, page 40), the performance of fibres from rats of a given age is not consistent across a number of E-C coupling parameters, with fibres of a given age group performing

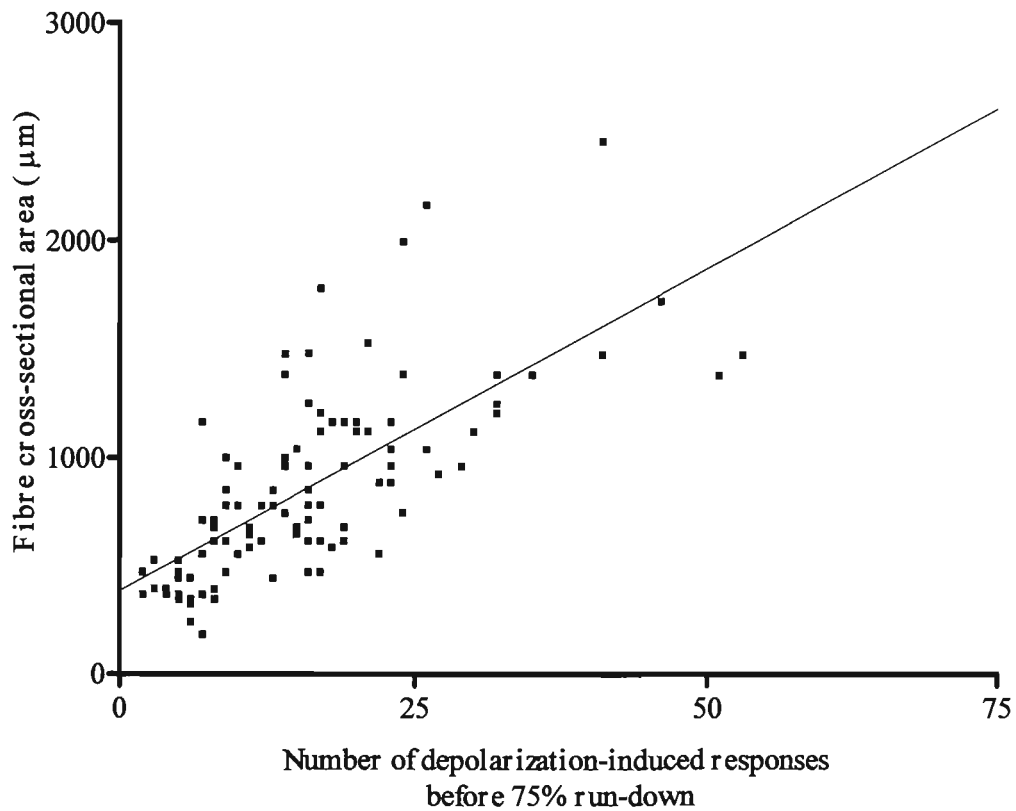


Figure 3.5 Correlation between fibre cross-sectional area and the number of depolarization-induced force responses obtained before 75% run-down.

The data from 4-wk, 8-wk, 10-wk, 15-wk, and 21-wk fibres were plotted together regardless of age. Coefficient of determination (r^2) = 0.51.

well with respect to some (e.g. maximum depolarization-induced force response) but not other (e.g. 75% run-down) parameters.

Age related differences in E-C coupling characteristics

Maximum depolarization-induced force response

In this study, the amplitude of the maxDIFR produced by skinned fibres was normalised to the respective maxCaF response. This excluded the possibility that the differences observed in maxDIFR between age groups were due to potential differences in the force per cross sectional area developed by these fibres (an issue not specifically investigated as part of this study). As explained in section *Parameters describing skinned fibre responsiveness to T-system depolarization* (Chapter 2, page 67), the maxDIFR is determined by the amount of Ca^{2+} released from and sequestered by the SR (i.e. the functional competence of the SR) and by the sensitivity to Ca^{2+} of the contractile apparatus. In turn, Ca^{2+} release from the SR is affected by events occurring at the triad such as depolarization/repolarization of the T-system and signal transmission between functionally coupled voltage-sensors and Ca^{2+} release channels.

In this study it was found that the maxDIFR in 4-wk (and 8-wk) fibres was significantly lower than that in 10-wk, 15-wk, and 21-wk fibres (Figure. 3.3A), which could suggest that the contractile apparatus in fibres from the younger rats was less sensitive to Ca^{2+} (and/or that less SR Ca^{2+} was released in these fibres). The data showed that the sensitivity of the contractile apparatus to Ca^{2+} was actually higher in 4-wk fibres as compared to 10-wk fibres (see Results), indicating that the smaller DIFRs developed by fibres from the youngest rats are more likely to be related to less SR Ca^{2+} release.

As reviewed in Chapter 1 (see *Aspects of postnatal development of rat skeletal muscle relevant to the E-C-R cycle*, page 32), it appears that by ~4-6 wks postnatal, the organization of the T-system and SR and the amount/structure of the major proteins involved in Ca^{2+} release from the SR (i.e. voltage-sensors and Ca^{2+} release channels) are essentially the same as those in adult muscle (Chaplin *et al.*, 1970; Edge, 1970; Kyselovic *et al.*, 1994; Pereon *et al.*, 1993). In other words, the results of these studies suggest that the components involved in E-C coupling, which are responsible for SR Ca^{2+} release, should be functionally competent by 4-6 wks of age. This is not confirmed by the results presented here, which show that the maxDIFR (a functional parameter of E-C coupling) was much lower in 4- and 8-wk fibres than that in 10-wk, 15-wk, and 21-wk fibres. The poor performance of the 4- and 8-wk fibres may have been related to (i) ineffective depolarization/repolarization of the T-system (compounded by differences in T-system membrane potential), (ii) ineffective signal transmission from the voltage-sensors to the Ca^{2+} release channels (due for example to a smaller number of functionally coupled voltage-sensor/ Ca^{2+} release channel units), and (iii) differences in the amount of Ca^{2+} released from the SR and the events involved thereafter. Regarding the first possibility, it is noteworthy that according to Conte Camerino *et al.* (1989) the resting E_m may not reach 'adult' values until 10 wk postnatal (see Table 1.2 in Chapter 1, page 40). Differences in the ability of the T-system membrane to seal (following mechanical skinning) and/or differences in the lipid composition of the T-system membrane cannot be ruled out as whole or partial contributors to the disparity in the maximum depolarization-induced response. Such differences may also account for the relatively large number of nF fibres (10/30) obtained from 4-wk rats compared to that obtained from each of the other age groups investigated (see Results).

Run-down

As already mentioned in Chapter 1 (see *Parameters describing skinned fibre responsiveness to T-system depolarization*, page 67), the exact cause of the run-down phenomenon observed in mechanically skinned fibre preparations, in which the contractile response is induced by T-system depolarization, is currently not well understood. It has been suggested that this phenomenon is related to the use-dependent loss of some factor (Lamb and Stephenson, 1990a). If this were the case, one might expect that the loss of such a factor would occur by diffusion and therefore that the time course of run-down (as indicated by the number of responses developed by a fibre to run-down) would be related to the cross-sectional area of the fibre. This study showed a good correlation ($r^2 = 0.51$; Figure 3.5) between the number of responses attained by a skinned fibre before $75\%R-D$ and the fibre cross-sectional area. While not directly confirming the theory of Lamb and Stephenson (1990a), our result is consistent with the hypothesis that the loss of responsiveness to T-system depolarization of the skinned fibre preparation involves a process of diffusion.

The results show that the run-down state was reached substantially faster with fibres obtained from 4-wk rats than with fibres obtained from 21-wk rats. It is worth noting that unlike maxDIFR , the values of the $75\%R-D$ parameter had not levelled off by 21wks. This result would not be surprising if fibre diameter played a major role in the $75\%R-D$ parameter because according to Alnaqeeb & Goldspink (1986) rat EDL fibres continue to increase in diameter up to the age of 27 wks. It must however be pointed out that age related difference in $75\%R-D$ found in this study can not be fully explained by developmental differences in EDL fibre diameter, given that the coefficient of

determination (r^2) for the relationship between fibre cross-sectional area and run-down was 0.51. Thus, functional differences, as well as size differences, in mechanically skinned fibre preparations may explain the age related differences in $75\%R-D$ reported here.

Methodological comments

The parameters most commonly examined so far in studies concerned with the mechanism/regulation of E-C coupling in skeletal muscle using the Lamb and Stephenson method (1990a) include the amplitude of the maximum depolarization-induced force response, and the number of responses to T-system depolarization obtained before the response declined to a given value relative to the maximum depolarization-induced response. When considering both these parameters, the best performing fibres were isolated from 21-wk rats.

In this study, a new parameter was introduced, *viz.* the number of consecutive responses with amplitudes between 80 and 100% of the maximum depolarization-induced response ($\#DIFR_{80-100\%}$). This parameter should be of particular benefit in studies where the effects of drugs or altered myoplasmic conditions on depolarization-induced force responses developed in mechanically skinned fibre preparations are examined by bracketing 'test' responses (produced in the presence of the desired drug/condition) with 'control' responses (e.g. Blazev & Lamb, 1999).

If one assumes that the minimum number of consecutive DIFRs (whose amplitudes are greater than 80% of the $\text{max}DIFR$) required for accurately determining the effect (and reversibility) of a drug on these responses is 6-7 (so that a combination of control-

test–control sequences can be carried out), then it is clear from the results obtained in this study that skinned fibres isolated from 4- or 8-wk LE rats would be inadequate. Furthermore, while it is apparent that skinned fibres isolated from 10- and 15-wk LE rats would be satisfactory for such studies (e.g. see Figure. 1 in Blazev & Lamb, 1999), it is also evident that the usefulness of these fibres would be limited in studies where a greater number of depolarization-induced force responses in the range 80-100% (of maxDIFR) was needed (e.g. see Figure. 3 in Blazev & Lamb, 1999). Therefore, skinned fibres isolated from 21-wk LE rats (where on average ~12 consecutive responses to depolarization >80% of the maxDIFR were obtained) would be the most suitable choice.

In summary, this study has shown that mechanically skinned fibres from 21wk old rats were the most responsive to T-system depolarization as indicated by the three main E-C coupling parameters examined (maxDIFR , $75\%R-D$, $\#DIFR_{80-100\%}$), while fibres from 4 wk old rats were the least responsive. By comparison, fibres from 10 wk old rats performed as well as 21 wk fibres with respect to maxDIFR but not with respect to $75\%R-D$ or $\#DIFR_{80-100\%}$.

Chapter 4

MHC-BASED FIBRE TYPE AND RESPONSIVENESS TO T-SYSTEM DEPOLARIZATION IN RAT MECHANICALLY SKINNED MUSCLE FIBRES

Introduction

In recent years, intense efforts have been directed towards the functional characterization of the contractile apparatus in single muscle fibres expressing specific MHC isoforms. These studies, in which MHC isoform analyses and determination of contractile parameters were carried out in the same fibre segment, have produced compelling evidence that the MHC isoform expressed in a single muscle fibre is a major determinant of maximum shortening velocity (Weiss *et al.*, 2001), maximum power output (Bottinelli *et al.*, 1991), optimal velocity of shortening (Bottinelli *et al.*, 1996), rate of tension development (Harridge *et al.*, 1996), rate of ATP consumption (Szentesi *et al.*, 2001), P_0/CSA (Geiger *et al.*, 2000) and stretch activation properties (Galler *et al.*, 1994). Because of the central role played by MHCs in muscle contractile performance and their relative abundance, MHC isoform expression (as detected by high resolution polyacrylamide gel electrophoresis or by immunohistochemistry) has become the method of choice for classifying skeletal muscle fibre types into distinct functional groups (for reviews see Bortolotto & Reggiani, 2002; Moss *et al.*, 1995; Stephenson, 2001).

To date, very little is known about the E-C coupling characteristics (involving the T-system and SR compartments) of different MHC-based fibre types. Qualitative molecular differences have been shown to exist between rodent EDL (containing predominantly fast fibre types) and SOL (containing predominantly slow fibre types) muscles, with varying amounts of cardiac α_{1C} -DHPR/voltage sensor isoform (Froemming *et al.*, 2000; Perea *et al.*, 1998), slow calsequestrin isoform (Damiani & Margreth, 1994) and neonatal Ca^{2+} release channel/RyR3 isoform (Bertocchini *et al.*, 1997) being found in adult SOL muscles but not in EDL. Studies using whole muscles or untyped single fibres have demonstrated functional and structural differences between rat EDL and SOL with respect to calcium transients (Delbono & Meissner, 1996; Eusebi *et al.*, 1980), DHPR/voltage sensor density (Lamb & Walsh, 1987), number of SR RyR/calcium release channels functionally coupled to T-tubular DHPR/voltage sensors (Delbono & Meissner, 1996), voltage dependence of DHPR/voltage sensor activation and inactivation (Chua & Dulhunty, 1988) and SR volume (Cullen *et al.*, 1984). Given the diversity of MHC-based fibre types that make up most commonly used mammalian skeletal muscles (including rat EDL and SOL) and the complexity of MHC isoform expression displayed by a large proportion of individual fibres (for review see Stephenson, 2001), it is clear that the methodological approaches using whole muscles or single fibres of unknown MHC composition cannot be used to answer the question of whether E-C coupling characteristics differ between MHC-based fibre types. So far there have been no studies examining the E-C coupling characteristics and MHC isoform composition in the same fibre segment.

As already stated in the Introductory chapter, currently the most efficient strategy for probing events spanning between T-system depolarization and force production in a single fibre involves the use of mechanically skinned fibre preparation and the experimental protocol for T-system system depolarization-induced activation of contraction developed by Lamb & Stephenson (1990a). Recently the Alanine-SDS PAGE method developed by Nguyen and Stephenson (1999 & 2002) was further refined to enable MHC analysis in rat single muscle fibre segments with a high degree of reproducibility. In the present study these two methods were combined to examine the E-C coupling characteristics and MHC isoform composition in single fibre segments from two predominantly fast-twitch, but functionally different muscles (EDL and the white region of sternomastoid, SM), and one predominantly slow-twitch (SOL) muscle.

Materials and methods

Animals and muscles

Based on the results of the study described in Chapter 3 the rats used in this study were aged between 20 – 21 wks. Muscle (EDL, SOL and SM) were carefully removed and handled as described in Chapter 2. The SM muscle has two distinct regions, red and white (Dulhunty & Dlutowski, 1979; Gottschall *et al.*, 1980). Both regions are considered fast twitch (Luff, 1985), but for comparison with the fast twitch fibres isolated from the white EDL muscle, single SM fibre segments were isolated from the white region only.

Mechanically skinned single fibre preparations and T-system depolarization experiments

Mechanically skinned fibre segments were prepared and their dimensions measured as described in Chapter 2. All T-system depolarization experiments were carried out at room temperature (20-25 °C) as described in Chapter 2.

Skinned fibre solutions

All solutions were as described in Chapter 2

Myosin heavy chain analysis

Sample preparation

After the completion of the depolarization-induced activation protocol, single fibre segments (volume range 1.0 - 8.8 nl) were removed from the force measuring apparatus and placed in 12 µl of solubilising buffer composed of 62.5 mM Tris, 2.3 % (w/v) SDS, 5 % (v/v) β-mercaptoethanol, 12.5 % (v/v) glycerol, 13.6 % (w/v) sucrose, 0.01 % (w/v) Bromophenol blue, 0.1 mM phenylmethylsulfonyl fluoride, 2 µM leupeptin , and 1 µM pepstatin. Fibre segments were incubated at room temperature for 24 hours and then boiled for 5 minutes and finally stored at -80°C.

Electrophoretic set up

All gels were prepared manually using 10 x 10.5 cm glass plates, 0.75 mm spacers and the SE 235 multiple gel caster (See Figure. 4.1A). The alanine SDS-PAGE protocol used in this study is a slightly modified version of the protocol developed for separating MHC isoforms expressed in toad skeletal muscle (Nguyen & Stephenson, 1999 & 2002). The

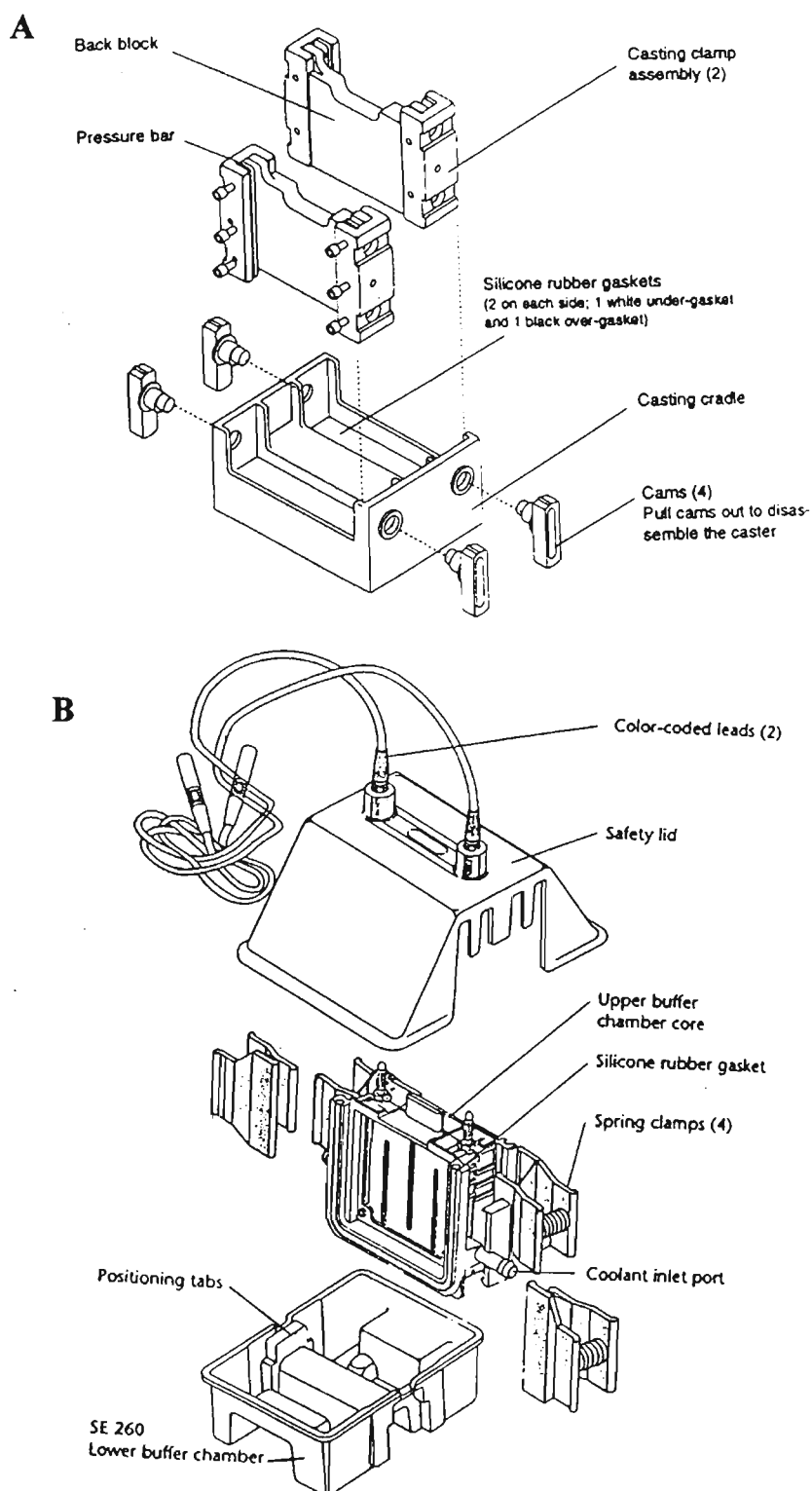


Figure 4.1. Electrophoresis equipment. **A.** Gels were prepared using the SE 235 multiple gel caster. **B.** Gels were run in the SE 260 electrophoresis setup connected to a power supply. (reproduced from Hoefer Gel Electrophoresis Unit instructions).

separating gel [total concentration of monomer (T) = 7.6 %; concentration of cross-linker relative to T (C) = 1.2 %] which contained 425 mM Tris pH 8.8, 30 % (v/v) glycerol, 75 mM alanine, 0.3 % SDS (w/v) was prepared in a glass conical flask and polymerized with 0.05 % (w/v) ammonium persulfate and 0.075 % (v/v) *N, N, N', N'*-tetramethylethylenediamine. Once poured, the gel was overlaid with running buffer (see below) and allowed to set overnight. The stacking gel (T = 4 %; C = 2.6 %) which contained 125 mM Tris pH 6.8, 40 % (v/v) glycerol, 4 mM EDTA, 0.3 % (w/v) SDS and polymerized with 0.1 % (w/v) ammonium persulfate and 0.05 % (v/v) *N, N, N', N'*-tetramethylethylenediamine, was poured and allowed to set for 2 hours with a 15-well comb inserted in the top. Once set and the comb removed, thin strips of filter paper were inserted into the wells to remove any excess unpolymerized polyacrylamide solution. After cleaning, the wells were filled with running buffer. The running buffer containing 175 mM Alanine, 25 mM Tris and 0.1 % (w/v) SDS was freshly prepared and precooled at 4 °C before use. After loading the sample into the wells, gels were mounted into the SE 260 electrophoresis setup (see Figure. 4.1B) and run for 26-27 hours at 4-6 °C at constant voltage (150 V).

Staining of polyacrylamide gels

The gels were stained with Bio-Rad Silver Stain Plus and MHC bands were analyzed using a Molecular Dynamics Personal densitometer and ImageQuaNT software (Version 4.1; Molecular Dynamics).

Statistics

All results are presented as means and standard error of the mean ($M \pm SEM$). Student's two-way t-test (GraphPad, Prism) was used for comparisons between two groups.

Significance was set at $P < 0.05$.

Results

Profiles of T-system depolarization induced force responses developed by electrophoretically typed single fibre preparations from EDL, SM and SOL

Profiles of T-system depolarization induced force responses (a qualitative descriptor of E-C coupling) developed by electrophoretically typed single fibre preparations from EDL, SM and SOL are shown in Figures 4.2, 4.3 and 4.4. A total of 58 mechanically skinned, single fibres from EDL (8), SM (18) and SOL (32) muscles were subjected to T-system depolarization by rapidly substituting K^+ with Na^+ in the Depolarizing solution. Under the conditions used in this study, the fibres produced three types of T-system depolarization-induced force responses: rapid transient responses (*rtF*) where force returned to a level equivalent to $<10\%$ of the peak within 2 -3 sec (Figure. 4.2), prolonged responses (*pF*; Figure.4.3A) where force remained higher than 10 % of the peak even when, as shown in Figure. 4.3B, the fibre was kept in the depolarizing solution for as long as 13 sec and no detectable force responses (*nF*; Figure. 4.4). Based on the profile of the maximum T-system depolarization-induced response developed by the fibre preparations examined, three groups of fibres were identified: fibres producing *rtF* responses (*rtF* fibres), fibres producing *pF* responses (*pF* fibres) and fibres that did not develop detectable force responses even after 4 – 6 successive depolarization

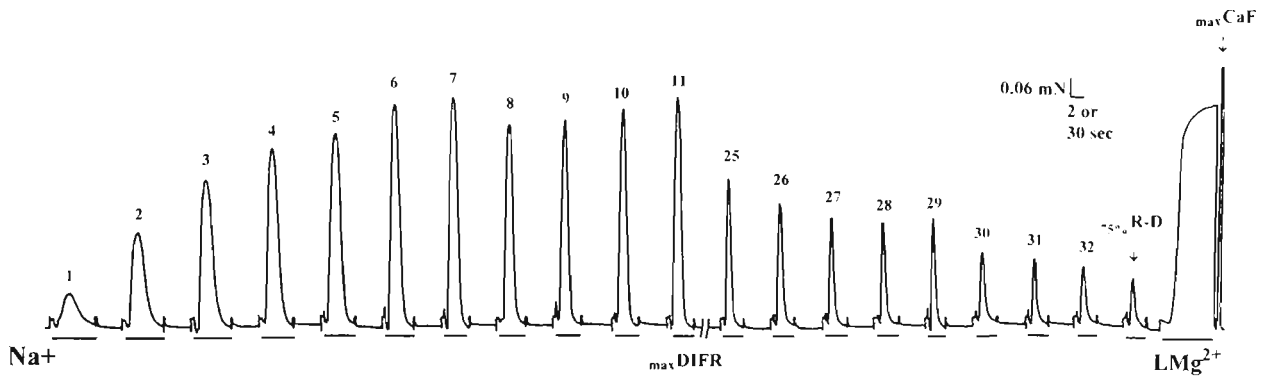
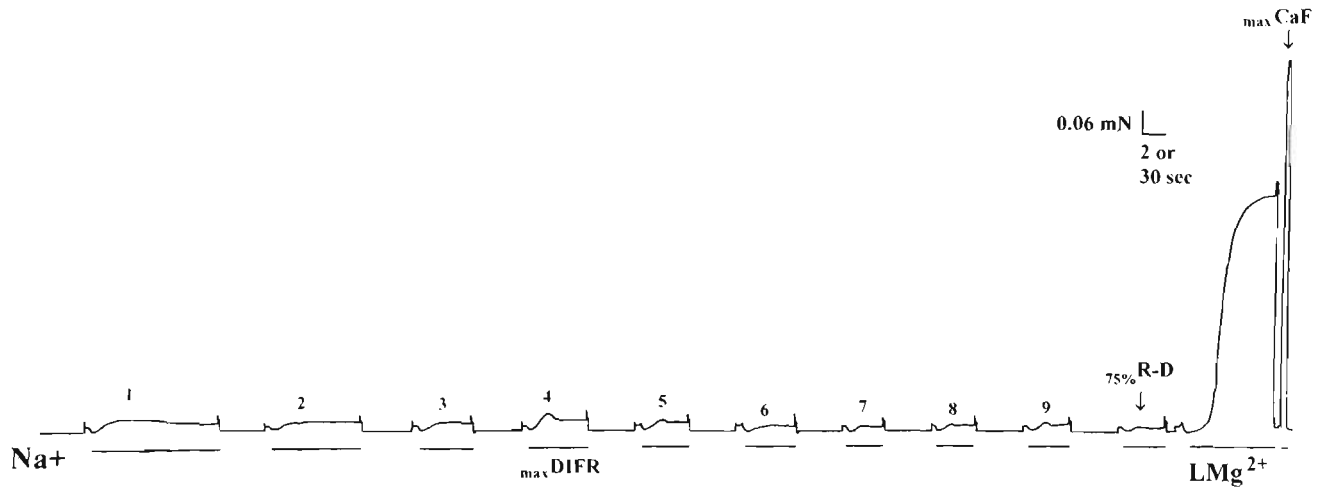


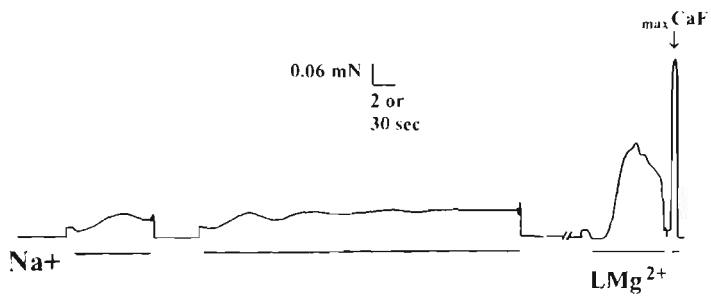
Figure. 4.2. An example of a rapid transient force (*rtF*) response developed by a type IIB EDL muscle fibre.

Time scale: 2 seconds during Na^+ depolarizations and low Mg^{2+} responses, and 30 seconds elsewhere.

A



B



C

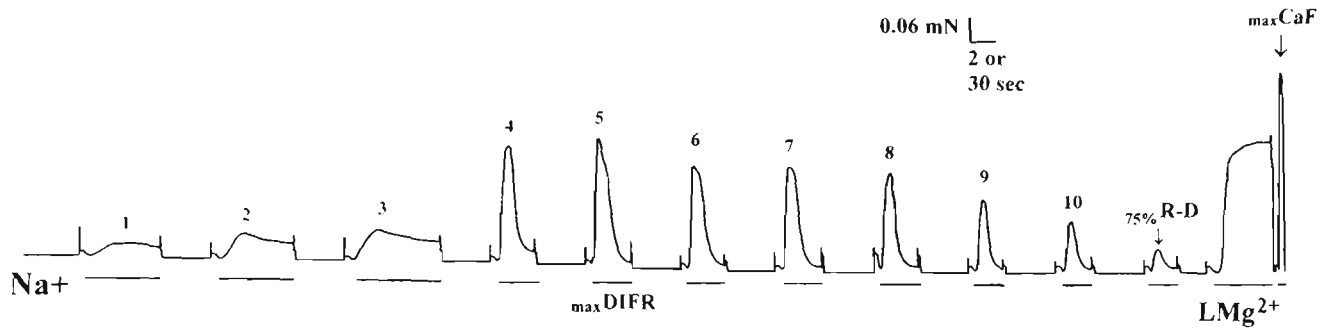


Figure. 4.3 Sample force responses produced by soleus fibres.

(A) An example of prolonged force (*pF*) responses developed by type I SOL fibres. (B) An example of a *pF* response developed by a SOL fibre subjected to prolonged (~ 13 secs) depolarization. (C) An example of the force response, developed by a SOL fibre, changing from *pF* to *rtF* during the work-up period. Time scale: 2 seconds during Na⁺ depolarizations and low Mg²⁺ responses, and 30 seconds elsewhere.

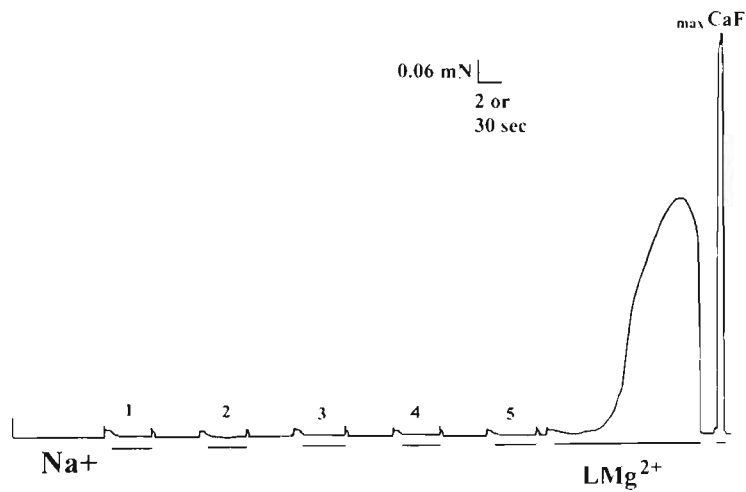


Figure. 4.4 An example of a trace from a soleus fibre that produced no force (nF) in response to T-system depolarization.

Time scale: 2 seconds during Na^+ depolarizations and low Mg^{2+} responses, and 30 seconds elsewhere.

/repolarization cycles (*nF* fibres). In this study, only fibres displaying *rtF* and *pF* responses were subjected to analyses of quantitative E-C coupling characteristics.

The type (based on MHC composition) of fibres dissected from EDL, SM and SOL muscles and the profiles of the force responses produced by T-system depolarization in these fibres are summarized in Table 4.1. Also shown in Table 4.1 are the low Mg^{2+} -induced force responses developed by *rtF* and *pF* fibres post run-down and by *nF* fibres after failing to respond to 4 - 6 successive depolarization/repolarization cycles. In Figure 4.5 are shown representative electrophoretograms of the four fibre type groups examined in this study comprising more than one fibre. It is important to note that, the number of Sol fibres displaying *pF* profiles (11) was large enough to validate their treatment as a separate group. However, only the data collected for 3 of these fibres were complete, and thus only these fibres were considered for further quantitative analyses. As shown in Figure 4.2C, three SOL fibres (two type I and one type I/IIA) initially developed *pF*-type force responses, but by the end of the work-up period these responses had changed into *rtF*-type responses.

Relationship between quantitative E-C coupling characteristics.

The two quantitative E-C coupling characteristics examined in this study are the maxDIFR and $75\%R-D$ (for full definition of these parameters see *Parameters describing skinned fibre responsiveness to T-system depolarization*, Chapter 2, page 67).

Table 4.1. Profiles of T-system depolarization induced force responses and the magnitude of low Mg^{2+} -induced force responses developed by electrophoretically typed single fibre preparations from EDL, SM and SOL.

Muscle of origin	MHC isoform based fibre type	Profile of T-system depolarization induced force response	Low Mg^{2+} induced force response (% max. Ca^{2+} -activated force)
EDL	IIB (8)	Rapid transient (8; 100%)	77.1 ± 3.3 % (8)
SM (white region)	IIB (15)	Rapid transient (13; 86.7%)	91.1 ± 2.4 % (13)
		No response (2; 13.3%)	100 % (1)
	IIB/D (3)	Rapid transient (3 ; 100%)	88.5 ± 8.2 % (3)
SOL	I (25)	Rapid transient (5; 20%)	77.8 ± 4.4 % (5)
		Prolonged (11; 44%)	72.8 ± 5.1 % (3)
		No response (9; 36%)	70.2 ± 4.7 % (9)
	I/IIA (6)	Rapid transient (4; 66.7%)	59.9 ± 6.8 % (4)
		No response (2; 33.3%)	67.7 ± 0.3 % (2)
	IIA (1)	No response (1; 100%)	59.4 % (1)

Note: The number of fibres and the proportion for each category is indicated in brackets.

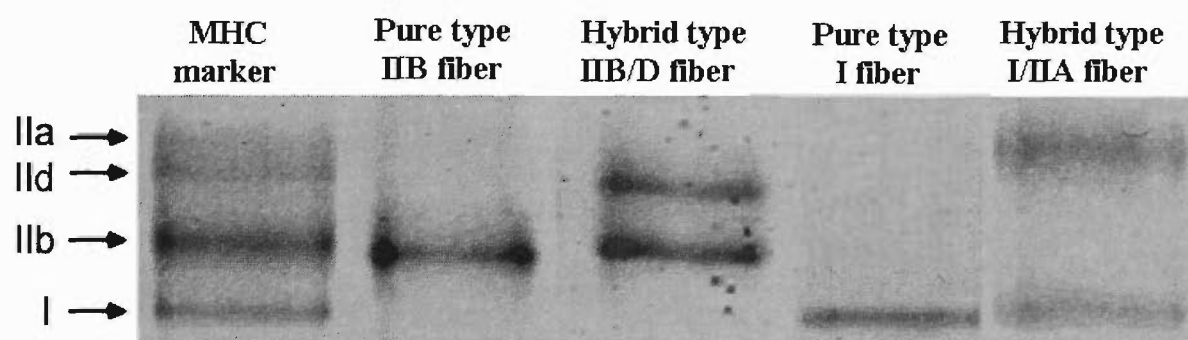


Figure. 4.5 Representative electrophoretogram of the muscle fibre types from extensor digitorum longus (EDL), sternomastoid (SM) and soleus (SOL).

MHC isoforms were identified by comparison with a marker, prepared from muscle homogenates containing all four rat hindlimb MHC isoforms.

The data obtained show (Figure. 4.6) no correlation between maxDIFR and $75\%R-D$ for pure type IIB fibres from EDL ($r^2 = 0.19$; $p = 0.2758$; $n = 8$; top panel) and SM ($r^2 = 0.20$; $p = 0.1458$; $n = 13$; middle panel), and for pure type I fibres from SOL ($r^2 = 0.02$; $p = 0.7587$; $n = 8$; bottom panel). This suggests that in these fibres the intracellular process(es) responsible for the use-dependent loss of contractile responsiveness to T-system depolarization is/are in large part independent of the factors determining the size of the maximum DIFR. In this analysis fibre type groups IIB/D (SM; $n = 3$) and I/IIA (SOL; $n = 4$) which comprised fewer than eight fibres were not included.

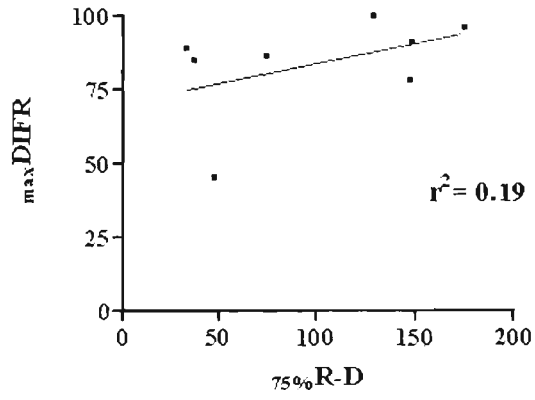
Quantitative E-C Coupling characteristics in electrophoretically typed single fibres from EDL, SM and SOL.

In this study maxDIFR and $75\%R-D$ were compared in: (i) fibres of the same type from different muscles (type IIB EDL fibres vs type IIB SM fibres), (ii) different fibre types from different muscles (type IIB EDL fibres and type IIB SM fibres vs type I SOL fibres), (iii) different fibre types (hybrid vs pure) from the same muscle (type IIB/D SM fibres vs type IIB SM fibres; type I/IIA SOL fibres vs type I SOL fibres) and (iv) fibres of the same type from the same muscle (type I SOL fibres).

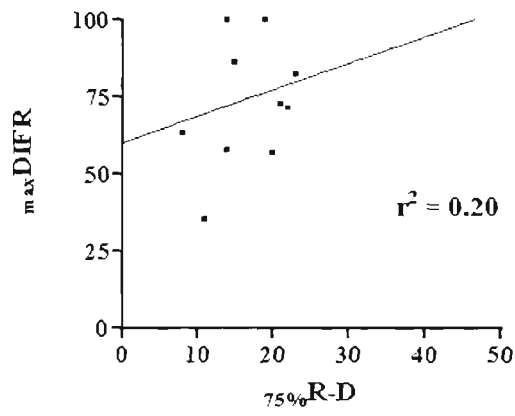
Type IIB EDL fibres vs type IIB SM fibres.

As shown in Figure 4.7A, the mean value of maxDIFR for type IIB fibres from EDL ($84.0\% \pm 6.0$) was not different from that for IIB SM fibres ($78.8\% \pm 2.9$). By comparison the mean value of $75\%R-D$ for IIB SM fibres (20.0 ± 2.9) was significantly lower than that for IIB EDL fibres (98.6 ± 20.1) (Figure. 4.7B). The inter-fibre variability (coefficient of

EDL type IIB fibers



SM type IIB fibers



SOL type I fibers

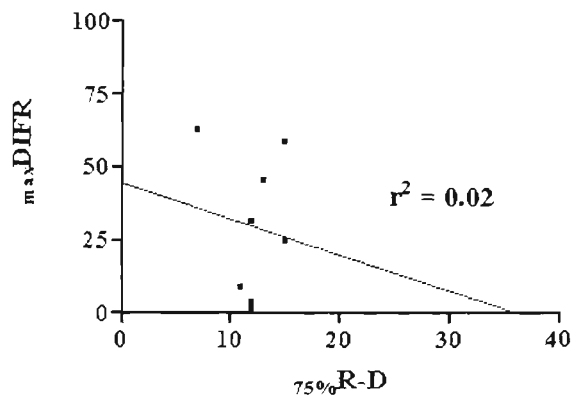


Figure. 4.6 Relationship between maxDIFR and 75 % run-down ($75\%R-D$) for type IIB EDL fibres ($r^2 = 0.19$), type IIB sternomastoid (SM) fibres ($r^2 = 0.20$), and type I SOL fibres ($r^2 = 0.02$).

variation; CV) with respect to the two E-C coupling characteristics considered was 20.2 % (maxDIFR) and 57.6 % ($75\%R-D$) for IIB fibres from EDL muscle and 26.7 % (maxDIFR) and 53.5 % ($75\%R-D$) for IIB fibres from SM muscle.

Type IIB EDL and type IIB SM fibres vs Type I SOL fibres.

Figure 4.7 also shows maxDIFR (Figure. 4.7A) and $75\%R-D$ (Figure. 4.7B) values for type I SOL fibres. These fibres displayed significantly lower values than pure type IIB EDL fibres for both maxDIFR (Figure. 4.7A) and $75\%R-D$ (Figure. 4.7B). As seen in Figure.4.7A, pure type I SOL fibres produced also significantly lower maximum depolarization-induced force responses (Figure. 4.7A) than pure type IIB SM fibres. However, while the number of responses to 75 % run-down developed by type I SOL fibres was lower (1.7 times) than that of IIB SM fibres, this difference just failed to reach statistical significance ($P = 0.0529$) (Figure. 4.7B). The CV for the two E-C coupling characteristics in SOL fibres was 81.2 % (for maxDIFR) and 20.7 % (for $75\%R-D$).

Type IIB/D SM fibres vs type IIB SM fibres; type I/IIA SOL fibres vs type I SOL fibres.

A comparison of the small group ($n = 3$) of hybrid IIB/D SM fibres with the pure type IIB SM fibres ($n = 13$) showed no significant difference with respect to either maxDIFR (78.8 ± 5.8 vs 95.1 ± 3.9) or $75\%R-D$ (20.0 ± 2.9 vs 26.0 ± 8.1). Taken together with the data presented in the previous section this finding could indicate that, under the conditions used in this study, mechanically skinned rat muscle fibres containing type II MHC isoforms are more responsive to T-system depolarization than fibres expressing MHCI isoform. Contrary to this conclusion, the four I/IIA hybrid SOL fibres examined here, all

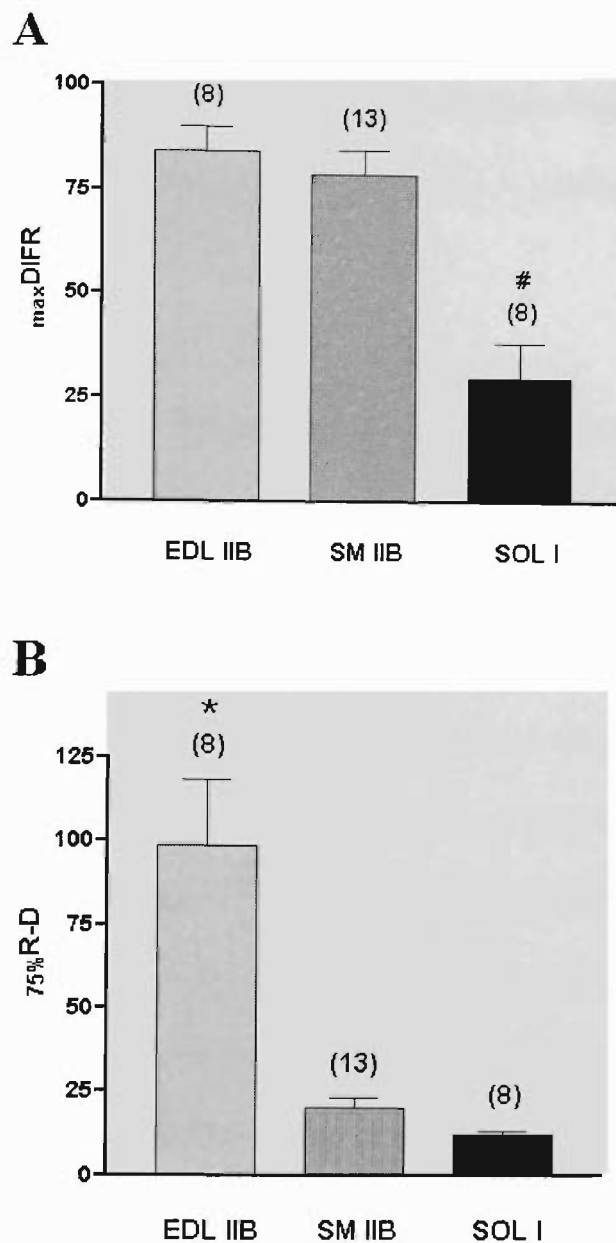


Figure. 4.7 (A) The amplitude of the maximum depolarization induced force response (max DIFR ; expressed as a % of the maximum Ca^{2+} activated force) for type IIB EDL, type IIB sternomastoid (SM) and type I SOL mechanically skinned muscle fibres. # significantly different from EDL and SM fibres ($P < 0.001$). **(B)** The number of depolarization induced force responses to 75 % run-down ($75\% \text{R-D}$) in type IIB EDL, type IIB sternomastoid (SM) and type I SOL mechanically skinned muscle fibres. * significantly different from SM ($p < 0.01$) and SOL ($p < 0.001$).

of which contained a larger proportion (mean = 72.5 %) of type IIa MHC isoforms were not significantly different from the pure type I SOL fibres (n = 8) in regards to either maxDIFR (23.1 % \pm 12.8 vs 29.8 % \pm 8.5) or $75\%R-D$ (10.3 \pm 0.6 vs 12.1 \pm 0.9).

Type I SOL fibres.

This analysis was applied to five pure type I SOL fibres producing rapid transient force responses and three fibres producing prolonged responses to T-system depolarization. A comparison of the E-C coupling characteristics in the two groups of type I SOL fibres showed that *rtF* fibres did not differ significantly from the *pF* fibres with respect to either maxDIFR (34.0 % \pm 8.5 vs 22.9 % \pm 19.9) or $75\%R-D$ (13.2 \pm 0.8 vs 10.3 \pm 1.7). To determine whether the prolonged elevated force responses developed by the *pF* fibres were artifacts due to contaminating Ca^{2+} in the depolarizing solution that would directly activate the contractile apparatus, *pF* fibres were incubated in a 2 % Triton/ K^+ -HDTA solution (to disrupt the t-tubular and SR membrane systems and abolish E-C coupling) for 10 mins after obtaining maximum Ca^{2+} activated force, washed in a Triton free K^+ -HDTA solution and then exposed to the depolarizing solution. Under these conditions, no force was developed by any of the *pF* fibres indicating that contaminating Ca^{2+} was not responsible for the prolonged profile of the force responses (data not shown).

Discussion

This is the first systematic investigation, at a single fibre level, of the relationship between functional parameters of the T-system and SR compartments and MHC-based fibre type in mammalian skeletal muscle. More specifically, this study was undertaken to

address the question of whether E-C coupling characteristics, measured in a mechanically skinned fibre preparation, are correlated to the MHC isoform(s) expressed in the same fibre segment. The experimental strategy involved the use of single muscle fibres from one predominantly slow-twitch (SOL) and two predominantly fast-twitch, but functionally distinct, muscles (EDL and white region of SM) of the adult rat.

maxDIFR and MHC-based fibre type

The maxDIFR values found in the present study for mechanically skinned IIB fibres from rat EDL muscle relative to maximum Ca^{2+} activated force (84.0 %) are similar to those reported for rat EDL fibres in previous investigations (70 - 90 %) using the same kind of preparation and experimental protocol (e.g. Lamb & Stephenson, 1991). In the present study, maxDIFR was also determined in fast-twitch fibre preparations from the white region of rat SM (Luff, 1985), a predominantly fast-twitch skeletal muscle not used in previous investigations of E-C coupling processes in mechanically skinned fibre segments. Interestingly, under the same conditions of T-system depolarization, IIB SM fibres also produced high force responses (78.8 %) that were not statistically different from IIB EDL fibres. While the membrane potential was not measured in any of the single fibres examined in this study, the relatively large depolarization induced force responses (compared to maxCaF) elicited in EDL and SM type IIB fibres suggest that in these preparations rapid replacement of K^+ with Na^+ achieved near maximal depolarization of the T-system membrane (Lamb & Stephenson, 1990a).

Slow-twitch fibres are known to be more sensitive than fast-twitch fibres to membrane depolarization (Dulhunty & Gage, 1983), and to have a higher SR luminal $[Ca^{2+}]$ (Fryer & Stephenson, 1996). Furthermore, the contractile apparatus in slow-twitch fibres is more sensitive to activating levels of Ca^{2+} than that in fast-twitch fibres (Stephenson & Williams, 1981). In spite of these factors which favour the production of force, mechanically skinned pure type I slow-twitch SOL fibres gave consistently smaller responses (29.8 ± 8.5 % of $_{max}CaF$, $n = 8$) to t-tubule membrane depolarization than the type IIB fast-twitch fibres from EDL and SM. This result is in agreement with the preliminary data of Stephenson *et al.* (1998) and with two studies in which mechanically skinned rat soleus fibres were used to investigate the effects of clenbuterol (Bakker *et al.*, 1998) and hydrogen peroxide (Plant *et al.*, 2002) on E-C coupling parameters. The value found in the present study for the $_{max}DIFR$ of SOL fibres (29.8 %) is lower than that reported by Plant *et al.* (47 ± 5 %, $n = 5$) (Plant *et al.*, 2002) but higher than that reported by Stephenson *et al.* (10 ± 4.5 %, $n = 8$) (1998), while Bakker *et al.* (1998) did not report the relative size of the SOL force responses.

The smaller responses produced by the type I slow-twitch fibres to T-system depolarization could be partly explained by the lower proportion of DHPRs functionally coupled to SR Ca^{2+} release channels (resulting in less Ca^{2+} released upon depolarization; Delbono & Meissner, 1996) and by the slower rate of Ca^{2+} release (Eusebi *et al.*, 1980) previously reported for SOL fibres. Other potential contributors include incomplete sealing of the t-tubules post-skinning and ineffective depolarization/repolarization of the T-system. From the data obtained from an extensive series of experiments, performed on

skinned fibre preparations from toad and rat in which fluorescent dyes were trapped within the T-system (Launikonis & Stephenson, 2002, and *personal communication*), Launikonis & Stephenson concluded that in all fibres (both fast and slow-twitch) mechanically skinned by the procedure used in this study, the T-system is invariably and uniformly sealed. This finding supports the possibility that, under the conditions used in this study, T-system depolarization and/or repolarization in slow-twitch type I fibres is less effective than in fast-twitch IIB fibres. This may be due to subtle fibre type specific differences in structure/function of the molecular components of the T-system, such as for example, Na^+/K^+ ATPase. To date no studies have quantified the number, density or activity of Na^+/K^+ pumps located in the t-tubule compartment of electrophoretically typed single fibres from slow- or fast-twitch muscle.

75%R-D and MHC -based fibre type

This study is the first to compare the number of DIFRs to run-down in fibres expressing the same MHC isoform from two different muscles. The data show that T-system depolarization induced force responses developed by type IIB fibres from the SM muscle declined 4.9 times faster than those developed by type IIB EDL fibres. This result is surprising, given the similarity displayed by IIB EDL and IIB SM fibres with respect to maxDIFR .

Here it was also shown that the T-system depolarization induced force responses developed by fibres expressing MHC I isoform from the SOL muscle decline faster than those developed by fibres expressing MHC Iib isoform from EDL (8.1 times) and SM

(1.7 times) muscles. This result is in agreement with the data of Plant *et al.* (2002) who reported that SOL fibres, classified as slow-twitch on the basis of the sensitivity of the contractile apparatus to strontium (Sr^{2+}), produced 2.9 times fewer responses to run-down than fast-twitch EDL fibres.

Within the framework of the previously discussed mechanisms involved in the run-down phenomenon (Lamb & Stephenson, 1990a), the differences in $_{75\%}\text{R-D}$ observed between type IIB fibres from EDL and SM muscles and between the type I (SOL) and type IIB (EDL & SM) fibres indicate that the processes associated with the use-dependent loss of E-C coupling in mechanically skinned fibre preparations may be both muscle of origin-specific and muscle fibre type-specific. It is unlikely that run-down in either of these fibre groups was related to SR dysfunction or depleted SR Ca^{2+} as the responses to low Mg^{2+} produced by these fibres (see Table 4.1) were relatively large ($>70\%$ of $_{\text{max}}\text{CaF}$).

EDL muscle fibres and the T-system depolarization/repolarization protocol described here have been used in several studies for determining the effects of particular compounds on E-C coupling (e.g. Bakker *et al.*, 1998; Blazev *et al.*, 2001; Dutka & Lamb, 2000). After the 'work up' period (see Methods for definition), test responses produced by the fibre preparations, when exposed to depolarization/repolarization solutions containing the compound of interest, are preceded and followed ('bracketed') by control responses (i.e. responses produced in the absence of the compound of interest). The sensitivity of this method is determined in large part by the number and amplitude of successive responses of similar height developed by a fibre between the end of the 'work

up' process and the onset of the run-down process. Given the relatively small number of total responses (12.1) to run-down found by us in mechanically skinned type I SOL fibres, it is reasonable to suggest that in its current form, the protocol developed by Lamb & Stephenson (1990a) may not be suitable for accurately determining the magnitude and reversibility of effects of particular compounds on E-C coupling characteristics in slow twitch fibre preparations.

Profile of T-system depolarization induced force responses produced by mechanically skinned fibres from EDL, SM and SOL muscles.

All previous studies using the T-system depolarization method of Lamb & Stephenson (1990) and mechanically skinned single fibre segments have reported only *rtF* type depolarization induced force responses for both rat EDL (e.g. Lamb & Stephenson, 1990a; Plant *et al.*, 2002) and SOL fibres (e.g. Bakker *et al.*, 1998; Plant *et al.*, 2002). Under the same conditions, the fibres examined in the present study produced, however, two different types of responses, *rtF* and *pF* (see Results for definition), or did not respond even after several depolarization/repolarization cycles. The lowest variability with respect to the profile of force responses induced by T-system depolarization was found among type IIB EDL fibres, all of which developed only *rtF* responses. By comparison, while the majority of type IIB SM fibre produced also *rtF* responses, a small proportion (13.3%) failed to respond. The highest variability with regard to this parameter was found in the population of type I SOL fibres, which contained a small proportion of fibres producing typical *rtF* responses, a small proportion of fibres producing *pF* responses and a large proportion of fibres that did not develop any force.

Taken together, these data suggest that, under the conditions used here, the profile of T-system depolarization induced force responses produced by mechanically skinned muscle fibre preparations is related to fibre type, muscle of origin and even individual fibre characteristics.

The finding that some SOL muscle fibres developed rapid transient forces (indicating complete inactivation) while others developed prolonged forces (indicating incomplete inactivation) in response to T-system depolarization provides the strongest support to date for the 'voltage window' model put forward in an earlier study by Chua & Dulhunty (1988). According to this model, the activation and inactivation curves for a given muscle preparation overlap to some extent thereby creating a 'window' like area, the size of which is related to the dependence of the activation and inactivation processes on the membrane potential at the peak of depolarization. Since the sensitivity of the voltage sensor to membrane potential in SOL is higher (activation) and lower (inactivation) than in EDL, the size of the voltage window is expected to be larger for SOL than for EDL muscle preparations. Chua & Dulhunty (1988) used the 'voltage window' model to explain the incomplete inactivation of K^+ contractures ('pedestal tensions') observed in bundles of intact SOL fibres and argued against the possibility that the profile of these contractures could have been due to a subpopulation of SOL fibres that did not inactivate. The single fibre study presented in this paper revealed the presence in the rat SOL muscle of *rtF* and *pF* fibres, whose responsiveness to T-system depolarization can be easily explained if one considers that, at the peak of depolarization, the membrane potential reached a value which was more positive (*rtF*) than the limit of the voltage window or

was within it (pF). Given the steepness of the activation and inactivation curves constructed for SOL muscles (see Figure 6 a & b in Chua & Dulhunty, 1988), it is suggested that despite the marked difference in the profile of the rtF and pF force responses, the actual difference between the membrane potentials of rtF and pF fibres could be very small.

It is interesting to note that the forces produced by a small number (two type I and one type I/IIA) of rtF SOL fibres during the work-up period displayed a pF type profile, with the pedestal component becoming smaller with successive depolarization/repolarization cycles such that the maxDIFR was of the rtF type. The work-up phenomenon has been related to the presence in the sealed T-system of Cl^- ions, which exert a polarizing effect on the membrane potential thereby reducing the effectiveness of the depolarization step (Coonan & Lamb, 1998). With successive depolarizations, Cl^- gradually diffuses out of the T-system, the membrane potential reaches more positive values, more DHPR/voltage sensors become activated and the fibre produces force responses of greater magnitude. Within this context, the transition of the aforementioned force responses, from pF to rtF , suggests that the membrane potential reached in these fibres in the depolarizing solution at the beginning of an experiment may be within the 'voltage window' and that successive depolarization/repolarization cycles (and subsequent loss of T-system Cl^-) causes the membrane potential reached during depolarization to shift out of the voltage window closer to zero.

An interesting finding of this study is that 11.1 % of IIB SM fibres and over 50 % of SOL type I fibres did not respond to T-system depolarization. The large proportion of SOL fibres not responding to T-system depolarization rat make studies on E-C coupling in type I fibres using the skinned fibre preparation and the Lamb & Stephenson depolarization protocol (Lamb & Stephenson, 1990a) a difficult task. It is unlikely that the *nF* fibres could have been damaged, since all single fibres used in this study were dissected, skinned and mounted by the same investigator. Furthermore, all the *nF* fibres examined here produced large force responses when exposed to a low Mg^{2+} solution (see Table 4.1) indicating that the SR compartment was not depleted of Ca^{2+} and that the RyR/ Ca^{2+} release channels were functional. Based on these data it is suggested that in *nF* fibres the DHPR/voltage sensors may have been irreversibly inactivated and/or that the coupling mechanism between the DHPR/voltage sensors and the RyR/ Ca^{2+} release channels may have been disrupted by some unknown causes.

Are functional characteristics of the T-system and SR compartments related to MHC-based fibre type?

Myosin heavy chains are the most widely used molecular markers of fibre type differentiation, specialization and adaptation, yet the extent to which the functional properties of the T-system and SR in different fibre types are related to MHC-based fibre type is far from being understood. One finding from the present study is that, regardless of the muscle of origin (EDL or SM), pure fast-twitch fibre preparations expressing MHC IIb isoform produce larger T-system depolarization induced responses than pure slow-twitch fibre preparations expressing MHC I isoform. Based on this finding, which

suggests a close relationship between MHC isoform expression and the amplitude of the responses, one would predict that DIFRs produced by pure muscle fibres expressing MHC IIa (type IIA fibres) or MHC II_d/x isoforms (type IID/X fibres) and by hybrid I/II fibres expressing a larger proportion of MHC II isoform should be larger than the DIFRs produced by fibres expressing only MHC I or a combination of MHC I and MHC II, with MHC I being the major component. Surprisingly, the force responses produced by four type I/IIA SOL fibres, expressing predominantly MHC IIa isoform (mean value of 73 %), were not different from those produced by pure type I SOL fibres. This result may indicate that, in the rat, type IIA fibres resemble type I rather than type IIB fibres with respect to the intracellular factors/events determining the amplitude of DIFR.

Unfortunately, this possibility could not be tested as the pool of fibres used in this study contained only one pure type IIA fibre, which failed to respond to T-system induced depolarization. Moreover, to date there is no published information on the E-C coupling phenotype of mechanically skinned fibre preparations expressing MHC IIa isoform. The similarity between the maxDIFR values for type I/IIA and type I SOL fibres may indicate, however, that the relationship between MHC isoform expression and the factors determining this parameter (see *Parameters indicating skinned fibre responsiveness to T-system depolarization* in Chapter 2, page 67) is stronger for MHC I than for MHC IIa.

This possibility seems unlikely though, given that for the population of type I SOL fibres, the inter-fibre variability (as indicated by the value of CV) with respect to maxDIFR was four times higher than that for IIB EDL and IIB SM fibres. A third possible explanation for the lower DIFRs developed by the I/IIA SOL fibres expressing predominantly the MHC IIa isoform is that the factors determining maxDIFR relate more to the muscle of

origin (SOL) and to its specific physiological role, than to the MHC isoform (IIa) expressed in the fibre. In this case one would expect that, if present in SOL muscle, even pure type IIB fibres, would produce lower force responses to T-system depolarization, comparable in height to those produced by the pure type I and type I/IIA SOL fibres. Again, the absence of type IIB fibres from the pool of rat SOL muscle fibres examined in this study made it impossible to validate/reject this point.

The possibility that responsiveness to T-system depolarization in a mechanically skinned fibre preparation relates to MHC-based fibre type as well as to the muscle from which the fibre was obtained is supported also by the data on $_{75\%R-D}$, the second E-C coupling parameter considered in this study: type I SOL fibres produced fewer force responses to run-down than type IIB fibres from EDL and SM (in agreement with a close relationship between E-C coupling characteristics and fibre type) and type IIB SM fibres produced fewer force responses to run-down than IIB EDL fibres (in agreement with a close relationship between E-C coupling characteristics and the muscle of origin). Recently Bortolotto *et al.* (2000) reported another example of functional/structural differences between fibres expressing the same MHC isoform, but originating from two different rat muscles. In this case, in which IIA SOL fibres displayed significantly higher sensitivity of the contractile apparatus to Ca^{2+} than IIA EDL fibres (Bortolotto *et al.*, 2000), the inter muscle difference involved most likely, components of the myofibrillar compartment (such as troponin C). Taken together with the results presented in this study, these data suggest that the optimum contractile function of a skeletal muscle fibre type is related to

both its MHC isoform composition and to the innervation pattern and functional role of the muscle of origin (Bottinelli, 2001).

In summary, this study has shown that pure type IIB fibres (from EDL or SM) produce larger DIFRs than SOL pure type I fibres suggesting that responsiveness to T-system depolarization of skinned muscle fibres varies with muscle fibre MHC isoform composition. When considering the second E-C coupling parameter, $75\%R-D$, EDL IIB fibres gave more DIFRs than both SM IIB and SOL I fibres suggesting that responsiveness to T-system depolarization may also vary according to the muscle of origin. The finding that a small group of SOL type I fibres responded to T-system depolarization with a prolonged force response, indicating incomplete inactivation of the DHPR, provided the first evidence at the single fibre level of the 'voltage window' model of voltage sensor function originally proposed by Chua & Dulhunty (1988).

Chapter 5

GLYCOGEN STABILITY AND GLYCOGEN PHOSPHORYLASE ACTIVITIES IN ISOLATED SKELETAL MUSCLES FROM RAT AND TOAD

Introduction

The study described in the next Chapter (Chapter 6) examines the relationship between glycogen content and the responsiveness to T-system depolarization of mechanically skinned fibres from the rat EDL muscle. A methodological prerequisite for such a study is that any loss of glycogen and associated enzymes occurring during muscle storage over the experimental period is kept to a minimum.

In this context it is worth pointing out that in studies involving mechanically skinned fibre preparations, whole muscles are dissected and single fibres are isolated and skinned at room temperature; when not being used for the generation of a new single fibre, the muscles are kept at 4°C. The time taken to perform these procedures, all of which are carried out under oil (for details see Chapter 2), with fibres isolated from the hindlimb muscles of one animal (i.e. the total time spent by the muscle tissue, under oil, at room temperature and at 4°C) depends on the skill of the experimenter and the functional state of the muscle, but does not usually exceed 6 hours. The stability of muscle glycogen over this time period has not been examined so far, but there is evidence to suggest that glycogen in mammalian skeletal muscle is relatively unstable (as compared for example with amphibian muscle). Thus, Calder and Geddes (1990) found very rapid glycogen loss (60% in the first 5 minutes after animal death,

82% within the first 2 hr) in rat hindlimb muscles left in the body post mortem. By comparison, Sahyun (1931) reported no decrease in glycogen content in frog (*Rana pipiens*) skeletal muscle left *in situ* for over 2 hours, at room temperature.

In the present study, the stability of glycogen in rat EDL muscle (the muscle used as a source of single fibres in Chapter 6) was determined and compared with that of rat SOL muscle and iliofibularis (IF) muscle of the cane toad.

As described in Chapter 1 (see Glycogenolysis and Glycogen phosphorylase, page 51 and 52, respectively), the enzyme predominantly responsible for the breakdown of skeletal muscle glycogen is glycogen phosphorylase, which is present in both active (phosphorylase a; Phos a) and inactive (phosphorylase b; Phos b) forms. To date there have been several reports concerned with glycogen phosphorylase activities in EDL and SOL muscles of the rat (Villa Moruzzi *et al*, 1981; James & Kraegen, 1984; Chasiotis, 1985; Chasiotis *et al*, 1985). In contrast, no equivalent studies have been performed using the IF muscle of the cane toad and there are no comparative studies on glycogen phosphorylase activities in rat and toad skeletal muscles. Thus, a second aim of the present study was to determine and compare total phosphorylase (Phos_{total}) and Phos a activities in isolated rat EDL and SOL and toad IF muscles at different time points over the period of muscle storage.

Materials and Methods

Animals

The animals used in this study were male rats (DRY and Sprague-Dawley; 11 – 13 weeks) and male and female cane toads (*Bufo marinus*; 160 - 400 g). The rats were

kept at room temperature and fed water and standard rat chow *ad libitum*, while toads were kept unfed in a dark, moist environment (16 – 24° C) for up to one week.

Muscle preparation

Rats were killed by deep halothane inhalation, while toads were double pithed.

Previous studies have demonstrated no adverse effect of rat exposure to anaesthetic halothane on skeletal muscle glycogen (Musch *et al.*, 1989; Ferreira *et al.*, 1998) or glycogen phosphorylase activity (Ferreira *et al.*, 1998). To minimise any diurnal variation in muscle glycogen, all rats were killed at the same time of day (Cohn & Joseph, 1971; Conlee *et al.*, 1976).

Rat EDL and SOL and toad IF muscles were dissected and handled as described in Chapter 2. The muscles to be stored, either at room temperature (RT) or at 4°C (see below), were placed in a Petri dish under Paraffin oil kept at RT. In all experiments (determination of glycogen content and phosphorylase activity), one muscle was used as a control and processed immediately while the contralateral muscle was stored as described below and processed as appropriate at the required time. In glycogen determination experiments, control muscles were homogenised immediately after weighing, while the contralateral muscles were homogenised after being incubated (see below). For glycogen phosphorylase assays, control muscles were rapidly clamped with aluminium tongs precooled in liquid N₂ and freeze-dried for 48 hrs, while stored muscles were blotted free of oil on filter paper, freeze clamped and freeze-dried. Due to technical constraints, glycogen determination and phosphorylase activity assays were performed, for each storage time point, on muscles obtained from different animals, and different rats were used to obtain the EDL and SOL muscles.

Muscle storage

Muscles were stored under paraffin oil at either RT (20 – 25°C) or at 4°C. These temperatures were chosen based on the protocol employed in studies using mechanically skinned single fibre preparations, which involves storage of the muscle tissue at low temperature and isolation of single fibres, mechanical skinning and fibre mounting onto the force measuring system at RT (Stephenson and Stephenson, 1996; Lamb and Cellini, 1999). For glycogen stability experiments, muscles were stored at RT for 0.5 (EDL and SOL), 3 hrs (EDL and SOL) and 6 hrs (EDL, SOL and IF) and at 4°C for 3 hrs (EDL and SOL) and 6 hrs (EDL, SOL and IF). For measurements of phosphorylase activity, rat SOL and EDL muscles were stored for 0.5 hr (RT) and 6 hrs (RT and 4°C), while toad muscles were stored for 6 hrs (RT and 4°C) only.

Glycogen determination

Whole muscle glycogen was determined using a two-step fluorometric method based on the analytical protocol of Passonneau & Lowry (1993). All enzymes were purchased from Boehringer-Mannheim. Whole muscles were mechanically homogenised (Omni, Warrenton, VA, USA) on ice in six volumes of ice cold 0.5 M acetate buffer (0.25 M acetic acid & 0.25 M sodium acetate), pH 5.0 to produce a smooth suspension. Amyloglucosidase (AG; amylo- α 1, 4- α -1, 6-glucosidase) was added to the homogenate at a final concentration of 20 μ g/ml and samples were incubated at RT for 4hrs (step 1; $Glycogen_{(n)} \xrightarrow{AG} Glycogen_{(n-1)} + glucose$). After this period, samples were centrifuged for 5 mins at 12,000 g. An aliquot of 7.5 to 10 μ l was taken from the supernatant and added to 3 ml of glucose reagent, which consisted of 0.05 mM Tris/HCl, pH 8.1, 1.0 mM MgCl₂, 0.5 mM DTT, 0.3 mM ATP, 0.05 mM NADP⁺ and 1.76 μ g/ml glucose-6-phosphate dehydrogenase (G-6-PDH).

To start the reaction, hexokinase (HK) was added at a final concentration of 0.4 $\mu\text{g/ml}$. The sample-reagent mixture was then incubated for 15 minutes in the dark (step 2; *Glucose + ATP + NADP⁺ ---HK & G-6-PDH---> NADPH + P-6-gluconolactone*) and subsequently read fluorometrically for NADPH content (Perkin Elmer, LC100) at a wavelength of 348 nm. The fluorescence NADPH signal is produced stoichiometrically with glucose monomers generated from glycogen in Step 1.

In order to determine the actual concentration of NADPH (and hence glycogen) from the fluorescence signal, a glycogen standard curve (0.5, 1.0, 2.0, 4.0, 8.0, 12.0, 16.0 & 20.0 μM) was prepared using commercial glycogen (Sigma) subjected to the same reaction steps as the samples. The fluorescence signals produced by the standards were then read on the fluorometer and the standard curve was plotted on GraphPad PrismTM program. The slope of the standard curve was finally used to convert the fluorescence signals produced by muscle samples to actual glycogen concentrations.

To determine any other endogenous contributors to the fluorescence signal (ie. glucose, G-6-P, NADH & NADPH), a portion of the original homogenate, without the addition of AG, was subjected to the second reaction step and the fluorescence signal analyzed. The concentration of these non-glycogen fluorescence contributors was subtracted from the glycogen concentration. Glycogen concentration was expressed as mmol glucosyl residues/kg wet weight or as mmol glucosyl residues/kg dry weight (mmol glucosyl residues X conversion factor /kg wet weight).

Wet weight/dry weight conversion

To allow the expression of glycogen concentration or phosphorylase activity relative to either wet or dry muscle mass, IF, EDL & SOL muscles were weighed wet, immediately after dissection and weighed again immediately after being freeze-dried for 48 hours. The muscle conversion factors used in this study, 3.66 (for EDL and SOL) and 4.34 (for IF), were calculated based on the finding that, for the three muscles examined, the dry weight (expressed as percent of wet weight), was 27.5 ± 0.3 % (n = 14; EDL), 27.5 ± 0.4 % (n = 15; SOL) and 22.7 ± 0.2 % (n = 15; IF).

Phosphorylase activities

Total phosphorylase (Phos_{total}) and phosphorylase a (Phos a) activities were determined at 30°C (the temperature commonly used in phosphorylase assays) in the direction of glycogen degradation using the two step method of Ren *et al.* (1992). All enzymes were purchased from Boehringer-Mannheim. Briefly, 10 – 25 mg of freeze dried muscle was homogenised on ice in 0.4 ml of ice cold homogenization solution containing 100 mM Tris/HCl, pH 7.5, 60% (v/v) glycerol, 50 mM NaF and 10 mM EDTA. The homogenate was then diluted with 1.6 ml of the above solution without glycerol and further homogenised on ice. Fifty microliters of homogenate was added to 0.5 ml of a phosphorylase stock reagent containing 50 mM Imidazole/HCl at pH 7.0, 1.25mM MgCl₂, 20 mM K₂HPO₄, 0.25% (w/v) BSA, 62.5 mM glycogen, 5 μM G-1-6-P, 0.5 mM DTT and 2.5 μg/ml phosphoglucomutase (PGM) (step 1; *Glycogen --- Phos---> G-1-P ---PGM---> G-6-P*). Phosphorylase activity was determined in the presence (Phos_{total}) or absence (Phos a) of 3 mM AMP.

After 10 mins at 30°C, the reaction was stopped with 60µl of 0.5 N HCl. The glucose-6-phosphate generated was measured by adding 50 µl sample (Phos_{total} assays) or 100 µl sample (Phos a assays) to 2 ml of G-6-P reagent containing 50 mM Tris/HCl at pH 8.1, 1 mM EDTA, 250 µM NADP⁺ and 0.5 µg/ml G-6-PDH (step 2; *G-6-P + NADP⁺ ---G-6-PDH---> NADPH + P-6-gluconolactone*). Samples were subsequently incubated for 15 mins in the dark at RT, then read fluorometrically for NADPH fluorescence signal at 348 nm.

In order to determine the actual concentration of NADPH (and hence G-6-P produced from the breakdown of glycogen by phosphorylase) from the fluorescence signal, a G-6-P standard curve (1.0, 2.0, 4.0, 8.0, 12.0, 16.0, 20.0 & 24.0 µM) was prepared using commercial G-6-P (Boehringer-Mannheim) subjected to reaction step 2. The fluorescence signals produced by the standards were then read on the fluorometer and the standard curve was plotted on GraphPad PrismTM program. The slope of the standard curve was then used to convert the fluorescence signals produced by the muscle sample to phosphorylase activity. Phos_{total} activity was expressed as µmol /min/g dry weight while Phos a activity was expressed both as µmol/min/g dry weight and as percentage of Phos_{total} activity.

Statistics

All results are presented as means and standard error of the mean (M ± SEM). Student's paired t test was used to detect differences between two groups. One way analysis of variance (ANOVA) with Boferroni's post test was used for multiple group comparisons. Significance was set at p< 0.05.

Results

Glycogen content in control muscles

As described in the Methods, muscle glycogen content was determined in homogenates prepared from wet (not freeze-dried) muscles. Control experiments showed no significant difference between the glycogen content of wet muscles and that of the rapidly frozen, freeze-dried contra-lateral muscles (data not shown). The glycogen content (expressed as mmol glucosyl residues/kg wet weight and in bracket as mmol glucosyl residues/kg dry weight), in freshly dissected EDL, SOL and IF muscles was 41.1 ± 1.5 (150.4 ± 5.5 ; $n=38$), 41.7 ± 1.5 (152.6 ± 5.5 ; $n=37$) and 51.4 ± 2.8 (223.1 ± 12.1 ; $n=18$), respectively. The conversion factors used are given in the Methods. The [glycogen] in both rat muscles was significantly lower than that in toad IF. There was no significant difference between EDL and SOL with respect to glycogen content.

Glycogen content in muscles stored under oil at RT

As seen in Figure. 5.1A, 6 hrs storage at RT was accompanied by a marked decrease in glycogen content both in EDL (by 74.7 ± 3.4 %; $n = 7$) and in SOL (by 62.6 ± 3.9 %; $n = 7$). In contrast, under the same conditions, there was only a slight decrease (by 13.5 ± 6.2 %; $n = 6$) in IF glycogen and this decrease was statistically non-significant. The proportions of glycogen retained in both EDL and SOL muscles after 6hrs storage at RT were not significantly different (ANOVA with Bonferroni's post-test; $p > 0.05$),

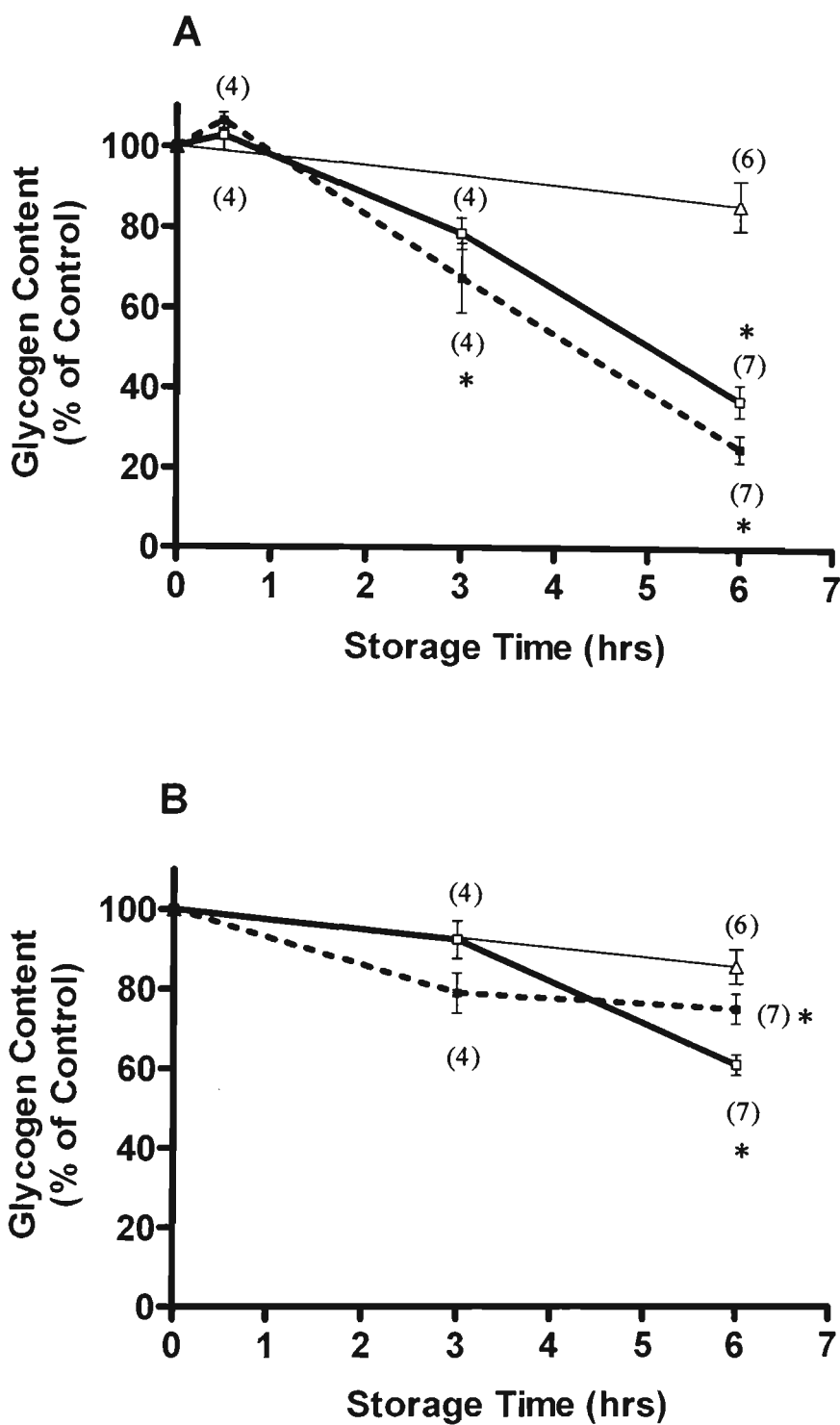


Figure 5.1. The time course of glycogen loss in rat EDL (■) and SOL (□) and in toad IF (Δ) muscles stored under oil at RT (20 – 25°C) (A) and 4°C (B).

Results are means \pm SEM. * significantly different ($p < 0.05$; ANOVA with Bonferroni's post test) from controls (0 hr storage).

but both were significantly lower than the proportion of glycogen found in IF muscle stored for the same length of time (ANOVA with Bonferroni's post-test; $p < 0.05$).

To determine the time course of glycogen loss in rat EDL and SOL over the 6hr time period, additional samples were stored at RT for 0.5 hr and 3 hrs. No change in the glycogen content of EDL ($106.5 \pm 1.9 \%$; $n = 4$) or SOL ($102.8 \pm 3.8 \%$; $n = 4$) was observed after 0.5 hr, while the 3 hr storage period decreased the glycogen content of both muscles by $32.4 \pm 8.7 \%$ ($n = 4$) and $21.3 \pm 4.0 \%$ ($n = 4$), respectively (Figure. 5.1A). No significant difference was observed between the proportions of glycogen retained in EDL and SOL after either 0.5 hr or 3 hrs storage (ANOVA with Bonferroni's post-test; $p > 0.05$).

Glycogen content in muscles stored under oil at 4°C.

As shown in Figure 5.1B, 6 hrs storage under oil at 4°C induced a significant loss of glycogen from both EDL ($24.8 \pm 3.8 \%$, $n = 7$) and SOL ($38.9 \pm 2.6 \%$, $n = 7$). By comparison, the same storage conditions produced only a small decrease in the glycogen content of IF muscles ($14.1 \pm 4.4 \%$; $n = 6$). The proportion of glycogen retained at 6 hrs in the two predominantly fast-twitch muscles (EDL and IF) was significantly higher than that in SOL (Student's t-test; $p < 0.05$). After 3 hrs storage at 4°C, the glycogen content in EDL and SOL decreased non-significantly by $21.0 \pm 5.1 \%$ ($n = 4$) and $7.5 \pm 4.8 \%$ ($n = 4$), respectively. No significant difference was found between the two muscles with respect to the proportions of glycogen retained at this time point.

Phos_{total} and Phos a activities in control muscles

The activities of Phos_{total} (A) and Phos a (B) in control, EDL, SOL and IF muscles are presented in Figure. 5.2. The Phos_{total} (expressed as $\mu\text{mol/g dry weight/min}$) for EDL (152.9 ± 4.4 ; $n = 23$) was significantly higher than for IF (66.3 ± 5.7 ; $n = 12$), which in turn was significantly higher than for SOL (29.9 ± 2.3 ; $n = 22$). By comparison, the Phos a activity (expressed both as $\mu\text{mol/g dry weight/min}$ and, in bracket, as % of Phos_{total} activity) was 72.4 ± 4.0 (48.1 ± 1.8 %; $n = 23$) for EDL, 6.0 ± 0.6 (19.2 ± 1.7 %; $n = 22$) for SOL and 3.1 ± 0.7 (4.9 ± 1.1 %; $n = 12$) for IF. The values of Phos a activity in SOL and IF, were significantly lower than the Phos a activity in EDL.

Phos_{total} and Phos a activity in muscles stored under oil at RT and 4°C.

In all three muscles examined in this study (EDL, SOL and IF), Phos_{total} did not change over the entire 6 hr period regardless of the storage temperature (Table 5.1), indicating no significant storage-induced degradation of glycogen phosphorylase. As shown in Figure.5.3A, after 6 hrs of storage at RT, Phos a activity (expressed both as $\mu\text{mol/g dry weight/min}$ and, in bracket, as a % of Phos_{total} activity) in EDL decreased 9 fold from 74.6 ± 4.7 (49.6 ± 2.3 %; $n = 11$) to 8.3 ± 1.5 (6.3 ± 1.1 %; $n = 6$). Six hours storage at RT of SOL muscles was accompanied by a 4 fold decrease in Phos a activity from 6.3 ± 0.9 (19.6 ± 2.5 %; $n = 12$) to 1.6 ± 0.6 (4.9 ± 1.7 %, $n = 6$). No decrease in Phos a activity was observed in IF muscles stored for 6 hrs at RT. [4.2 ± 1.7 (6.6 ± 3.2 %; $n = 6$) versus 3.5 ± 1.0 (5.5 ± 1.8 %)]. To find out how fast the Phos a activity decreased in EDL and SOL, the enzyme was assayed also in muscles stored at RT for 0.5 hr. As seen in Figure. 5.3A, a marked decrease in Phos a activity was observed relatively early both in EDL (4.1 fold) and in SOL (2.4 fold).

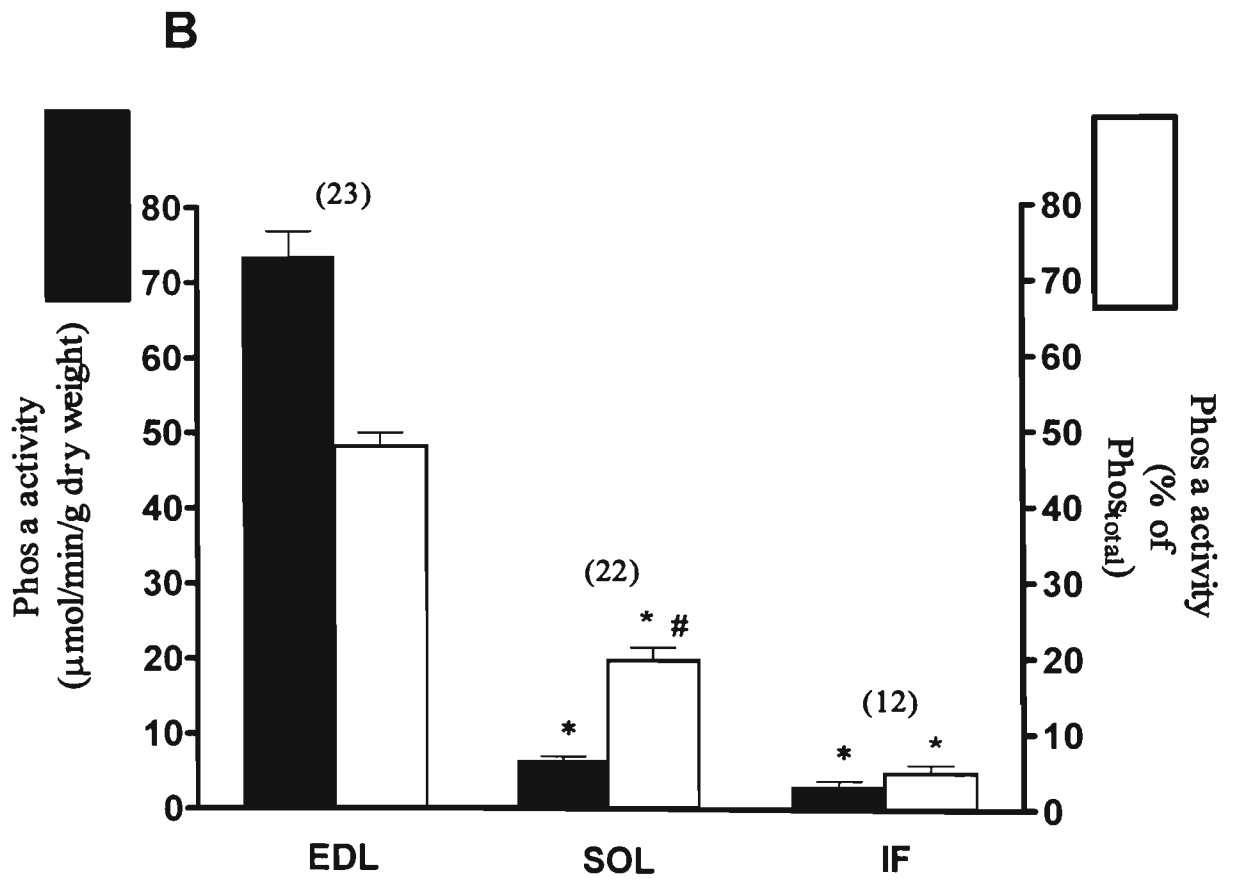
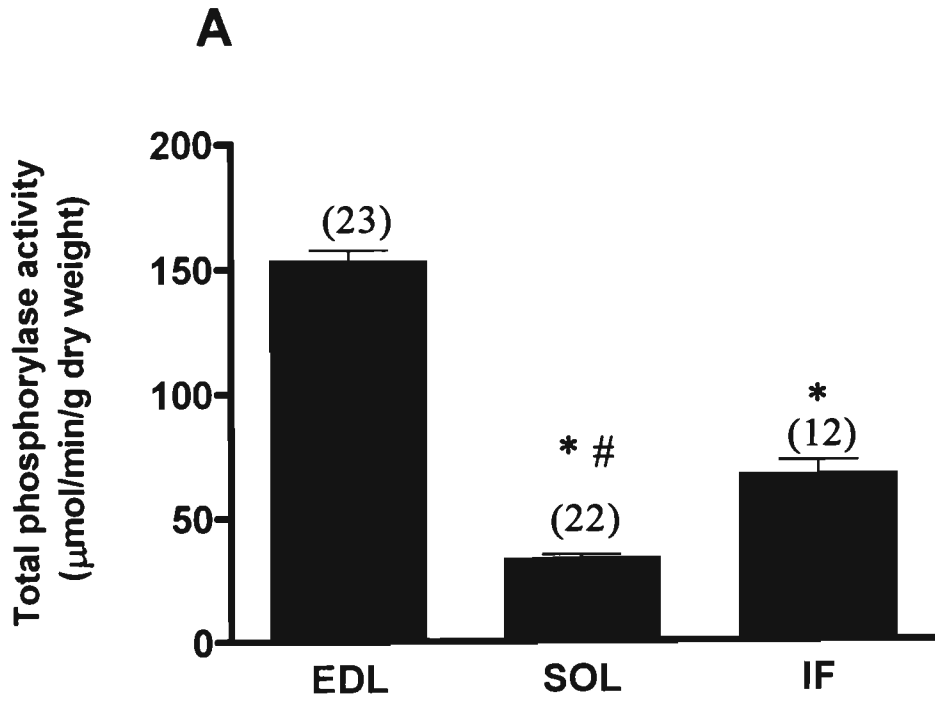


Figure 5.2 (A) Total phosphorylase activities ($\mu\text{mol}/\text{min}/\text{g}$ dry weight) in rat EDL and SOL and toad IF control muscles. Results are means \pm SEM. * significantly different ($p < 0.05$; ANOVA with Bonferroni's post test) from rat EDL; # significantly different ($p < 0.05$; ANOVA with Bonferroni's post test) from toad IF.

(B) Phosphorylase a activities (expressed: $\text{mol}/\text{min}/\text{g}$ dry weight and as % of total phosphorylase) in rat EDL and SOL and toad IF control muscles. Results are means \pm SEM. * significantly different from rat EDL. # significantly different ($p < 0.05$; ANOVA with Bonferroni's post test) from toad IF.

Table 5.1. Ratio $\text{Phos}_{\text{total}} \text{ 6 hrs} / \text{Phos}_{\text{total}} \text{ control}$ for EDL, SOL and IF. Number of samples shown in brackets.

Storage temperature	EDL	SOL	IF
RT (20-25°C)	0.97 ± 0.03 (6)	1.34 ± 0.15 (6)	1.06 ± 0.14 (6)
4°C	0.92 ± 0.05 (6)	0.92 ± 0.04 (6)	1.41 ± 0.23 (6)

After 6 hrs storage at 4°C, Phos a activities decreased 7.3 fold in EDL from 72.0 ± 5.3 (46.6 ± 2.8 %; n = 12) to 9.9 ± 0.6 (7.6 ± 0.6 %; n = 6) and only 3.3 fold in the SOL muscles [from 6.3 ± 0.7 (18.6 ± 2.3 %; n = 10) to 2.0 ± 0.4 (6.2 ± 0.8 %; n = 6)] (Figure. 5.3B). There was no decrease in the Phos a activity of IF muscles stored for 6 hrs at 4°C.

In Figure 5.3B are also shown the values for Phos a activity in rat muscles stored for 0.5 hr at 4°C. After this period of time, the Phos a activity decreased 2.5 fold to 29.3 ± 2.1 (19.6 ± 1.5 %; n = 6) in EDL and 1.3 fold to 4.9 ± 1.7 (13.7 ± 4.2 %; n = 4) in SOL muscles.

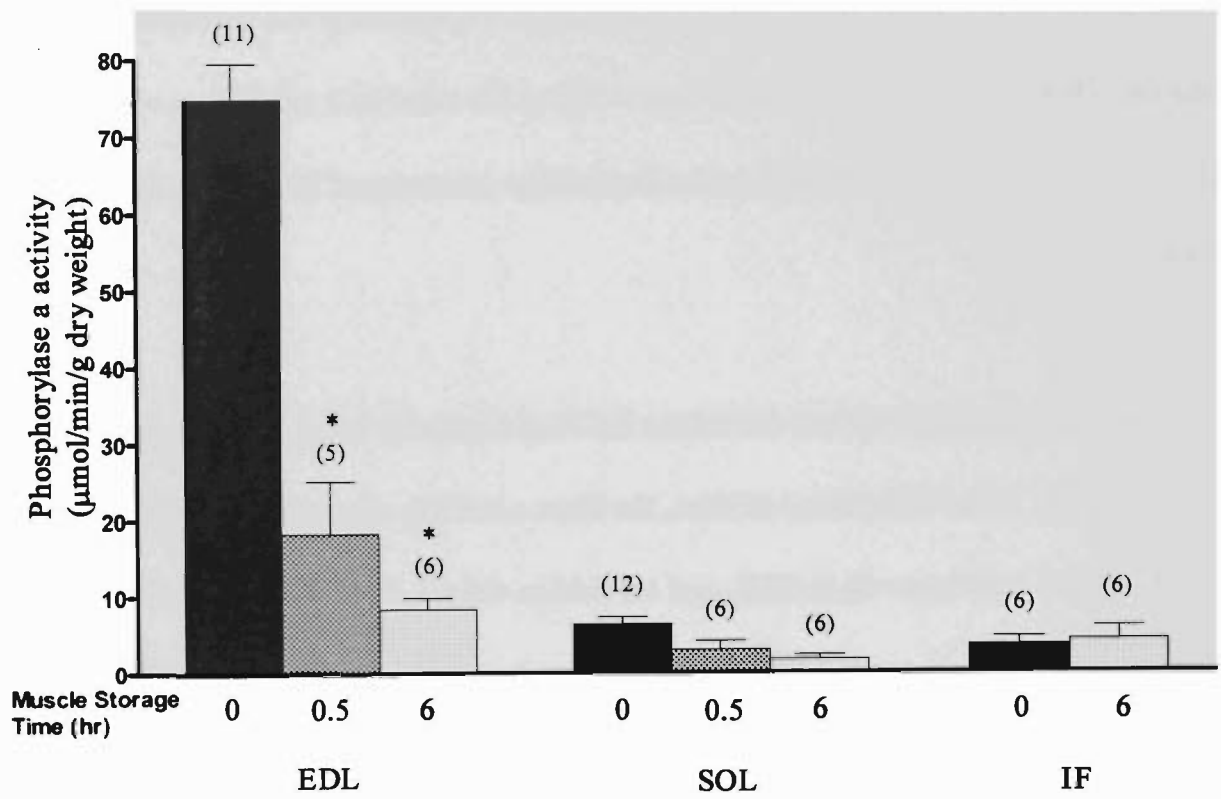
Discussion

The results presented in this study clearly show that storage under oil for up to 6 hrs at RT or 4°C, is accompanied by a time- and temperature-dependent glycogen loss in rat EDL and SOL and by minimal glycogen loss in toad IF irrespective of temperature. These data confirm that glycogen is less stable in skeletal muscle of the rat (mammal) than in skeletal muscle of the toad (amphibian).

Glycogen content and phosphorylase activities in freshly dissected (control) muscles

The absolute values for EDL and SOL glycogen determined in the present study are similar to those reported by other investigators who used Sprague-Dawley rats (Witzmann *et al*, 1983; Chasiotis, 1985). In this study, no significant difference was found in the glycogen content of these two rat muscles. This result is in agreement with the data of Witzmann *et al* (1983) and James and Kraegen (1984), but in

A



B

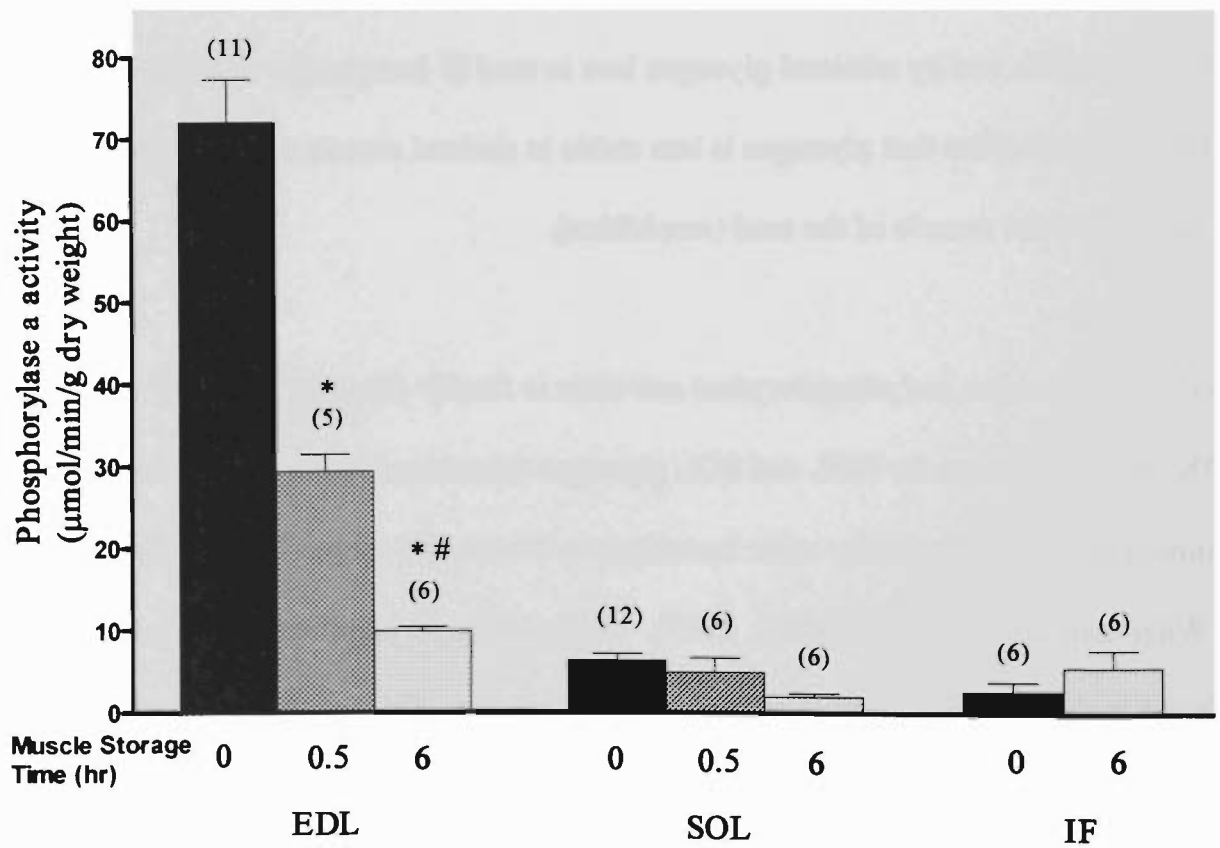


Figure 5.3. Phosphorylase 'a' activities (expressed as % of total phosphorylase) in rat EDL and SOL and toad IF muscles stored under oil at room temperature (20 – 25°C) (A) and 4°C (B) for up to 6 hrs.

Results are means \pm SEM. * significantly different ($p < 0.05$; ANOVA with Bonferroni's post test) from controls (0 hrs).

disagreement with those of Villa Moruzzi and Bergamini (1983), Chasiotis (1985) and Hutber and Bonen (1989), who reported that the glycogen content in EDL is slightly higher than in SOL. This discrepancy between different studies can be explained by the large animal-related variability in muscle glycogen content observed both by us [the coefficient of variance (CV) for both EDL and SOL glycogen was about 20%], and by others (Villa Moruzzi & Bergamini, 1983; James & Kraemer, 1984; Chasiotis, 1985).

This is the first study in which the glycogen content of rat EDL and SOL is compared with that of the cane toad IF muscle, using the same experiment. The data show that the toad IF (a predominantly fast-twitch muscle; Nguyen and Stephenson, 1999) contains a significantly higher concentration of glycogen than EDL and SOL of the rat. This somewhat surprising result, given that the toads were kept unfed while the rats had access to food *ad libitum*, may be explained by species-related differences in dietary habits, muscular activity patterns, or metabolic adaptations to environmental conditions.

The absolute values of $\text{Phos}_{\text{total}}$ determined in this study for freshly dissected and rapidly freeze-dried EDL and SOL muscles are similar to those reported by others for Sprague-Dawley rats (Chasiotis, 1985; Chasiotis *et al*, 1985). Under the experimental conditions used in this study, the rat EDL $\text{Phos}_{\text{total}}$ activity was 4 - 5 fold higher than that in the SOL. This result is in agreement with previous reports that rat fast-twitch muscles have a higher $\text{Phos}_{\text{total}}$ activity than slow-twitch muscles (Villa Moruzzi *et al*, 1981; Chasiotis *et al*, 1985). In this context, it is interesting to note that the $\text{Phos}_{\text{total}}$

activity displayed by toad IF, also a predominantly fast-twitch muscle, was also higher than that in rat SOL, but was lower (less than half) than that found in EDL.

According to earlier reports (Ren & Hultman, 1988; Ren *et al*, 1992), the proportion of Phos a activity in resting mammalian muscle (rat and human) represents approximately 5-10% of the total phosphorylase. In contrast, Conlee *et al*. (1979) found that the proportion of Phos a in the 'resting' red region (slow-twitch) of rat gastrocnemius was 52% whereas that in the white region (fast-twitch) was 60% of the total phosphorylase. The authors attributed the high values found for Phos a in gastrocnemius muscle to the activation of glycogen phosphorylase by the cutting and pulling of the tissue prior to freeze-drying. The proportions of Phos a in the freshly dissected and rapidly freeze-dried rat muscles used in the present study were also high (48.1% in EDL and 19.2% in SOL). These values may also be attributed to the Ca^{2+} release induced by stretching the muscle during freeze clamping (as suggested by Conlee *et al*, 1979) and/or inadvertent mechanical stimulation during dissection (Cohen, 1983a), because, as it will be discussed later, the proportion of Phos a activity in the rat muscles (particularly in EDL) decreased markedly when the tissues were freeze-clamped after being stored under oil for at least 0.5 hr.

In contrast to the rat muscles, the freshly dissected toad IF, which was subjected to the same dissecting and freeze-drying protocol, displayed a low Phos a activity (4.9% of $\text{Phos}_{\text{total}}$). This difference in Phos a activity between the toad and rat muscles suggests that the mechanisms of regulation of phosphorylase kinase and phosphorylase activities in the toad may be different from those in the rat. There is currently no

information regarding the proportion of Phos a or the cellular mechanisms involved in the regulation of the glycogenolytic system in 'resting' toad IF muscles.

Glycogen loss and phosphorylase activities in muscles stored under oil at RT and at 4°C

In this study no glycogen breakdown was found in the rat muscles stored for 0.5 hrs, under paraffin oil, at either RT or 4°C. This result strongly suggests that, under these conditions, stored muscles are not strongly hypoxic because in the experiments performed by Ren *et al.* (1992) on rat epitrochlearis, muscles stored for 20 min under strongly hypoxic conditions (Krebs-Hansleit bicarbonate buffer bubbled with 95%N₂-5% CO₂) lost 36% of the initial glycogen, while the controls (muscles stored in oxygenated Krebs-Hansleit bicarbonate buffer) lost only 1%.

Calder and Geddes (1990) previously reported that in rat 'hindlimb' muscle of a non-specified type, glycogen was rapidly broken down (60% in the first 5 min post-animal death and over 80 % within 2hr) when the muscles were left within the animal carcass. Under the conditions of the present study, the EDL and SOL muscles retained most of their glycogen (67.6% and 78.7% of the control, respectively) even after 3 hr of storage. Glycogen losses similar to those reported by Calder & Geddes (1990) were found only after EDL and SOL muscles had been kept at RT for 6 hr.

The most obvious difference between these two studies, which may explain the discrepancy between the present data and those of Calder and Geddes (1990), is the temperature at which the muscle was kept prior to glycogen determination. Thus, Calder and Geddes (1990) left the muscle tissue after death inside the body, where the

temperature, at least initially, would have been close to normal body temperature of the rat (37-38°C; Severinsen & Munch, 1999). In the present study muscles were stored at RT (20-24°C), which was approximately 15°C lower than that in the Calder and Geddes (1990) study. At this temperature the rate of all enzyme activities (including glycogenolytic enzymes) would have been considerably lower.

Storing EDL and SOL under oil at RT produced no glycogen loss at 0.5 hrs, a small loss (32-21%) after 3 hrs and more than 60% loss after 6 hrs. By comparison, storing EDL and SOL under oil at 4°C produced less than 25% glycogen loss after 3 hrs and less than 40% after 6 hrs. This result indicates clearly that in studies concerned with the correlation between initial single fibre glycogen and rat skinned fibre responsiveness to T-system depolarization, the muscles can be stored at either RT or preferably at 4°C up to 3 hrs and at 4°C up to 6 hrs with only minor loss in muscle glycogen content.

In contrast to the rat muscles, which displayed a temperature and storage time-related glycogen stability, toad IF muscle lost only a very low proportion of glycogen after being stored under oil at RT or 4°C, for up to 6 hrs. One possible explanation for the greater glycogen stability in toad IF muscle is that toads have a lower body temperature (23 – 27°C in cane toads kept at 20°C; Pörtner *et al*, 1994) and a lower resting metabolic rate (as indicated by the rate of oxygen consumption; Pörtner *et al*, 1994) than the rat (Ballor & Poehlman, 1993; Severinsen & Munch, 1999). The toad muscle should therefore have a lower energy requirement at rest than the rat, resulting in less glycogen being broken down over the same period of tissue storage.

An interesting observation made in this study is that the high proportion of Phos a activity recorded in the freshly dissected EDL declined markedly and rapidly during tissue storage at RT, reaching values within the range (5-10%) reported by other laboratories (Conlee *et al*, 1979; Ren & Hultman, 1988; Ren *et al*, 1992). A rapid decrease in the Phos a fraction in human muscles was also reported by Ren and Hultman (1988) in a study in which the freezing of the tissue post-dissection was delayed by a few minutes. When the muscles were stored at 4°C, the drop in the proportion of Phos a activity was slightly smaller. This result could be due to the low temperature induced inhibition of protein phosphatase –1, the enzyme believed to be responsible for the dephosphorylation and inactivation of Phos a (Cohen, 1983b).

In this study no quantitative correlation was found between the amount of glycogen broken down and Phos a activity in isolated ‘resting’ EDL, SOL and IF muscles, stored under oil. For example, after 6 hrs storage at RT, SOL and EDL lost a similar amount of glycogen (112.8 and 97.7 mmol glucosyl residues/kg dry weight, respectively), yet the Phos a activity in SOL was 5.2 fold lower than that in EDL. By comparison, Phos a activity in IF stored at RT for 6 hrs was only 1.9 fold lower than that in EDL, yet the proportion of glycogen lost from IF was 3.9 lower than that from EDL. The finding that SOL lost during storage almost the same amount of glycogen as EDL, even though it displayed a lower Phos a activity, can be explained, at least in part, by its higher content of inorganic phosphate (3.6 mM) relative to EDL (1.1 mM) (Kushmerick *et al.*,1992). Inorganic phosphate is known to activate both Phos a and b, and as a consequence may increase the rate of glycogenolysis (Newgard *et al.*, 1989). A storage-related build up of inorganic phosphate may also explain why, despite the decrease in Phos a activity, glycogenolysis occurred consistently in both SOL and

EDL during the 6 hrs period. The lack of available information on the P_i content of IF in cane toad, precludes us from extending the line of reasoning used for EDL and SOL to explain the lack of correlation between the Phos a activity and rate of glycogen breakdown found in EDL and IF.

In summary, the results of this study indicate that storage under paraffin oil for up to 6 hrs at RT or 4°C is accompanied by a time- and temperature-dependent glycogen loss in EDL and SOL muscles of the rat and minimal glycogen loss in toad IF muscles. Importantly in the context of this thesis, the rat EDL muscle, handled as required in the study described in the next Chapter, retained ~ 80% of its initial glycogen content when stored for 3 hrs at 4°C. Rat EDL had a greater Phos_{total} activity than toad IF which in turn had a higher Phos_{total} activity than rat SOL. Rat EDL and SOL Phos a activity declined also in a time and temperature dependent manner, while toad Phos a activity remained low and constant over six hours of storage at both 4°C and RT.

Chapter 6

GLYCOGEN CONTENT AND RESPONSIVENESS TO T-SYSTEM DEPOLARIZATION IN RAT MECHANICALLY SKINNED MUSCLE FIBRES

Introduction

Skeletal muscle glycogen is an intensely researched area of inquiry particularly with respect to metabolism and biological function(s). So far most studies concerned with these issues involved the use of whole muscles, whole muscle extracts or enzymes isolated from whole muscle homogenates. The main drawback of this experimental strategy is that it provides little insight into potential inter-fibre differences in the regulation of glycogen metabolism (see Kobayashi *et al.*, 1999 for supporting evidence of such differences) or into cellular events that mediate the role of glycogen in the E-C-R cycle. Further advances in these areas could be made with single fibre preparations containing different glycogen concentrations, under conditions where (i) the molecular participants in the glycogen metabolism and other signaling pathways of interest were accessible for functional testing *in situ* and (ii) the composition of the myoplasmic environment could be manipulated as required.

Such a study was conducted by Stephenson *et al.* (1999) with single fibres freshly dissected from the iliofibularis muscle of the cane toad. When mechanically skinned under oil and then incubated in aqueous solutions mimicking the myoplasmic environment at rest, the toad fibre preparations retained a large proportion of glycogen

and a Ca^{2+} -sensitive glycogenolytic system that was activated during T-system depolarization induced isometric contraction. By exploiting these features it was established that, in mechanically skinned fibres of toad iliofibularis muscle, initial fibre glycogen content and fibre responsiveness to T-system are positively correlated under conditions where [ATP] and [creatine phosphate] in the activating solution is kept high and constant. This finding is the strongest supporting evidence so far for the idea that glycogen may also play a non-metabolic role in skeletal muscle contractility (Green, 1991; Fitts, 1994).

The data produced by the toad study strongly indicate that the mechanically skinned fibre is a promising preparation for skeletal muscle glycogen studies at a cellular level in amphibians, but does not predict its applicability to mammalian systems. The present study fills in this cognitive gap by examining the glycogen content and responsiveness to T-system depolarization in mechanically skinned fibres of the rat EDL muscle, using the same T-system depolarization protocol as that described in the toad study.

Materials and methods

Note that in this study depolarization experiments were performed by Dr R Blazev.

Animals and muscles

The animals used were Long Evans hooded rats, aged 20-21 weeks. EDL muscles were carefully removed and mechanically skinned fibre segments were prepared as described in Chapter 2. The age of the animal and the specific muscle used as a source of single fibres in this study were chosen based on the results of Chapters 3 and 4 respectively. All experiments were carried out at room temperature (20-25 °C). To

minimize storage-related glycogen loss, each muscle was used within 3 hours from dissection (See Chapter 5). Due to this time constraint only 3 - 4 fibres were used from each rat muscle.

Skinned fibre responsiveness to T-system depolarization

The protocol used to determine fibre responsiveness to T-system depolarization is described in detail in Chapter 2 (see *The protocol for T-system depolarization induced activation in mechanically skinned fibres*, page 66). The overall indicator of contractile responsiveness to T-system depolarization used in this study was that introduced by Stephenson *et al.* (1999). This indicator, referred to as ‘fibre response capacity’ or ‘response capacity’ was calculated by dividing the sum of amplitudes of the depolarization induced force responses to 75 % run-down (see Chapter 2 for definition of the phrase 75% run-down) by the maximum Ca^{2+} -activated force response.

Skinned fibre solutions

All solutions were as described in Chapter 2.

Glycogen analysis in single fibre segments

Glycogen concentration in freshly skinned (not freeze dried) single fibres was determined using the microfluorometric technique described previously (Nguyen *et al.*, 1998a & b and Stephenson *et al.*, 1999). This analytical protocol distinguished two glycogen pools in toad skinned muscle fibres (Stephenson *et al.*, 1999) incubated in 100 mM Na acetate buffer (pH 7.0): one that was lost from the fibre relatively fast (within 2 min) and another which remained associated with the fibre for at least

another 30 min. Note: the two min wash step is used to mimic the incubation of the test fibre segment in aqueous solution immediately prior to the commencement of an E-C coupling experiment. In the toad study these two glycogen pools were referred to as washable glycogen (**WGlyc**) and non-washable glycogen (**NWGlyc**), respectively. However, both in the toad study and in the present work it was observed that if the mechanically skinned fibre was incubated in a solution mimicking the myoplasmic environment (such as the Polarizing solution; see *Solution composition* in Chapter 2, page 70), the loss of endogenous glycogen followed a different pattern. In this case, the glycogen retained by the fibre after the 2 min wash continued to move gradually into the solution by a non-enzymatic process (Stephenson et al., 1999; see also below). Based on this observation, it was decided to refer to the pool of glycogen retained in the skinned fibre preparations after 2 min incubation in Polarizing solution as skinned fibre glycogen (**SFGlyc**) rather than **NWGlyc**. **SFGlyc** was the parameter of interest in the present study and thus was determined in all fibres.

During the initial 2 min wash in Polarizing solution, an amount of fluorogenic material is washed (**WFluo**) out of the fibre (Nguyen *et al.*, 1998b). This pool includes not only **WGlyc** but also other non-glycogen (**NGlyc**) compounds that contribute to the fluorescence signal such as NADPH, NADH, G-6-P and glucose. To properly determine what proportion of **WFluo** is **WGlyc**, the **NGlyc** signal needs to be subtracted from the **WFluo** signal (i.e. $\text{WGlyc} = \text{WFluo} - \text{NGlyc}$). **WGlyc** (and by implication **Wfluo** and **Nglyc**) was determined only in some fibres.

Preparation of Petri dishes for enzymatic reactions in μ l volumes

The micorfluorometric technique of Nguyen et al. (1998a & b) involves the determination of minute amounts of metabolic analytes in small droplets of reagent formed under oil on the bottom of a Petri dish to avoid evaporation into the atmosphere. Before making the droplets, Petri dishes were first cleaned thoroughly to remove any biological or non-biological contaminants that could potentially interfere with the reaction steps, and to also help the formation of spherical droplets. To this end, glass Petri dishes (20 x 100mm, Schott & Gen Main, Germany) were rinsed with acetone, washed with detergent and hot water, rinsed with 6M KOH/ethanol, rinsed 4 times with hot water and then rinsed 6 times with milliQ water. Clean Petri dishes were left 'face' down to dry at room temperature.

Solutions

Polarizing/Washing solution – 50 mM HDTA²⁻, 90 mM HEPES, pH 7.1. 1 mM free Mg²⁺ (8.5 mM total), 1 mM azide, 8 mM ATP, 10 mM CP, 126 mM K⁺, 37 mM Na⁺.

AG reagent – 100 mM Na⁺-acetate buffer, pH 5.0, 2.5 mM Tris, 0.002% BSA, 10 μ g/ml amyloglucosidase (AG).

GLU reagent – 676 mM Tris-HCl, pH 8.8, % mM MgCl₂, 0.8 mM NADP⁺, 0.8 mM ATP, 0.1 mM DTT, 2.4 μ g/ml hexokinase (HK), 1.6 μ g/ml glucose-6-phosphate dehydrogenase (G-6-PDH).

Reaction steps

Glycogen was assayed using the two step analytical protocol of Passonneau & Lowry (1993):

Step 1/reaction 1 *Glycogen* ---AG---> *n- glucose*

Step 2/reaction 1 *Glucose + ATP* ---HK---> *G-6-P + ADP*

Step 2/reaction 2 *G-6-P + NADP⁺* --G-6-PDH--> *P-6-gluconolactone + NADPH + H⁺*

Preparation of reaction droplets

On the day of an experiment each dish was covered with a ~ 2 mm layer of oil mixture (30 % hexadecodane & 70 % light mineral oil; Sigma). Droplets of reagent were then dispensed under oil on the bottom of the dish using a 2.5 µl micro-pipette (Eppendorf, Germany), aided by a dissecting microscope (Olympus). The arrangement of droplets used in this study is shown in Figure 6.1. In one dish a column of 0.75 µl droplets of Polarizing/washing solution was created, while in a second dish three droplets of solutions were injected as follows: (i) 0.25 µl of 100 mM Na⁺- Acetate buffer, pH 5.0 (no AG); (ii) 0.25 µl of AG reagent; and (iii) 0.5 µl of AG reagent.

Determination of SFGlyc in washed fibre segments

To analyze the glycogen content of a washed single fibre segment, the segment was transferred through the air from the washing droplet to a 0.5 µl droplet of AG reagent in a second dish (see Figure 6.1). The fibre was left to incubate in the AG reagent (Step 1) for 45 minutes while glycogen was broken down to individual glucose units after which 2.0 µl of GLU reagent was added to the droplet to initiate step 2 and left for 30 minutes.

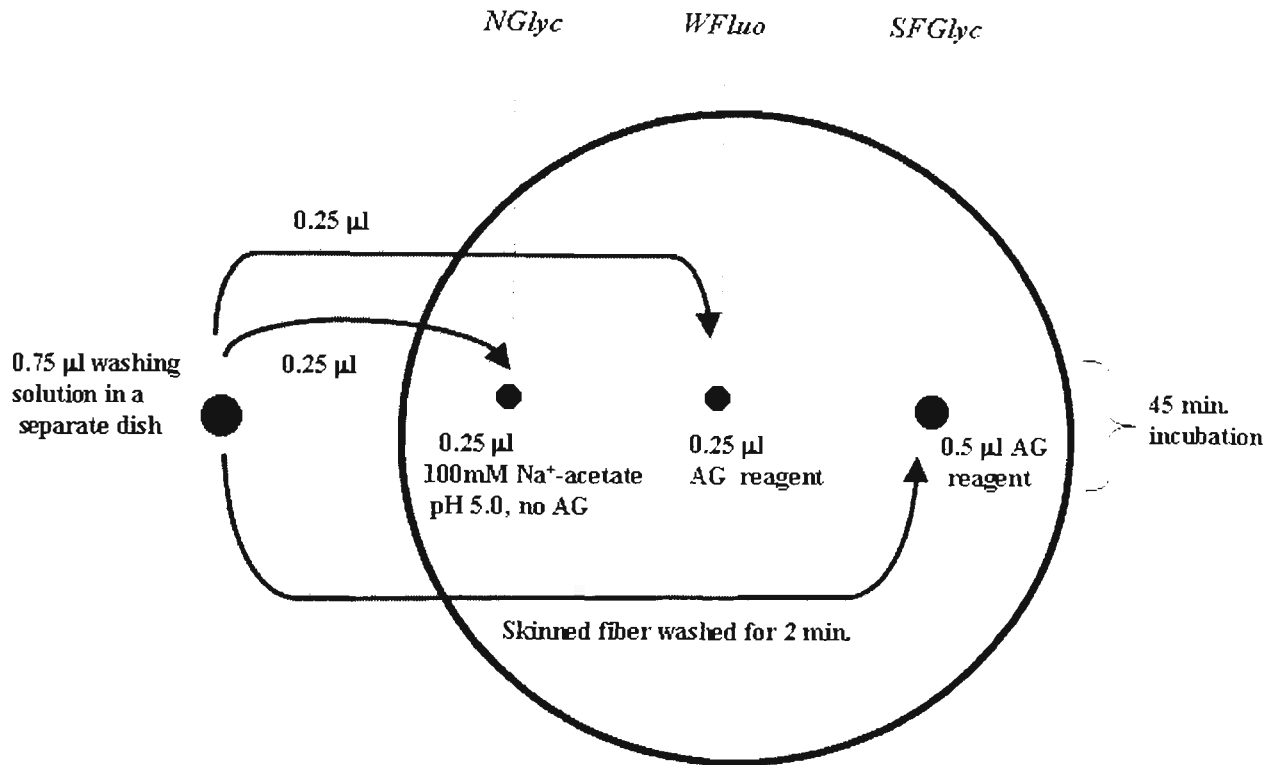


Figure 6.1. Arrangement of reagent droplets under a layer of mineral oil on the bottom of a Petri dish.

After the 45 mins incubation period, 2.0 μl of GLU reagent was added to each droplet and incubated for an additional 30 mins. Note: **WGlyc** was determined by subtracting **NGlyc** from **WFluo** (see *Glycogen analysis in single fibre segments*, page 155).

Determination of fluorogenic material in washing solution

To determine the amount of fluorogenic material washed out of the fibre during the two minute washing step (i.e. **WFluo**), 0.25 μl of the washing solution in the first dish was withdrawn and added to the 0.25 μl droplet of AG reagent (Step 1) in the second dish (see Figure 6.1) and then left for 45 minutes. At the end of 45 minutes, 2.0 μl of GLU reagent was added to the droplet (Step 2) and left for 30 another minutes.

*Determination of **NGlyc** material in the washing solution*

To assess the **NGlyc** in the washing solution, 0.25 μl was withdrawn from the washing droplet and added to a 0.25 μl droplet (see Figure 6.1) of a solution identical to the AG reagent except that AG had been omitted (i.e. no Step 1/reaction 1). After 45 minutes, 2.0 μl of GLU reagent was added to the droplet to start Step 2 and left for 30 minutes.

Microfluorometric reading of samples

After the 30 minute incubation time for Step 2, a micropipette was used to withdraw 0.75 μl from each droplet which was then aspirated by capillarity into individual rectangular borosilicate glass microcells with dimensions of 0.05 x 0.5 x 50 mm (Vitro Dynamics Inc., USA). As illustrated in Figure 6.2, the microcells were then carefully placed side by side in separate grooves on a custom built brass frame with dimensions of 3 x 30 x 75 mm. This brass frame could then be placed on the stage of the epifluorescence microscope for fluorometric readings.

Fluorescence signals were measured in a dark room using an inverted epifluorescence microscope (Axiovert 100TV, Zeiss) with a bialkali photomultiplier

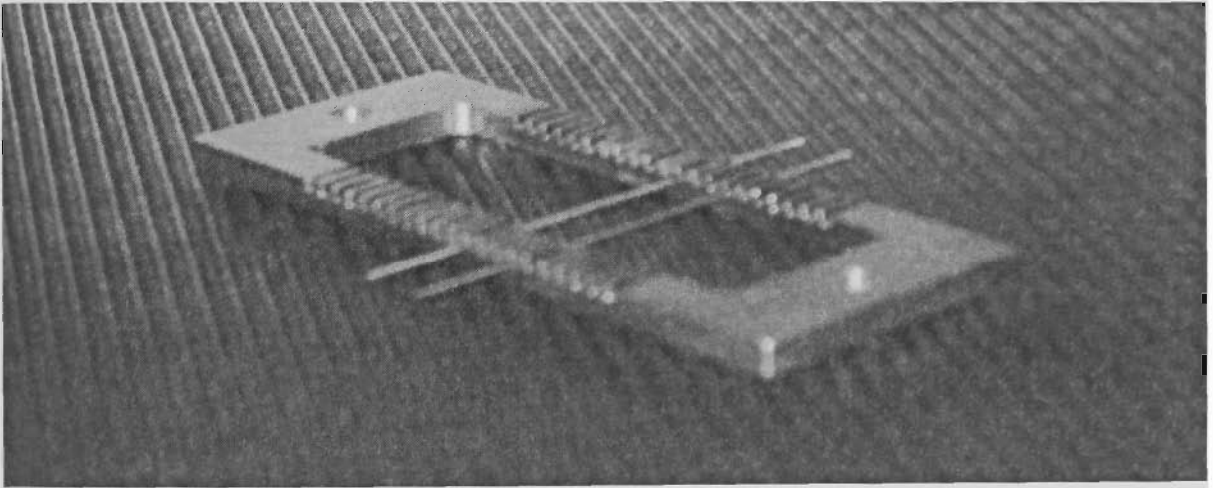


Figure 6.2. Custom designed brass frame with two microcells.

The frame holds a total of 22 microcells.

(Thorn, EMI) and personal computer with Power Lab software (ADInstruments) (Figure 6.3). Zeiss excitation (365 nm), beamsplitter (425 nm) and emission (420 nm) filters were used with a Xenon lamp as the light source. The light field was adjusted so that it covered a 1 mm (25 nl) section of an individual microcell. Fluorescence signals were recorded over a 5 – 10 second period over which no significant bleaching was observed. The fluorescence signal was measured at three places along the length of each microcell with the final values given as an average of the three readings

STD curves

In order to determine the actual amount of NADPH (and hence glycogen) from the fluorescence signal, a glycogen standard curve was prepared using commercial glycogen (Sigma) subjected to the same reaction steps as the samples. The standard solutions were then aspirated into the microcells and the fluorescence signal produced by each standard was then read on the fluorometer and the standard curve was plotted on GraphPad PrismTM program. Finally, the slope of the standard curve was used to convert the fluorescence signals to an amount of glycogen and this value was then divided by the fibre segment volume (see *Measurement of muscle fibre dimensions* in Chapter 2, page 62). The minimum amount of fibre glycogen (NADPH) that could be accurately detected by the fluorometric method used here, defined as the amount of glycogen corresponding to 3 standard deviations of the blank (Bergmeyer *et al.*, 1983), was 6.1 mmol GU for a 5 nl fibre.

Total fibre glycogen (**tGlyc**) was calculated by adding **WGlyc** and **SFGlyc**. Total glycogen was expressed as mmol glucosyl units/litre fibre volume (mmol GU/l fibre),

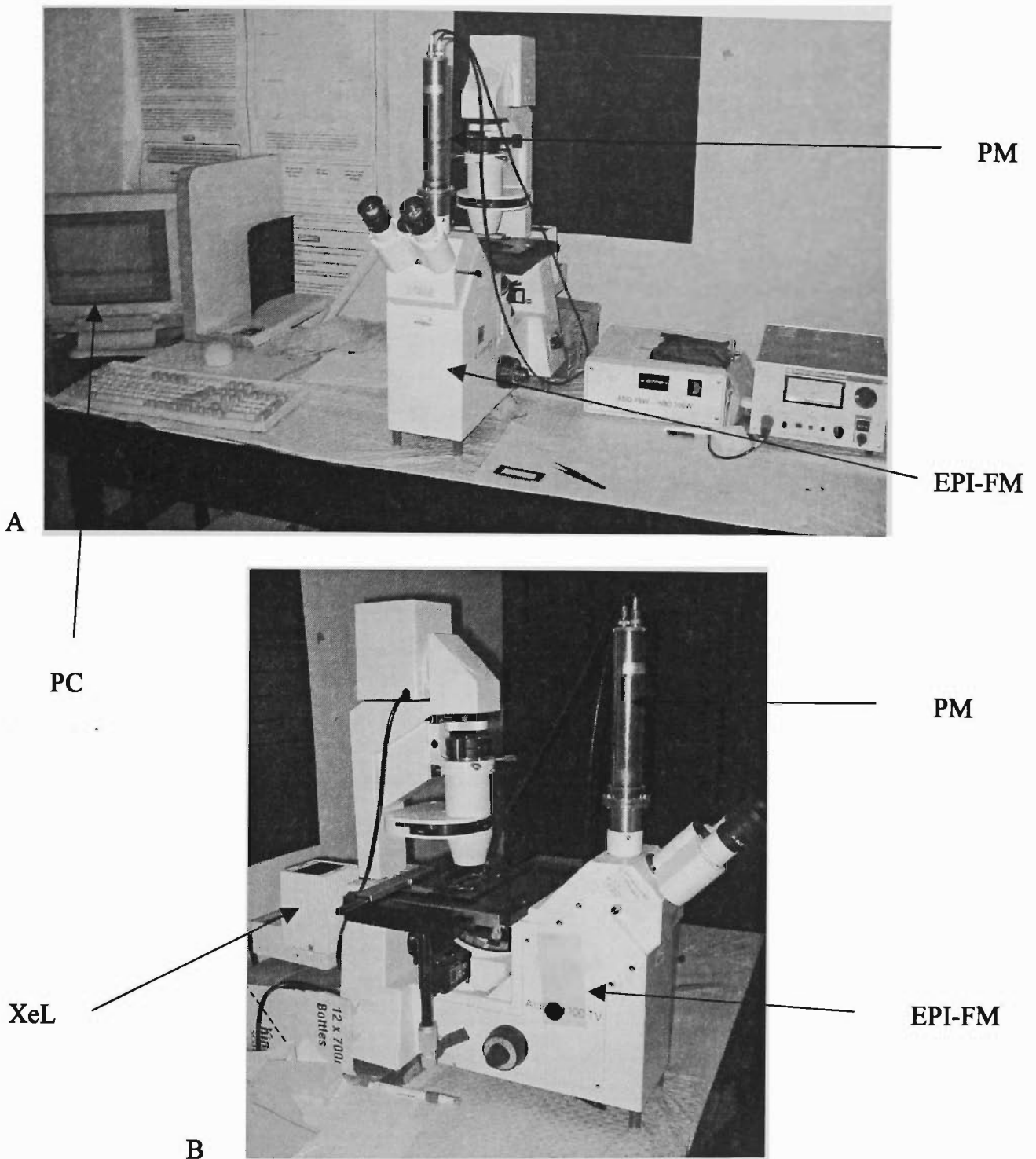


Figure 6.3 A & B. Microfluorometric system used in single fibre glycogen content experiments. PC, personal computer; XeL, xenon lamp; EPI-FM, epifluorescence microscope; PM, photo multiplier.

while **WGlyc** and **SFGlyc** were expressed either as a percentage of **tGlyc** or as mmol GU/l fibre.

Glucose and insulin treatment

In a small number of experiments, glycogen content was determined in single fibres from muscles treated with glucose and insulin. For these experiments, the test EDL muscles were incubated for 2 hours at room temperature (20-25°C) in a Krebs solution containing (in mM): 118 NaCl, 4.75 KCl, 1.18 KH₂PO₄, 1.18 MgSO₄, 24.8 NaHCO₃, 2.5 CaCl₂, 10 glucose and insulin (20 U/L), pH 7.4, which was constantly bubbled with 95 % O₂/5 % CO₂. The control muscles were incubated in a Krebs solution without glucose and insulin for the same length of time and at the same temperature as the test muscles.

Statistics

All results are presented as means and standard error of the mean ($M \pm SEM$) where n represents the number of fibres. Two-tailed paired and non-paired Student's t-tests (GraphPad, Prism) were used for comparisons between two groups of fibres (test and control). Significance was set at $p < 0.05$.

Results

Glycogen content in mechanically skinned fibres from rat EDL muscle

Under the experimental conditions of this study, the average total glycogen content (**tGlyc**) in 53 mechanically skinned fibres from 16 freshly dissected muscles (16 rats) was 58.1 ± 4.2 mmol GU/l fibre (range 7.7-139.2 mmol GU/l fibre), with 88% of the values falling between 20 and 90 mmol GU/l fibre. After 2 min exposure to an

aqueous solution mimicking the myoplasmic environment at rest, the average glycogen content in the skinned fibres (**SFGlyc**) was 40.9 ± 3.3 mmol GU/l fibre, which represents 73.1 ± 2.8 % of the total glycogen.

Fibres dissected from 6 muscles (6 rats) pre-incubated with glucose and insulin had significantly ($p = 0.0095$, Student's two tailed unpaired t-test) higher **tGlyc** (79.7 ± 7.8 mmol GU/l fibre, $n = 32$) than fibres isolated from freshly dissected muscles. In the fibres from treated muscles, **tGlyc** ranged between 8.0 and 200.8 mmol GU/l fibre, with 88 % of values falling between 20 and 140.3 mmol GU/l fibre. The proportion (81.6 ± 2.8 %) of **SFGlyc** (64.5 ± 7.1 mmol GU/l fibre) in fibres from glucose and insulin treated muscles was slightly higher, but not statistically significant ($p = 0.0502$, Student's two tailed unpaired t-test, $n = 32$), than that in the non-treated fibres.

In the experiments described below, the glycogen content in a skinned fibre segment subjected to a given set of conditions ('test') was related to that of an adjacent skinned fibre segment used as 'control'. To validate this experimental strategy the difference in **SFGlyc** between two adjacent segments of the same fibre was determined. The data obtained with 7 individual fibres showed that this difference (mean value: 2.9 ± 4.4 mmol GU/l fibre) was not statistically significant from zero (Student's two-tailed paired t-test).

The contractile responsiveness to T-system depolarization of mechanically skinned fibres from rat EDL muscles

There was no significant difference ($p = 0.2862$; two tailed unpaired t-test) in contractile responsiveness to T-system depolarization between fibres from freshly

dissected muscles and those from muscles incubated with glucose and insulin.

Therefore in this section only the data obtained from fibres prepared from freshly dissected muscles are presented.

Figure 6.4 shows a sample trace of the isometric force responses produced by rat skinned fibres when subjected first to a series of depolarization/repolarization cycles, then briefly to a low $[Mg^{2+}]$ solution, which promotes T-system independent-SR Ca^{2+} release, and finally to a maximally Ca^{2+} -activating solution. The fibre that produced the data shown in Figure 6.4 developed twenty T-system depolarization-induced force responses to 75 % run-down ($R-D_{75\%}$), with the highest response being equal in amplitude with the maximum Ca^{2+} -activated force response (CaF_{max}) and the low Mg^{2+} -induced response being equivalent to 70% of CaF_{max} . As explained in the Methods, for each fibre activated by T-system depolarization to run-down and then by exposure to the high $[Ca^{2+}]$ solution (i.e. subjected to the complete depolarization/repolarization protocol) the response capacity was calculated by adding the amplitudes of the depolarization-induced responses to 75% run-down and then dividing this sum by CaF_{max} . The response capacity for the fibre depicted in Figure 6.4 was 12.8 equivalent maximum Ca^{2+} -activated force responses.

Under the conditions used in this study, the average number of responses to 75% run-down and the average response capacity of a population of 17 skinned fibre segments from freshly dissected rat EDL muscles was 18.4 ± 1.7 and 26.4 ± 2.7 , respectively.

Ten of these fibre segments were subjected to the complete depolarization/repolarization protocol described in the Methods, but the other seven were not exposed to the maximum Ca^{2+} -activating solution since they were

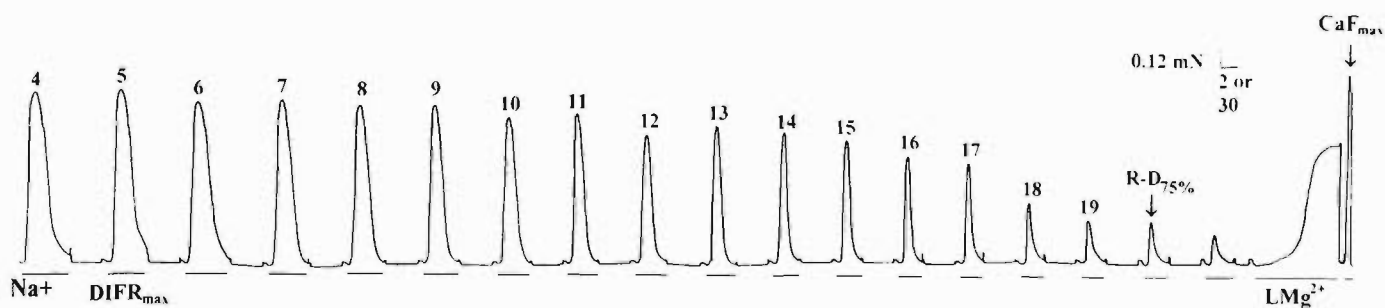


Figure 6.4 An example of the depolarization-induced force responses developed by an EDL fibre to 75 % run-down.

Time scale, 30 s, except during Na^+ depolarizations and low $[\text{Mg}^{2+}]$ (LMg^{2+}) responses (2 s). CaF_{max} , maximum Ca^{2+} -activated force; DIFR_{max} , maximum T-system depolarization -induced force response; $\text{R-D}_{75\%}$, the force response elicited by the fibre at 75 % run-down (for this fibre this was the 20th response in the sequence). The response capacity for this fibre was 12.8 equivalent maximum Ca^{2+} -activated force responses.

subsequently used for determining SFGlyc at run-down (see below). For these 7 fibres, the response capacity was calculated using a value for CaF_{max} that was estimated from the average relative amplitude of the maximum depolarization-induced force responses ($82.2 \pm 6.8\%$ of CaF_{max}) developed by the 10 fibres subjected to the complete protocol. Note that there was no statistically significant difference between the response capacities of the fibres subjected to the complete or incomplete depolarization/repolarization protocol (Student's unpaired two-tailed t-test; $p = 0.2554$). Nine of the 10 fibres that were subjected to the complete protocol were also exposed to the low $[\text{Mg}^{2+}]$ solution, immediately after the 75% run-down point (see Methods). The average force response produced by the fibres in this solution was $77.8 \pm 7.2\%$ of CaF_{max} , suggesting that, under the experimental conditions used in this study, the loss of fibre response capacity at run-down was not due to SR Ca^{2+} depletion or to use-related alterations in the functional status of RyRs.

SR Ca^{2+} - release induced by T-system depolarization in mechanically skinned fibres from rat EDL muscle is not accompanied by detectable loss of fibre glycogen.

Since in this study the average time spent by the test fibre segments in an aqueous solution, as part of the depolarization/repolarization experiment, was 38.4 ± 4.3 min (range: 20.6 to 54.2 min), it was necessary to determine the proportion of SFGlyc lost from the fibres into the bathing solution, independent of the T-system depolarization-induced events. For this purpose SFGlyc was measured in 4 pairs of skinned fibre segments, where one segment of a pair was incubated for 2 min (control) and the other for 32 min (test) in the Polarizing solution. As shown by this experiment, the test skinned fibre segments lost on average $36.0 \pm 12.3\%$ of their initial glycogen content during the 30 min incubation in the Polarizing solution.

To establish the extent of glycogen loss from rat mechanically skinned muscle fibres during the T-system depolarization-induced events, **SFGlyc** was measured in seven fibre segments that were run-down to 75% (without being subsequently exposed to the low $[Mg^{2+}]$ or maximally $[Ca^{2+}]$ activating solutions) and compared to the initial **SFGlyc** measured in the adjacent control segments. The result of this experiment showed that **SFGlyc** in the run-down fibre segments was $33.5 \pm 13.5\%$ lower ($p < 0.05$, Student's two-tailed paired t-test) than that in the paired controls.

From the two sets of data given above it is clear that under the experimental conditions used in this study, there was no detectable loss of glycogen from the skinned fibre preparation directly related to T-system depolarization-induced SR Ca^{2+} release. One possible reason for this finding is that the rat skinned muscle fibres do not contain a Ca^{2+} -sensitive glycogenolytic system. This possibility was tested by placing one group of skinned fibres into a high $[Ca^{2+}]$ solution ($30 \mu M$), and another (the control group) into the Polarizing solution in which the free $[Ca^{2+}]$ was less than $0.2 \mu M$. This strategy, which was used by this laboratory for the same purpose in the toad study (Stephenson *et al.*, 1999), is based on earlier reports (e.g. Ebashi & Endo, 1968) that at high concentrations, Ca^{2+} directly activates phosphorylase kinase, which in turn phosphorylates/activates glycogen phosphorylase thereby initiating glycogenolysis (for review see Picton *et al.*, 1981). After 30 minutes of incubation at room temperature, **SFGlyc** in fibres exposed to $30 \mu M Ca^{2+}$ ($n = 8$) decreased by $71.6 \pm 6.4\%$ compared with the control fibres ($n = 8$) and this difference was statistically significant ($p = 0.0007$, Student's two-tailed unpaired t-test). This result suggests that mechanically skinned fibres of rat EDL, like those of toad iliofibularis muscle,

contain an active glycogenolytic system, which is stimulated when the fibre is exposed to high $[Ca^{2+}]$ for a relatively long (30 min) period of time. However, this glycogenolytic system, unlike that in the toad skinned fibres, was not activated during the brief (3-5 sec) bouts of T-system depolarization-induced sarcoplasmic reticulum (SR) Ca^{2+} release.

Initial SFGlyc and response capacity in mechanically skinned fibres from rat EDL muscle

Previously, Stephenson et al. (1999) reported that, under conditions where the concentrations of ATP and creatine phosphate were maintained high and constant, the capacity of toad mechanically skinned fibres to respond to T-system depolarization was positively correlated ($P < 0.0001$) with initial fibre glycogen concentration. In other words, toad fibres with a lower initial glycogen content developed fewer force responses to run-down. In the present study, using the same protocols for measuring fibre glycogen content and testing contractile responsiveness to T-system depolarization as those used in the toad study, no significant correlation ($r^2 = 0.2249$; $P = 0.0544$) was found between fibre response capacity and initial glycogen content for 17 rat mechanically skinned fibres, whose SFGlyc ranged from 11.9 to 97.2 mmol GU/l fibre (Figure. 6.5).

Discussion

This is the first study in which single mechanically skinned fibres of rat EDL muscle were investigated with respect to glycogen content and contractile responsiveness to T-system depolarization when activated in solutions containing high levels of ATP (8 mM) and creatine phosphate (10 mM).

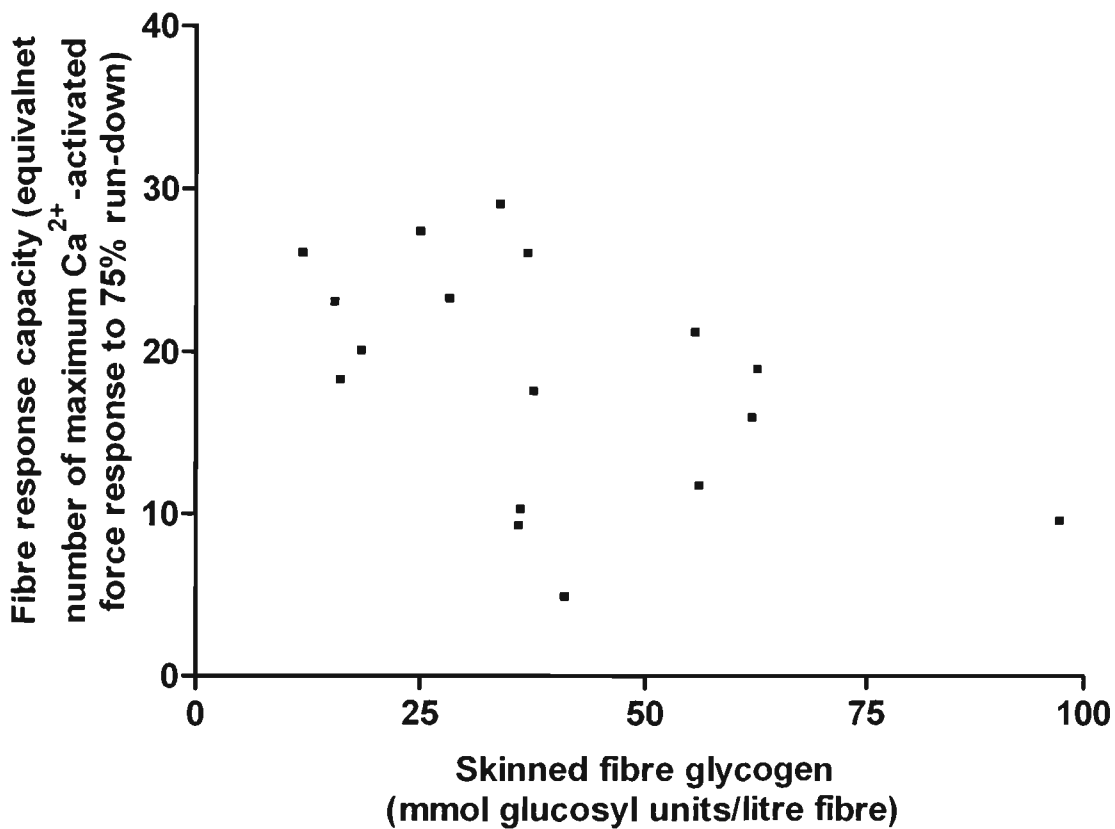


Figure 6.5 Correlation between initial fibre glycogen concentration and fibre response capacity in mechanically skinned fibres.

Data from 17 freshly dissected fibres. Co-efficient of determination $r^2 = 0.2249$; $p = 0.0544$). Fibre response capacity and skinned fibre glycogen were measured in paired segments of the same single fibre.

The mean total glycogen concentration in 53 rat fibres from freshly dissected muscles was 58.1 mmol GU/l fibre or 162.7 mmol GU/kg dry weight. The unit conversion was made on the basis that 1g mammalian muscle contains 0.23g protein, 0.125g extracellular water and 0.645g intracellular water (Meissner *et al.*, 1973). The average total glycogen value for freshly dissected fast-twitch rat EDL fibres, determined by a microfluorometric technique not involving analyte amplification (Nguyen *et al.*, 1998b), is similar to that (~162 mmol/kg dry weight) previously found by Hintz *et al.* (1982) for freeze dried fast-twitch fibres from rat plantaris muscle by conventional fluorometry with analyte amplification.

As part of the T-system depolarization/repolarization protocol, a skinned fibre was first incubated for 2 mins in the Polarizing solution, which is an aqueous relaxing solution mimicking the myoplasmic environment. At the end of this period a large proportion (~73 %) of the total glycogen pool remained associated with the skinned fibre preparation, possibly trapped within or tightly associated with intracellular structures such as the SR (Wanson & Drochmans, 1972; Entman *et al.*, 1980; Friden *et al.*, 1989; Cuenda *et al.*, 1995), while the rest moved as glycogen into the bathing solution. This value is not significantly different from that previously reported for toad skinned fibres (74–85 %; Nguyen *et al.*, 1998b). If the rat skinned fibre was kept in the Polarizing solution for 30 min, the proportion of glycogen retained by it decreased only by another 9% (to ~64% of the initial value), indicating that the glycogen loss from the fibre occurred in a biphasic manner, at a fast rate ($13.50\% \text{min}^{-1}$) in the first 2 min and ~42 times slower ($0.32\% \text{min}^{-1}$) thereafter. Based on this result and that from the toad study (Nguyen *et al.*, 1998b), it is reasonable to suggest that the two pools of glycogen, which are distinguishable by the pattern of elution from a

skinned fibre preparation (of rat or toad) exposed to an aqueous relaxing solution, represent two different glycogen species which differ either by size and/or by intracellular location.

When the Ca^{2+} concentration in the incubating solution was increased to 30 μM , the rate of glycogen loss from rat skinned fibre preparations was markedly higher ($2.40\% \text{min}^{-1}$) than that in the relaxing solution ($0.32\% \text{min}^{-1}$), such that after 30 min the pool of glycogen retained by the fibre was only $\sim 28\%$ of the initial. This rate of fibre glycogen loss is similar to that recorded under the same conditions in the toad study ($2.66\% \text{min}^{-1}$, Stephenson *et al.*, 1999), in which it was ascertained that $\sim 80\%$ of the glycogen lost in the bathing solution was broken down into glucose-1-phosphate, the end product of glycogen phosphorolysis. Based on this result it is concluded that rat skinned fibres, like toad skinned fibres, retain a Ca^{2+} -sensitive glycogenolytic enzyme system even when exposed to an aqueous solution for up to 30 min.

So far, most studies on the regulation of glycogen catabolism in skeletal muscle have been carried out on whole tissue extracts or on purified enzymes (see references in Chebotareva *et al.*, 2001; Roach, 2002). Such studies have two major intrinsic limitations: (i) they involve biochemical alteration of enzyme structure and microenvironment and (ii) they cannot address issues related to the fibre type specificity of the glycogenolytic process. From the data presented here and in the previous study of Stephenson *et al.* (1999), it is clear that, single, mechanically skinned fibres of both rat and toad skeletal muscle possess an endogenous glycogenolytic system as well as an experimentally accessible intracellular milieu.

Furthermore, these fibres can be typed by microelectrophoretic analysis of MHC composition (Nguyen & Stephenson, 2002; O'Connell *et al.*, 2003). On this basis it is proposed that mechanically skinned, single fibre preparations, which proved to be extremely valuable in studies of muscle contractility (Lamb 2002 a & b), heterogeneity (Bortolotto *et al.*, 2000) and plasticity (Bortolotto *et al.*, 1999; Bortolotto *et al.*, 2001) would be well suited for more physiologically meaningful studies of regulation of glycogen catabolism in vertebrate skeletal muscle.

It has been previously reported (Barnes *et al.*, 2001) that the total glycogen content of rat EDL muscle (determined colorimetrically by the PAS method in bundles of fibres) is significantly increased following incubation of the whole muscle in a Krebs solution containing glucose and insulin. In the present study, the average total glycogen content of single fibres isolated from rat EDL muscles treated with glucose and insulin was significantly higher than that of fibres from control muscles, confirming the data of Barnes *et al.* (2001). The glucose-insulin treatment did not eliminate low glycogen fibres, but increased the glycogen content and relative proportion of the high glycogen fibres. Since the outcome of these effects is an increase in muscle heterogeneity with respect to fibre glycogen content (as reflected by the broader range of values recorded for fibres from treated muscles), it is concluded that in studies concerned with the relationship between glycogen concentration and other biochemical or physiological properties of single fibres, the parameter of interest and glycogen content should be determined in the same fibre, particularly if the muscle glycogen level is manipulated experimentally prior to single fibre analyses. It should also be noted that the average value of **SFGlyc** (expressed as a proportion of **tGlyc**) in fibres from muscles incubated with glucose and insulin was

not significantly different from that in fibres from control muscles indicating that this treatment affected in a similar manner the pool of glycogen retained by and that lost from the skinned fibre exposed to an aqueous relaxing solution.

In toad skinned fibres (Stephenson *et al.*, 1999), T-system depolarization-induced SR Ca^{2+} release was accompanied by a substantial loss of fibre glycogen (~76% of initial). This was not observed with rat skinned fibre preparations even though they contained, as argued above, a Ca^{2+} -activatable glycogenolytic system. The apparent lack of glycogen depletion in rat fibres subjected to the same depolarization/repolarization protocol as that used in the toad study (Stephenson *et al.*, 1999) could be explained for example by too little Ca^{2+} being released from the SR during the depolarization step in the rat fibres or by a lower sensitivity to Ca^{2+} of the rat glycogenolytic system.

Both in this study and in the toad study, the amount of Ca^{2+} released from the SR in response to T-system depolarization could be estimated from the amplitude of the depolarization-induced force developed by the skinned fibre. However, this parameter is determined not only by the amount of Ca^{2+} released from the SR for each depolarization bout, but also by the sensitivity to Ca^{2+} of the contractile apparatus. The sensitivity of the contractile apparatus to Ca^{2+} in rat EDL fibres is comparable to that in toad iliofibularis fibres (Fink *et al.*, 1986). Moreover, the average amplitude of the maximum depolarization-induced force responses produced by the rat EDL skinned fibres was similar (~80% of CaF_{max}) to that observed previously for the toad iliofibularis fibres. Taken together, these data suggest that the amount of Ca^{2+} released from the SR in response to T-system depolarization is similar in the rat and toad

fibres, and that the inability to detect T-system depolarization-induced glycogen depletion in rat skinned fibres is more likely to be related to a lower sensitivity to Ca^{2+} of the rat glycogenolytic system. Currently there is no published information regarding potential differences between rat and toad skeletal muscles with respect to the sensitivity to Ca^{2+} of the glycogen phosphorylase kinase activity.

Another possibility for explaining the differences in the extent of T-system depolarization-induced glycogen depletion in skinned fibres from rat and toad muscles is that toad fibres were used at the normal physiological temperature for amphibians (Pörtner *et al.*, 1994) while rat fibres were used at temperatures well below the normal physiological range for mammalian muscle (Severinsen & Munch, 1999).

Earlier research on muscle fatigue in humans has produced compelling evidence that glycogen content and mammalian skeletal muscle performance are positively correlated (for reviews see Green, 1991; Fitts, 1994). Later it was found that the depletion of intracellular glycogen stores associated with exercise-induced decrease in human muscle function is not accompanied by drastic changes in the cellular pool of ATP (Vollestad *et al.*, 1988; reviewed by Green, 1991; Fitts, 1994), a surprising result given the well established role of glycogen as a rapid metabolic source of ATP for anaerobic glycolysis. One of the ideas put forward to explain the tight correlation between exercise-induced reduction in human muscle performance and endogenous glycogen depletion, when the whole cell ATP concentration is still relatively high, is that muscle glycogen plays a protective role in excitation-contraction (E-C) coupling processes that is independent of its metabolic function (Green, 1991; Fitts, 1994). So far, the strongest support for this idea has come from the toad study (Stephenson *et*

al., 1999) in which it was shown that when activated in high [ATP]-[creatine phosphate] solutions, mechanically skinned iliofibularis muscle fibres containing lower levels of initial glycogen produce fewer T-system depolarization induced force responses to run-down than skinned fibres with higher glycogen content.

In the present study, the same protocols for fibre dissection, skinning and depolarization/repolarization as those used in the toad study (Stephenson *et al.*, 1999) found no close correlation between initial glycogen content and fibre response capacity in rat mechanically skinned EDL muscle fibres. A possible explanation for this result is that glycogen does not play a protective, non-metabolic role in E-C coupling events in rat mechanically skinned fibres. This possibility is not fully consistent, however, with the finding that rat skinned fibres, which retained a relatively large proportion (~67%) of initial glycogen throughout the process of T-system depolarization induced activation, displayed an average response capacity (18.4) that was about 4 times higher ($P < 0.0001$) than that obtained previously for toad mechanically skinned fibres (4.6 ± 0.8 , $n = 22$; see Figure. 4 in Stephenson *et al.*, 1999) in which the rate of fibre glycogen loss associated with the T-system depolarization induced activation process was quite high (at least one order of magnitude higher than that elicited by exposure of the skinned fibres to a high $[Ca^{2+}]$ containing solution for 30 min). Indeed, the largest response capacity value displayed by a single fibre segment in the present study was 29.1, while the highest response capacity value displayed by a fibre segment in the toad study was 12.9 (Stephenson *et al.*, 1999). The possibility that glycogen does not play a protective role in the contractile responsiveness of rat skinned muscle fibres to T-system depolarization activation is also inconsistent with the data of Barnes *et al.* (2001), who found that

mechanically skinned fibres from rat EDL muscles in which the glycogen content (determined in bundles of fibres) was elevated by the glucose-insulin treatment discussed above reached 50% run-down after a larger number of T-system depolarizations than their paired controls.

An alternative explanation for the lack of correlation between initial glycogen content and responsiveness to T-system depolarization in rat skinned fibres is that the experimental strategy, which proved to be well suited for probing the non-metabolic role of glycogen in toad iliofibularis muscle fibre excitability cannot be used for the same purpose with fibres of rat EDL muscle. This is because, under the conditions used in this study, the endogenous glycogen level in the skinned fibre preparations activated in the presence of high [ATP] and [creatine phosphate] does not fall below a 'critical value' (with respect to E-C coupling processes) before other non-glycogen related factors, such as the redox and/or Ca^{2+} -dependent phosphorylation status of reactive groups on the RYR/ Ca^{2+} release channel or DHPR/voltage sensor (Han & Bakker, 2003; Stephenson *et al.*, 1995), ultimately limit the capacity of the fibres to respond to T-system depolarization. Based on this rationale one would predict that a strategy similar to that used in the toad study, but including a method that would increase the rate of glycogen depletion during T-system depolarization induced contractions without affecting the E-C coupling related processes in a glycogen-dependent manner, should enable the experimenter to gain further insights into the non-metabolic role of glycogen in mammalian muscle fibre excitability by using rat mechanically skinned fibres as an experimental model.

In summary, this study has shown that mechanically skinned fibres of rat EDL retain a large proportion of endogenous glycogen when exposed to an aqueous low $[Ca^{2+}]$ solution, but lost most of it when exposed to a high $[Ca^{2+}]$ solution for 30 min, probably due to the action of a Ca^{2+} -sensitive glycogenolytic system. These data suggest that rat mechanically skinned EDL fibres, like toad iliofibularis muscle fibres could be easily used in studies concerned with vertebrate skeletal muscle glycogen and its regulation as they relate to MHC-based fibre type. When subjected to T-system depolarization (by ionic substitution), rat mechanically skinned fibres did not appear to lose any detectable glycogen above that lost through incubation in a relaxing aqueous solution and there was no correlation between their initial glycogen content and their excitability.

CONCLUDING REMARKS

The data obtained from the four studies described in this thesis lead to several major conclusions of conceptual and methodological nature:

- The responsiveness of rat EDL mechanically skinned fibres to T-system depolarisation induced by ion substitution (described by the parameters maxDIFR and $75\%R-D$), using the Lamb & Stephenson (1990a) method, varies with animal age over the broad period currently regarded as the ‘adult’ stage of rat development (4-21 wks), with 4 wks and 21 wks fibres being the worst and the best performers, respectively. Two potential contributors to this phenomenon are the age-related changes in the molecular structure/function of the T-system membrane and fibre diameter.
- In rat skeletal muscle, participants/events in E-C coupling reach the adult stage in a non-synchronized manner. This idea (suggested also by a number of published studies) is supported by the finding that the two seemingly unrelated descriptors of E-C coupling processes in mechanically skinned fibres of the rat EDL muscle examined in this work, maxDIFR and $75\%R-D$, display a slightly different pattern of change with age over the period 4-21 wks postnatal.
- The responsiveness to T-system depolarisation of mechanically skinned fibres from 21 wk-old rat skeletal muscle [determined with the Lamb & Stephenson protocol (1990a)] varies with the fibre type (indicated by MHC composition) and identity (probably the function) of the muscle of origin, such that type IIB

EDL fibres perform overall significantly better than type I SOL fibres and type IIB sternomastoid fibres. The data obtained in this thesis indicate that the Lamb & Stephenson protocol (1990a) would require further refinement if needed to investigate at the cellular level, E-C coupling processes in rat skeletal muscles other than EDL.

- The “voltage window” phenomenon, first described by Chua & Dulhunty (1988) for bundles of rat SOL fibres, can also be observed in single, mechanically skinned rat SOL fibres subjected to the T-system depolarisation protocol developed for rat EDL fibres.
- Under a set of storage conditions simulating those used in T-system depolarisation experiments with mechanically skinned fibres (alternating, brief incubations under oil, at RT and at 4° C), rapidly dissected rat skeletal muscles (EDL and SOL) retain a large proportion (> ~ 70%) of endogenous glycogen and phosphorylase activities for up to 3 hrs.
- The temperature sensitivity of glycogenolytic processes in skeletal muscle may be species specific. This idea is supported by the finding that the stability of glycogen and phosphorylase activities in rat EDL and SOL muscles incubated under oil at RT or 4°C was markedly lower than that of glycogen and phosphorylase activities in toad iliofibularis muscle stored under the same conditions.

- Mechanically skinned fibres of rat skeletal muscle may be used to investigate the relationship between glycogenolytic processes and fibre type. This conclusion is based on the well established feasibility of MHC isoform analyses in single rat fibres and on the finding that, when exposed to aqueous relaxing solutions, mechanically skinned fibre preparations retain a large proportion of glycogen, which decreases quite markedly in the presence of high $[Ca^{2+}]$.
- The experimental protocol used to investigate the relationship between glycogen content and responsiveness to T-system depolarisation of toad mechanically skinned muscle fibres when glycogen was not required as an energy source may not be used, without further modification, for the same purpose with rat mechanically skinned fibres. This is likely to be due to the stability of the glycogen pool associated with rat skinned fibre preparation, during the T-system depolarisation-induced activation process.

REFERENCES

- Adams GR, McCue SA, Zeng M & Baldwin KM (1999). Time course of myosin heavy chain transitions in neonatal rats: importance of innervation and thyroid state. *Am J Physiol* **276**, R954-R961.
- Aidley, DJ (1998). *The physiology of excitable cells*. 4th Ed. Cambridge University Press, Cambridge, UK.
- Albis A, Couteaux R, Janmot C & Roulet A (1989). Specific programs of myosin expression in the postnatal development of rat muscles. *Eur J Biochem* **183**, 583-590.
- Allen DG, Lannergren J & Westerblad H (1995). Muscle cell function during prolonged activity: cellular mechanisms of fatigue. *Exp Physiol* **80**, 497-527.
- Alnaqeeb MA & Goldspink G (1986). Changes in fibre type, number and diameter in developing and ageing skeletal muscle. *J Anat* **153**, 31-45.
- Armstrong RB & Phelps RO (1984). Muscle fibre type composition of the rat hindlimb. *Am J Anat* **171**, 259-272.
- Asmussen E (1979). Muscle fatigue. *Med Sci Sports*. **11**, 313-21

Bagshaw CR (1993). Muscle contraction. 2nd Ed. London: Chapman & Hall.

Bakker AJ, Head SI, Wareham AC and Stephenson DG (1998). Effect of clenbuterol on sarcoplasmic reticulum function in single skinned mammalian skeletal muscle fibers. *Am J Physiol* 274, C1718-C1726.

Bakker AJ & Berg HM (2002). Effect of taurine on sarcoplasmic reticulum function and force in skinned fast-twitch skeletal muscle fibres of the rat. *J Physiol* 538, 185-194.

Baldwin KM (1984). Muscle development: neonatal to adult. In: Ed RL Terjung, *Exercise and sport sciences reviews*. MacMillan Pub Co., NY, USA. 12, 1-19.

Ballor DL & Poehlman ET (1993). Exercise intensity does not affect depression of resting metabolic rate during severe diet restriction in male *Sprague-Dawley* rats. *J Nutr* 123, 1270-1276.

Bar A & Pette D (1988). Three fast myosin heavy chains in adult rat skeletal muscle. *FEBS Lett* 235, 153-155.

Barnard RJ, Edgerton VR, Furukawa T & Peter JB (1971). Histochemical, biochemical and contractile properties of red, white, and intermediate fibers. *Am J Physiol* 220, 410-414.

Barnes M, Gibson LM & Stephenson DG (2001). Increased muscle glycogen content is associated with increased capacity to respond to T-system depolarization in mechanically skinned skeletal muscle fibres from the rat. *Pflugers Arch* **442**, 101-106.

Beam KG, Knudson CM & Powell JA (1986). A lethal mutation in mice eliminates the slow calcium current in skeletal muscle cells. *Nature* **320**, 168-170.

Beam KG & Knudson CM (1988). Effect of postnatal development on calcium currents and slow charge movement in mammalian skeletal muscle. *J Gen Physiol* **91**, 799-815.

Bergmeyer HU, Horder M & Markowetz D (1983). Reliability of laboratory results and practicability of procedures. In: Eds Bergmeyer HU, Bergmeyer J & Grable M. *Methods of enzymatic analysis*. Weinheim: Verlag Chemie. pp. 21-39.

Bergstrom J, Hermansen L, Hultman E & Saltin B (1967). Diet, muscle glycogen and physical performance. *Acta Physiol Scand* **71**, 140-150

Bertocchini F, Ovitt CE, Conti A, Barone V, Scholer HR, Bottinelli R, Reggiani C & Sorrentino V (1997). Requirement of the ryanodine receptor type 3 for efficient contraction in neonatal skeletal muscles. *EMBO J* **16**, 6956-6963.

Blazev R & Lamb GD (1999). Adenosine inhibits depolarization-induced Ca^{2+} release in mammalian skeletal muscle. *Muscle Nerve* **22**, 1674-1683.

Blazev R, Hussain M, Bakker AJ, Head SI & Lamb GD (2001). Effects of the PKA inhibitor H-89 on excitation-contraction coupling in skinned and intact skeletal muscle fibres. *J Muscle Res Cell Motil* **22**, 277-86.

Bortolotto S, Stephenson DG & Stephenson GMM (1999). Fibre type populations and Ca^{2+} -activated properties of single fibres in soleus muscle from SHR and WKY rats. *Am J Physiol* **276**, C628-C637.

Bortolotto SK, Cellini M, Stephenson DG & Stephenson GM (2000). MHC isoform composition and Ca^{2+} - or Sr^{2+} -activation properties of rat skeletal muscle fibers. *Am J Physiol* **279**, C1564-C1577.

Bortolotto SK, Stephenson DG & Stephenson GM (2001). Caffeine thresholds for contraction in electrophoretically typed, mechanically skinned muscle fibres from SHR and WKY rats. *Pflugers Arch* **441**, 692-700.

Bortolotto S & Reggiani C (2002). Cellular and molecular basis of heterogeneity in contractile performance of human muscles. *Basic Appl Myol* **12**, 7-16.

Bottinelli R, Schiaffino S & Reggiani C (1991). Force-velocity relations and myosin heavy chain isoform compositions of skinned fibres from rat skeletal muscle. *J Physiol* **437**, 655-672.

Bottinelli R, Canepari M, Pellegrino MA & Reggiani C (1996). Force-velocity properties of human skeletal muscle fibres: myosin heavy chain isoform and temperature dependence. *J Physiol* **495**, 573-586.

Bottinelli R & Reggiani C (2000). Human skeletal muscle fibres: molecular and functional diversity. *Prog Biophys Mol Biol* **73**, 195-262.

Bottinelli R (2001). Functional heterogeneity of mammalian single muscle fiber: do myosin isoforms tell the whole story? *Pflugers Arch* **443**, 6-17.

Brenner B (1998). Muscle mechanics II: skinned muscle fibres. In: H Sugi (Ed). *Current methods in muscle physiology: advantages, problems and limitations*. Oxford University Press, NY, USA. pp. 33-69.

Briggs FN, Poland JL & Solaro RJ (1977). Relative capabilities of sarcoplasmic reticulum in fast and slow mammalian skeletal muscles. *J Physiol* **266**, 587-594.

Broberg S & Sahlin K (1989). Adenine nucleotide degradation in human skeletal muscle during prolonged exercise. *J Appl Physiol* **67**, 116-22.

Brook MH & Kaiser KK (1970). Muscle fiber types: how many and what kind? *Arch Neurol* **23**, 369-379.

Brown DH (1994). Glycogen metabolism and glycolysis in muscle. In: AG Engel & C Franzini-Armstrong (Eds), *Myology*. Vol 1, Chpt 25. McGraw-Hill, New York: US. pp. 648 - 664.

Brum G, Stefani E & Rios E (1987). Simultaneous measurements of Ca current and intracellular Ca concentrations in single muscle fibres of the frog. *Can J Physiol Pharmacol* **65**, 681-685.

Calder PC & Geddes R (1990). Post mortem glycogenolysis is a combination of phosphorolysis and hydrolysis. *Int J Biochem* **22**, 847-856.

Carraro U & Catani A (1983). A sensitive SDS-PAGE method separating myosin heavy chain isoforms of rat skeletal muscles reveals the heterogeneous nature of the embryonic myosin. *Biochem Biophys Res Comm* **116**, 793-802.

Chandler WK, Rakowski RF & Schneider MF (1976). Effects of glycerol treatment and maintained depolarization on charge movement in muscle. *J Physiol* **254**, 285-316.

Chaplin ER, Nell GW & Walker SM (1970). Excitation-contraction latencies in postnatal rat skeletal muscle fibers. *Exp Neurol* **29**, 142-151.

Chasiotis D (1985). Effects of adrenaline infusion on cAMP and glycogen phosphorylase in fast twitch and slow twitch rat muscles. *Acta Physiol. Scand* **125**, 537-540.

Chasiotis D, Edstrom L, Sahlin K & Sjöholm H (1985). Activation of glycogen phosphorylase by electrical stimulation of isolated fast twitch and slow twitch muscles from rat. *Acta Physiol Scand* **123**, 43-47.

Chebotareva NA, Klinov SV & Kurganov BI (2001). Regulation of muscle glycogen phosphorylase by physiological effectors. *Biotechnol Genet Eng Rev* **18**, 265-297.

Chin ER & Allen DG (1997). Effects of reduced muscle glycogen concentration on force, Ca^{2+} release and contractile function in intact mouse skeletal muscle. *J Physiol* **498**, 17-29.

Chua M & Dulhunty AF (1988). Inactivation of excitation-contraction coupling in rat extensor digitorum longus and soleus muscles. *J Gen Physiol* **91**, 737-757.

Clausen T (2003). $Na^+ - K^+$ pump regulation and skeletal muscle contractility. *Physiol Rev* **83**, 1269-1324.

Close R (1964). Dynamic properties of fast and slow skeletal muscles of the rat during development. *J Physiol* 173, 74-95.

Close RI (1972). Dynamic properties of mammalian skeletal muscles. *Physiol Rev* 52, 129-97.

Cohen P (1983a). Phosphorylase kinase from rabbit skeletal muscle. *Meth Enzymol* 99, 243-250.

Cohen P (1983b). Protein phosphorylation and the control of glycogen metabolism in skeletal muscle. *Philos Trans R Soc Lond B Biol Sci.* 302, 13-25.

Cohn C & Joseph D (1971). Feeding habits and daily rhythms in tissue glycogens in the rat. *Proc Soc Exp Biol Med* 137, 1305-1306.

Conlee RK, Rennie MJ & Winder WW (1976). Skeletal muscle glycogen content: diurnal variation and effects of fasting. *Am J Physiol* 231, 614-618.

Conlee RK, Mclane JA, Rennie MJ, Winder WW & Holloszy JO (1979). Reversal of phosphorylase activation in muscle despite continued contractile activity. *Am J Physiol* 237, R291-R296.

Conte Camerino D, De Luca A, Mambrini M & Vrbova G (1989). Membrane ionic conductances in normal and denervated skeletal muscle of the rat during development. *Pflügers Arch* **413**, 568-570.

Coonan JR & Lamb GD (1998). Effect of transverse-tubular chloride conductance on excitability in skinned skeletal muscle fibres of rat and toad. *J Physiol*. **509**, 551-564.

Corconado R, Morrissette J, Sukhareva M & Vaughan DM (1994). Structure and function of ryanodine receptors. *Am J Physiol* **266**, C1485-C1504.

Craig R (1994). The structure of the contractile filaments. In: C Franzini-Armstrong & AG Engel (Eds). *Myology*. 2nd ed. Chpt 5. McGraw-Hill, NY: USA. pp. 134-175.

Csernoch L (1999). Regulation of the ryanodine receptor calcium release channel of the sarcoplasmic reticulum in skeletal muscle. *Acta Physiol Hung* **86**, 77-97.

Cuenda A, Nogues M, Gutierrez-Merino C & de Meis L (1993). Glycogen phosphorylation can form a metabolic shuttle to support Ca^{2+} uptake by sarcoplasmic reticulum membranes in skeletal muscle. *Biochem Biophys Res Comm* **196**, 1127-1132.

Cuenda A, Henao F, Nogues M & Gutierrez-Merino C (1994). Quantification and removal of glycogen phosphorylase and other enzymes associated with sarcoplasmic reticulum membrane preparations. *Biochim Biophys Acta* **1194**, 35-43.

Cuenda A, Nogues M, Henao F & Gutierrez-Merino C (1995). Interaction between glycogen phosphorylase and sarcoplasmic reticulum membranes and its functional role. *J Biol Chem* **270**, 11998-12004.

Cullen MJ, Hollingworth S & Marshall MW (1984). A comparative study of the transverse tubular system of the rat extensor digitorum longus and soleus muscles. *J Anat* **138**, 297-308.

Curtis BM & Catterall WA (1983). Solubilization of the calcium antagonist receptor from the rat brain. *J Biol Chem* **258**, 7280-7283.

Curtis BM & Catterall WA (1986). Reconstitution of the voltage-sensitive calcium channel purified from skeletal muscle transverse tubules. *Biochem* **25**, 3077-3083.

Damiani E & Margreth A (1994). Characterization study of the ryanodine receptor and of calsequestrin isoforms of mammalian skeletal muscles in relation to fibre types. *J Muscle Res Cell Motil* **15**, 86-101.

Damiani E, Sacchetto R & Margreth A (1999). Regulatory protein phospholamban is not expressed in rat soleus muscle. *J Muscle Res Cell Motil* **20**, 90.

De Barsey T & Hers H-G (1990). Normal metabolism and disorders of carbohydrate metabolism. In: JB Harris & DM Turnbull (Eds), *Clinical endocrinology and metabolism*. **4**, 499-522.

Delbono O & Meissner G (1996). Sarcoplasmic reticulum Ca²⁺ release in rat slow- and fast-twitch muscles. *J Membrane Biol*. **151**, 123-130.

Dirksen RT (2002). Bi-directional coupling between dihydropyridine receptors and ryanodine receptors. *Front Biosci* **7**, d659-70.

Donaldson SKB (1985). Peeled Mammalian skeletal muscle fibers. Possible stimulation of Ca²⁺ release via a transverse tubule-sarcoplasmic reticulum mechanism. *J Gen Physiol* **86**, 501-525.

Drachman DB & Johnston DM (1973). Development of a mammalian fast muscle: dynamic and biochemical properties correlated. *J Physiol* **234**, 29-42.

Dulhunty AF (1992). The voltage-activation of contraction in skeletal muscle. *Prog Biophys Molec Biol* **57**, 181-223.

Dulhunty AF & Dlutowski M (1979). Fiber types in red and white segments of the rat sternomastoid muscle. *Am J Anat* **156**, 51-62.

Dulhunty AF & Gage PW (1983). Asymmetrical charge movement in slow- and fast-twitch mammalian muscle fibres in normal and paraplegic rats. *J Physiol* **341**, 213-231.

Dulhunty AF & Gage PW (1988). Effects of extracellular calcium concentration and dihydropyridines on contraction in mammalian skeletal muscle. *J Physiol* **399**, 63-80.

Dulhunty AF, Haarmann CS, Green D, Laver DR, Board PG & Cararotto MG (2002). Interactions between dihydropyridine receptors and ryanodine receptors in striated muscle. *Prog Biophys Molec Biol* **79**, 45-75.

Dulhunty AF & Pouliquin P (2003). What we don't know about the structure of ryanodine receptor calcium release channels. *Clin Exp Pharmacol Physiol* **30**, 713-723.

Dutka TL & Lamb GD (2000). Effect of lactate on depolarization-induced Ca^{2+} release in mechanically skinned skeletal muscle fibers. *Am J Physiol* **278**, C517-C525.

Dux L (1993). Muscle relaxation and sarcoplasmic reticulum function in different muscle types. *Rev Physiol Biochem Pharmacol* **122**, 69-147.

Ebashi S & Endo M (1968). Calcium ion and muscle contraction. *Prog Biophys Mol Biol* **18**, 123-178.

Edge MB (1970). Development of apposed sarcoplasmic reticulum at the T system and sarcolemma and the change in orientation of triads in rat skeletal muscle. *Dev Biol* **23**, 634-650.

Edman KA, Reggiani C, Schiaffino S, & te Kronnie G (1988). Maximum velocity of shortening related to myosin isoform composition in frog skeletal muscle fibres. *J Physiol* **395**, 679-694.

Endo M (1977). Calcium release from the sarcoplasmic reticulum. *Physiol Rev* **57**, 71-108.

Endo M & Iino M (1980). Specific perforation of muscle cell membranes with preserved SR functions by saponin treatment. *J Muscle Res Cell Motil* **1**, 89-100.

Enoka RM (1995). Mechanisms of muscle fatigue: central factors and task dependency. *J Electromyogr Kinesiol* **5**, 141-149.

Entman M. L, Keslensky SS, Chu A & Van Winkle WB (1980). The sarcoplasmic reticulum-glycogenolytic complex in mammalian fast twitch skeletal muscle. *J Biol Chem* **255**, 6245-625.

Eusebi F, Miledi R & Takahashi T (1980). Calcium transients in mammalian muscles. *Nature* **284**, 560-561.

Ferreira LDM, Palmer TN & Fournier PA (1998). Prolonged exposure to halothane and associated changes in carbohydrate metabolism in rat muscles in vivo. *J Appl Physiol* **84**, 1470-1474.

Fill MD & Best PM (1988). Contractile activation and recovery in skinned frog muscle stimulated by ionic substitution. *Am J Physiol* **254**, C107-C114.

Fill M & Copello JA (2002). Ryanodine receptor calcium release channels. *Physiol Rev* **82**, 893-922.

Fink RH, Stephenson DG & Williams DA (1986). Potassium and ionic strength effects on the isometric force of skinned twitch muscle fibres of the rat and toad. *J Physiol* **370**, 317-337.

Fink RH & Stephenson DG (1987). Ca^{2+} -movements in muscle modulated by the state of K^{+} -channels in the sarcoplasmic reticulum membranes. *Pflügers Arch* **409**, 374-380.

Fitts RH (1992). Substrate supply and energy metabolism during brief high intensity exercise: importance in limiting performance. In DR Lamb & CV Gisolfi (Eds). *Energy metabolism in exercise and sport*. Chpt 2. Cooper Publishing, Carmel, IN, USA. pp. 53-106.

Fitts R (1994). Cellular mechanisms of muscle fatigue. *Physiol Rev* **74**, 49-94.

Flucher BE, Conti A, Takeshima H & Sorrentino V (1999). Type 3 and type 1 ryanodine receptors are localized in triads of the same mammalian skeletal muscle fibers. *J Cell Biol* **146**, 621-629.

Fosset M, Jaimovich E, Delpont E & Lazdunski M (1983). [3H] Nitrendipine receptors in skeletal muscle. *J Biol Chem* **258**, 6086-6092.

Franzini-Armstrong C (1970). Studies of the triad. I. Structure of the junction in frog twitch fibres. *J Cell Biol* **47**, 488-498.

Franzini-Armstrong C (1994). The sarcoplasmic reticulum and the transverse tubules. In: AG Engel & C Franzini-Armstrong (Eds). *Myology*. 2nd Ed. Chpt 6. McGraw-Hill, NY, USA, pp. 176-199.

Franzini-Armstrong C & Protasi F (1997). Ryanodine receptors of striated muscles: a complex channel capable of multiple interactions. *Physiol Rev* 77, 699-729.

Friden J, Seger J & Ekblom B (1985). Implementation of periodic acid-thiosemicarbazide-silver proteinate staining for ultrastructural assessment of muscle glycogen utilization during exercise. *Cell Tissue Res* 242, 229-232.

Friden J, Seger J & Ekblom B (1989). Topographical localization of muscle glycogen: an ultrahistochemical study in the human vastus lateralis. *Acta Physiol. Scand* 135, 381-391.

Froemming GR, Murray BE, Harmon S, Pette D & Ohlendieck K (2000). Comparative analysis of the isoform expression pattern of Ca(2+)-regulatory membrane proteins in fast-twitch, slow-twitch, cardiac, neonatal and chronic low-frequency stimulated muscle fibers. *Biochim Biophys Acta* 1466, 151-68.

Fryer MW & Stephenson DG (1996). Total and sarcoplasmic reticulum calcium contents of skinned fibres from the rat. *J Physiol* 493, 357-370.

Futatsugi A, Kuwajima G & Mikoshiba K (1995). Tissue-specific and developmentally regulated alternative splicing in mouse skeletal muscle ryanodine receptor mRNA. *Biochem J* **305**, 373-378.

Galler S, Schmitt TL & Pette D (1994). Stretch activation, unloaded shortening velocity, and myosin heavy chain isoforms of rat skeletal muscle fibres. *J Physiol.* **478**, 513-521.

Galler S, Hilber K, Gohlsch B & Pette D (1997). Two functionally distinct myosin heavy chain isoforms in slow skeletal muscle fibres. *FEBS Let* **410**, 150-152.

Geddes R (1986). Glycogen: a metabolic viewpoint. *Biosci Rep* **6**, 415-428.

Geiger PC, Cody MJ, Macken RL & Sieck GC (2000). Maximum specific force depends on myosin heavy chain content in rat diaphragm muscle fibers. *J Appl Physiol* **89**, 695-703.

Gillis JM (1985). Relaxation of vertebrate skeletal muscle. A synthesis of the biochemical and physiological approaches. *Biochim Biophys Acta* **811**, 97-145.

Goldspink G (1980). Alterations in myofibril size and structure during growth, exercise, and changes in environmental temperature.. In: LD Peachy (Ed), *Skeletal muscle*. Handbook of Physiology. Sect. 10, Chpt. 18, American Physiological Society, Bethesda, Maryland, USA. pp. 539-554.

Gordon AM, Homsher E & Regnier M (2000). Regulation of contraction in striated muscle. *Physiol Rev* **80**, 853-924.

Gordon AM, Regnier M & Homsher E (2001). Skeletal and cardiac muscle contractile activation: tropomyosin “rocks and rolls”. *News Physiol Sci* **16**, 49-55.

Gorza I (1990). Identification of a novel type 2 fiber population in mammalian skeletal muscle by combined use of histochemical myosin ATPase and anti-myosin monoclonal antibodies. *J Histochem Cytochem* **38**, 257-265.

Gottschall J, Zenker W, Neuhuber W, Mysicka A & Muntener M (1980). The sternomastoid muscle of the rat and its innervation. Muscle fiber composition, perikarya and axons of efferent and afferent neurons. *Anat Embryol (Berl)* **160**, 285-300.

Green HJ (1991). How important is endogenous muscle glycogen to fatigue in prolonged exercise? *Can J Physiol Pharmacol* **69**, 290-297.

Hamilton SL, Serysheva I & Straburg GM (2000). Calmodulin and excitation-contraction coupling. *News Physiol Sci* **15**, 281-284.

Han JW, Thieleczek R, Varsanyi M & Heilmeyer LM (1992). Compartmentalized ATP synthesis in skeletal muscle triads. *Biochemistry* **31**, 377-84.

Han R & Bakker AJ (2003). The effect of chelerythrine on depolarization-induced force responses in skinned fast skeletal muscle fibres of the rat. *Brit J Pharmacol* **138**, 417-426.

Hannon JD, Lee NKM, Yandong C & Blinks JR (1992). Inositol trisphosphate (InsP₃) causes contraction in skeletal muscle only under artificial conditions: evidence that Ca²⁺ release can result from depolarization of t-tubules. *J Muscle Res Cell Motil* **13**, 447-456.

Harridge SDR, Bottinelli R, Canepari M, Pellegrino MA, Reggiani C, Esbjorsson M & Saltin B (1996). Whole-muscle and single-fibre contractile properties and myosin heavy chain isoforms in humans. *Pflugers Arch* **432**, 913-920.

Hazlewood CF & Nichols BL (1967). In vitro investigation of resting muscle membrane potential in preweanling and weanling rat. *Nature* 935-936.

Herrmann-Frank A, Luttgau HC & Stephenson DG (1999). Caffeine and excitation-contraction coupling: a stimulating story. *J Muscle Res Cell Motil* **20**, 223-237.

Hintz CS, Chi MM, Fell RD, Ivy JL, Kaiser KK, Lowry CV & Lowry OH (1982).

Metabolite changes in individual rat muscle fibers during stimulation. *Am J Physiol* **242**, C218-C228.

Hirata Y, Atsumi M, Ohizumi Y & Nakahata N (2003). Mastoparan binds to glycogen phosphorylase to regulate sarcoplasmic reticular Ca^{2+} release in skeletal muscle. *Biochem J* **371**, 81-88.

Hutber CA & Bonen A (1989). Glycogenesis in muscle and liver during exercise. *J Appl Physiol* **66**, 2811-2817.

Illingworth B, Lerner J & Cori GT (1952). Structure of glycogens and amylopectins.1. Enzymatic determination of chain length. *J Biol Chem* **199**, 631-640.

Jacquemond V, Csernoch L, Klein MG & Schneider MF (1991). Voltage-gated and calcium-gated calcium release during depolarization of skeletal muscle fibers. *Biophys J* **60**, 867-873.

James DE & Kraegen EW (1984). The effect of exercise training on glycogen, glycogen synthase and phosphorylase in muscle and liver. *Eur J Appl Physiol* **52**, 276-281.

Johnson LN (1992). Glycogen phosphorylase: control by phosphorylation and allosteric effectors. *FASEB J* **6**, 2274-2282.

Kelly AM (1980). T tubules in neonatal rat soleus and extensor digitorum longus muscles. *Dev Biol* **80**, 501-505.

Kennedy LD, Kirkman BR, Lomako J, Rodriguez IR & Whelan WJ (1985). The biogenesis of rabbit-muscle glycogen. In: MC Berman, W Gevers & LH Opie (Eds), *Membranes and Muscle*. ICSU Symposium Series Volume 6. IRL Press.

Kobayashi M, Takatori T, Nakajima M, Saka K, Iwase H, Nagao M, Niijima M & Matsuda Y (1999). Does the sequence of onset of rigor mortis depend on the proportion of muscle fibre types and on intra-muscular glycogen content? *Int J Legal Med* **112**, 167-171.

Korge P & Campbell KB (1995). The importance of ATPase microenvironment in muscle fatigue: a hypothesis. *Int J Sports Med* **16**, 172-9.

Kruszynska YT, Ciaraldi TP & Henry RR (2001). Regulation of glucose metabolism in skeletal muscle. In: LS Jefferson & AD Cherrington (Eds), *The endocrine pancreas and regulation of metabolism*. Handbook of Physiology, Sect. 7, Vol 2. Oxford University Press, USA. pp. 579-607.

Kushmerick MJ, Moerland TS & Wiseman RW (1992). Mammalian skeletal muscle fibers distinguished by contents of phosphocreatine, ATP and Pi. *Proc Natl Acad Sci USA*. **89**, 7521-7525.

Kyselovic J, Leddy JJ, Ray A, Wigle J & Tuana BS (1994). Temporal differences in the induction of dihydropyridine receptor subunits and ryanodine receptors during skeletal muscle development. *J Biol Chem* **269**, 21770-21777.

Laemmli UK (1970). Cleavage of structural proteins during the assembly of bacteriophage T₄. *Nature* **227**, 680-685.

La Framboise WA, Daood MJ, Guthrie RD, Butler-Browne GS, Whalen RG & Ontell M (1990). Myosin isoforms in neonatal rat extensor digitorum longus, diaphragm, and soleus muscles. *Am J Physiol* **259**, L116-L122.

Lamb GD (1992). DHP receptors and excitation-contraction coupling. *J Muscle Res Cell Motil* **13**, 394-405.

Lamb GD (1993). Ca²⁺-inactivation, Mg²⁺ inhibition and malignant hyperthermia. *J Muscle Res Cell Motil* **14**, 554-556.

Lamb GD (2000). Excitation-contraction coupling in skeletal muscle: comparison with cardiac muscle. *Clin Exp Pharmacol Physiol* **27**, 216-224.

Lamb GD (2002a). Excitation-contraction coupling and fatigue mechanisms in skeletal muscle: studies with mechanically skinned fibres. *J Muscle Res Cell Motil* **23**, 81-91.

Lamb GD (2002b). Voltage-sensor control of Ca²⁺ release in skeletal muscle: insights from skinned fibers. *Front Biosci* **7**, d834-d842.

Lamb GD & Walsh T (1987). Calcium currents, charge movement and dihydropyridine binding in fast- and slow-twitch muscles of the rat and rabbit. *J Physiol* **393**, 595-617.

Lamb GD & Stephenson DG (1990a). Calcium release in skinned muscle fibres of the toad by transverse tubule depolarization or by direct stimulation. *J Physiol* **423**, 495-517.

Lamb GD & Stephenson DG (1990b): Control of calcium release and the effect of ryanodine in skinned muscle fibres of the toad. *J Physiol* **423**, 519-542.

Lamb GD & Stephenson DG (1991). Excitation-contraction coupling in skeletal muscle fibres of rat and toad in the presence of GTP gamma γ S. *J Physiol* **444**, 65-84.

Lamb GD & Stephenson DG (1994). Effects of intracellular pH and $[Mg^{2+}]$ on excitation-contraction coupling in skeletal muscle fibres of the rat. *J Physiol* **478**, 331-339.

Lamb GD & Stephenson DG (1996). Effects of FK506 and rapamycin on excitation-contraction coupling in skeletal muscle fibres of the rat. *J Physiol* **49**, 569-576.

Lamb GD & Cellini MA (1999). High intracellular $[Ca^{2+}]$ alters sarcoplasmic reticulum function in skinned skeletal muscle fibres of the rat. *J Physiol* **519**, 815-27.

Lamb GD, Junankar PR & Stephenson DG (1995). Raised intracellular $[Ca^{2+}]$ abolishes excitation-contraction coupling in skeletal muscle fibres of rat and toad. *J Physiol* **489**, 349-362.

Larner J, Illingworth B, Cori GT & Cori CF (1952). Structure of glycogens and amylopectins.2. Analysis by stepwise enzymatic degradation. *J Biol Chem* **199**, 641-651.

Launikonis BS & Stephenson DG (1999). Effects of β -escin and saponin on the transverse-tubular system and the sarcoplasmic reticulum membranes of rat and toad skeletal muscle. *Pflugers Arch* **437**, 955-965.

- Launikonis BS & Stephenson DG (2001). Effects of membrane cholesterol manipulation on excitation-contraction coupling in skeletal muscle of the toad. *J Physiol* **534**, 71-85.
- Launikonis BS & Stephenson DG (2002). Tubular system volume changes in twitch fibres from toad and rat skeletal muscle assessed by confocal microscopy. *J Physiol* **538**, 607-18.
- Lee AG (2002). A calcium pump made visible. *Curr Opin Struct Biol* **12**, 547-554.
- Lee YS, Ondrias K, Duhl AJ, Ehrlich BE & Kin DH (1991). Comparison of calcium release from sarcoplasmic reticulum of slow and fast twitch muscles. *J Memb Biol* **122**, 155-163.
- Lees SJ, Franks PD, Spangenburg EE & Williams JH (2001). Glycogen and glycogen phosphorylase associated with sarcoplasmic reticulum: effects of fatiguing activity. *J Appl Physiol* **91**, 1638-1644.
- Loughlin M (1993). *Muscle biopsy. A laboratory investigation*. Butterworth-Heinemann, Oxford, UK
- Luff AR (1985). Dynamic properties of fiber bundles from the rat sternomastoid muscle. *Exp Neurol* **89**, 491-502.

Luttgau HC & Spiecker, H (1979). The effects of calcium deprivation upon mechanical and electrophysiological parameters in skeletal muscle fibres of the frog. *J Physiol* **296**, 411-429.

Luttgau HC & Stephenson DG (1986). Ion movements in skeletal muscle in relation to the activation of contraction. In: TE Androli, JF Hoffman, DD Fanestil & SG Schultz (Eds), *Physiology of membrane disorders*. 2nd Ed. Plenum, NY, USA. pp. 449-468.

Mackrill JJ (1999). Protein-protein interactions in intracellular Ca²⁺-release channels function. *Biochem J* **337**, 345-361.

Marchand I, Chorneyko K, Tarnopolsky M, Hamilton S, Shearer J, Potvin J & Graham TE (2002). Quantification of subcellular glycogen in resting human muscle: granule size, number, and location. *J Appl Physiol* **93**, 1598-1607.

Martonosi AN (1994). Regulation of calcium by the sarcoplasmic reticulum. In: AG Engel & C Franzini-Armstrong (Eds). *Myology*. 2nd Ed. Chpt 21 A. McGraw-Hill, NY, USA, pp. 553-584.

- Matterson DR (1994). Ionic channels in excitable cells. In: AG Engel & C Franzini-Armstrong (Eds). *Myology*. 2nd Ed. Chpt 14 A. McGraw-Hill, NY, USA, pp. 391-404.
- Meissner G, Conner GE & Fleischer S (1973). Isolation of sarcoplasmic reticulum by zonal centrifugation and purification of Ca²⁺-pump and Ca²⁺-binding proteins. *Biochim Biophys Acta* **298**, 246-69.
- Meissner G, Darling E & Eveleth J (1986). Kinetics of rapid Ca²⁺ release by sarcoplasmic reticulum. Effects of Ca²⁺, Mg²⁺ and adenine nucleotides. *Biochem* **26**, 236-244.
- Meissner G (1994). Ryanodine receptor/Ca²⁺ release channels and their regulation by endogenous effectors. *Annu Rev Physiol* **56**, 485-508.
- Melendez R, Melendez-Hevia E & Cascante M (1997). How did glycogen structure evolve to satisfy the requirement for rapid mobilization of glucose? A problem of physical constraints in structure building. *J Mol Evol* **45**, 446-455.
- Melendez R, Melendez-Hevia E, Mas F, Mach J & Cascante M (1998). Physical constraints in the synthesis of glycogen that influence its structural homogeneity: a two-dimensional approach. *Biophys J* **75**, 106-114.

Melzer W (1995). The role of calcium ions in excitation-contraction coupling of skeletal muscle fibres. *Biochim Biophys Acta* 1241, 59-116.

Meyer F, Heilmeyer LMG, Haschke RH & Fischer EH (1970). Control of phosphorylase activity in a muscle glycogen particle. *J Biol Chem* 245, 6642-6648.

Moisescu DG & Pusch H (1975). A pH-metric method for the determination of the relative concentration of calcium to EGTA. *Pflugers Arch* 355, R122.

Moisescu DG & Thieleczek R (1978). Calcium and strontium concentration changes within skinned skeletal muscle preparations following a change in the external bathing solution. *J Physiol* 275, 241-262.

Moss RL, Diffie GM & Greaser ML (1995). Contractile properties of skeletal muscle fibers in relation to myofibrillar protein isoforms. *Rev Physiol Biochem Pharmacol* 126, 1-62.

Murayama T & Ogawa Y (2002). Roles of two ryanodine receptor isoforms coexisting in skeletal muscle. *Trends Cardiovasc Med* 12, 305-311.

Musch TI, Warfel BS, Moore RL & Larach DR (1989). Anaesthetic effects on liver and muscle glycogen concentrations: rest and post exercise. *J Appl Physiol* 66, 2895-2900.

Natori R (1949). On the mechanism of muscle contraction (in Japanese). *J Physiol Soc Jpn* 11, 14-15.

Newgard CB, Hwang PK & Fletterick RJ (1989). The family of glycogen phosphorylases: structure and function. *Crit Rev Biochem Mol Biol* 24, 69-95.

Newgard CB, Brady MJ, O'Doherty RM & Saltiel AR (2000). Organizing glucose disposal: emerging roles of the glycogen targeting subunits of protein phosphatase-1. *Diabetes* 49, 1967-1977.

Newsholme EA & Leech AR (1995). *Biochemistry for the medical sciences*. John Wiley & Sons, Chichester: UK.

Nguyen LT & Stephenson GMM (1999). An electrophoretic study of myosin heavy chain expression in skeletal muscles of the toad *Bufo marinus*. *J Muscle Res Cell Motil* 20, 687-695.

Nguyen LT & Stephenson GM (2002). Myosin heavy chain isoform expression and Ca^{2+} -stimulated ATPase activity in single fibres of toad rectus abdominis muscle. *J Muscle Res Cell Motil* 23, 147-56.

Nguyen LT, Stephenson DG & Stephenson GMM (1998a). A direct microfluorometric method for measuring subpicomole amounts of nicotinamide adenine dinucleotide phosphate, glucose and glycogen. *Anal Biochem* **259**, 274-278.

Nguyen LT, Stephenson DG & Stephenson GMM (1998b). Microfluorometric analyses of glycogen in freshly dissected, single skeletal muscles of the cane toad using a mechanically skinned fibre preparation. *J Muscle Res Cell Motil* **19**, 631-638.

O'Connell B, Nguyen LT & Stephenson GM (2003). A single fibre study of the relationship between MHC and TnC isoform composition in rat skeletal muscle. *Biochem J in press* DOI: 10.1042/BJ20031170.

Owen VJ, Lamb GD, Stephenson DG & Fryer MW (1997). Relationship between depolarization-induced force responses and Ca^{2+} content in skeletal muscle fibres of rat and toad. *J Physiol* **498**, 571-586.

Passonneau JV & Lowry OH (1993). *Enzymatic analysis: A practical guide*. Humana Press, Totowa, NJ.

Peachy LD & Franzini-Armstrong C (1980). Structure and function of membrane systems of skeletal muscle cells. In: LD Peachy (Ed). *Skeletal muscle*. Sect 10. Handbook of Physiology. Williams & Wilkins, Baltimore, USA. pp. 23-71.

Pearson AM & Young RB (1989). *Muscle and meat biochemistry*. Academic Press. San Diego, California, USA.

Pereon Y, Louboutin JP & Noireaud J (1993). Contractile responses in rat extensor digitorum longus muscles at different times of postnatal development. *J Comp Physiol [B]* **163**, 203-211.

Pereon Y, Dettbarn C, Lu Y, Westlund KN, Zhang JT & Palade P (1998). Dihydropyridine isoform expression in adult rat skeletal muscle. *Pflugers Arch.* **436**, 309-314.

Peter JB, Barnard RJ, Edgerton VR, Gillespie CA & Stempel KE (1972). Metabolic profiles of three fiber types of skeletal muscle in guinea pigs and rabbits. *Biochem* **11**, 2627-2633.

Pette D & Staron RS (1990). Cellular and molecular diversities of mammalian skeletal muscle fibers. *Rev Physiol Biochem Pharmacol* **116**, 1-76.

Pette D & Staron RS (1997). Mammalian skeletal muscle fiber type transitions. *Int Rev Cytol* **170**, 143-223.

Pette D, Peuker H & Staron RS (1999). The impact of biochemical methods for single muscle fibre analysis. *Acta Physiol Scand* **166**, 261-277.

Pette D & Staron RS (2000). Myosin isoforms, muscle fiber types, and transitions.

Micros Res Tech 50, 500-509.

Picton C, Klee CB & Cohen P (1981). The regulation of muscle phosphorylase kinase by calcium ions, calmodulin and troponin-C. *Cell Calcium* 2, 281-294.

Plant DR, Lynch GS & Williams DA (2002). Hydrogen peroxide increases depolarization-induced contraction of mechanically skinned slow twitch fibres from rat skeletal muscles. *J Physiol* 539, 883-891.

Polishchuk SV, Brandt NR, Meyer HE, Varsanyi M & Heilmeyer LMG (1995). Does phosphorylase kinase control glycogen biosynthesis in skeletal muscle? *FEBS Lett* 362, 271-275.

Pörtner HO, Branco LGS, Malvin GM & Wood SC (1994). A new function for lactate in the toad *Bufo marinus*. *J Appl Physiol* 76, 2405-2410.

Posterino GS (2001). "Current" advances in mechanically skinned skeletal muscle fibres. *Clin Exp Pharmacol Physiol*. 28, 668-74.

Posterino GS, & Fryer MW (2000). Effects of high myoplasmic L-lactate concentration on E-C coupling in mammalian skeletal muscle. *J Appl Physiol* **89**, 517-528.

Posterino GS, Lamb GD & Stephenson DG (2000). Twitch and tetanic force responses and longitudinal propagation of action potentials in skinned skeletal muscle fibres of the rat. *J Physiol*. **527**,131-7.

Posterino GS, Dutka TL & Lamb GD (2001). L(+)-lactate does not affect twitch and titanic responses in mechanically skinned mammalian muscle fibres. *Pflugers Arch* **442**, 197-203.

Ranvier L (1873). Propriétés et structures différentes des muscles rouges et des muscles blancs chez les lapins et chez les raies. *Comptes rendus hebdomadair des séances de l'Academie des sciences (Paris)* **77**, 1030-1034.

Rassier DE, MacIntosh BR and Herzog W (1999). Length dependence of active force production in skeletal muscle. *J Appl Physiol* **86**, 1445-1457.

Ren JM & Hultman E (1988). Phosphorylase activity in needle biopsy samples – factors influencing transformation. *Acta Physiol Scand* **133**, 109-114.

- Ren JM, Gulve EA, Cartee GD & Holloszy JO (1992). Hypoxia causes glycogenolysis without an increase in percent phosphorylase a in rat skeletal muscle. *Am J Physiol* **263**, E1086-E1091.
- Roach PJ (2002). Glycogen and its metabolism. *Curr Mol Med* **2**, 101-120.
- Rodney GG, Williams RY, Stracburg GM, Beckingham K & Hamilton SI (2000). Regulation of RYR1 activity by Ca^{2+} and calmodulin. *Biochem* **39**, 7807-7812.
- Rossi D & Sorrentino V (2002). Molecular genetics of ryanodine receptors Ca^{2+} -release channels. *Cell Calcium* **32**, 307-319.
- Ruegg JC (1992). *Calcium in muscle contraction*. 2nd ed. Springer-Verlag, Berlin, Germany.
- Rybicka KK (1996). Glycosomes – the organelles of glycogen metabolism. *Tissue Cell* **28**, 253-265.
- Sahyun M (1931). On the carbohydrate of the muscles of the frog (*Rana Pipiens*). *J Biol Chem* **94**, 29-38.
- Sadow A (1965). Excitation-contraction coupling in skeletal muscle. *Pharmacol Rev* **17**, 265-320.

Schiaffino S & Margreth A (1969). Coordinated development of the sarcoplasmic reticulum and t-system during postnatal differentiation of rat skeletal muscle. *J Cell Biol* **41**, 855-875.

Schiaffino S, Gorza L, Sartore S, Saggin L, Ausoni S, Vianello M, Gunderson K & Lomo T (1989). Three myosin heavy chain isoforms in type 2 skeletal muscle fibres. *J Muscle Res Cell Motil* **10**, 197-205.

Schiaffino S & Reggiani C (1994). Myosin isoforms in mammalian skeletal muscle. *J Appl Physiol* **77**, 493-501.

Schiaffino S & Reggiani C (1996). Molecular diversity of myofibrillar proteins: gene regulation and functional significance. *Physiol Rev* **76**, 371-423.

Schiaffino S & Salviati G (1997). Molecular diversity of myofibrillar proteins: isoform analysis at the protein and mRNA level. *Meth Cell Biol* **52**, 349-369.

Schneider MF (1994). Control of calcium release in functioning skeletal muscle fibers. *Annu Rev Physiol* **56**, 463-484.

Schneider MF & Chandler WK (1973). Voltage dependent charge movement in skeletal muscle. *Nature* **242**, 244-246.

Schwartz LM, McCleskey EW & Almers W (1985). Dihydropyridine receptors in muscle are voltage-dependent but most are not functional calcium channels. *Nature* 314, 747-751.

Severinsen T & Munch IC (1999). Body core temperature during food restriction in rats. *Acta Physiol Scand* 165, 299-305.

Shearer J & Graham TE (2002). New perspectives on the storage and organization of muscle glycogen. *Can J Appl Physiol* 27, 179-203.

Sjostrom M, Friden J & Ekblom B (1982). Fine structural details of human muscle fibres after fibre type specific glycogen depletion. *Histochem* 76, 425-438.

Smythe C & Cohen P (1991). The discovery of glycogenin and the priming mechanism for glycogen biogenesis. *Eur J Biochem* 200, 625-631.

Squire JM & Morris EP (1998). A new look at thin filament regulation in vertebrate skeletal muscle. *FASEB J* 12, 761-771.

Stephenson, DG & Williams DA (1981). Temperature effect on Ca^{2+} -activation curves in fast and slow-twitch skinned muscle fibres of the rat. *J Physiol* 317, 281-302.

Stephenson, DG & Williams DA (1982). Effects of sarcomere length on the force-pCa relation in fast- and slow-twitch skinned muscle fibres from the rat. *J Physiol* **333**, 637-653.

Stephenson DG, Lamb G, Stephenson GMM & Fryer MW (1995). Mechanisms of excitation-contraction coupling relevant to skeletal muscle fatigue. *Adv Exp Med Biol*. **384**, 45-56.

Stephenson DG, Lamb GD & Stephenson GMM (1998). Events of the excitation-contraction-relaxation (E-C-R) cycle in fast- and slow-twitch mammalian muscle fibres relevant to muscle fatigue. *Acta Physiol Scand* **162**, 229-245.

Stephenson DG, Nguyen LT & Stephenson GMM (1999). Glycogen content and excitation-contraction coupling in mechanically skinned muscle fibres of the cane toad. *J Physiol* **519**, 177-187.

Stephenson EW (1981). Activation of fast skeletal muscle: contributions of studies on skinned fibers. *Am J Physiol* **240**, C1-C19.

Stephenson GM & Stephenson DG (1996). Effects of ammonium ions on the depolarization-induced and direct activation of the contractile apparatus in mechanically skinned fast-twitch skeletal muscle fibres of the rat. *J Muscle Res Cell Motil* **17**, 611-616.

Stephenson GMM (2001). Hybrid skeletal muscle fibers: a rare or common phenomenon? *Clin Exp Pharmacol Physiol* **28**, 692-702.

Stryer L (1995). *Biochemistry*. 4th Ed. WH Freeman & Co. New York, NY, USA. pp. 581-602

Sutko JL & Airey JA (1996). Ryanodine receptor Ca^{2+} release channels: Does diversity in form equal diversity in function? *Physiol Rev* **76**, 1027- 1071.

Szczesna D & Potter JD (2002). The role of troponin in the Ca^{2+} -regulation of skeletal muscle contraction. *Results Prob Cell Diff* **36**, 171-190.

Szentesi P, Zaremba R, Van Mechelen W & Stienen GJM (2001). ATP utilization for calcium uptake and force production in different types of human skeletal muscle fibres. *J Physiol* **531**, 393-403.

Szent-Gyorgyi A (1949). Free-energy relations and contractions of actomyosin. *Biol Bull* **96**, 140-161.

Takeyasu K, Kawase T & Yoshimura SH (2003). Intermolecular interaction between Na^+/K^+ -ATPase α subunit and glycogen phosphorylase. *Ann NY Acad Sci* **986**, 522-524.

Talmadge RJ, Roy RR & Edgerton VR (1993). Muscle fiber types and function. *Curr Opin Rheumatol* **5**, 695-705.

Talmadge RJ (2000). Myosin heavy chain isoform expression following reduced neuromuscular activity: potential regulatory mechanisms. *Muscle Nerve* **23**, 661-679.

Tamaki T & Uchiyama S (1995). Absolute and relative growth of rat skeletal muscle. *Physiol Behav* **57**, 913-919.

Tanabe T, Beam KG, Powell JA & Numa S (1988). Restoration of excitation-contraction coupling and slow calcium current in dysgenic muscle by dihydropyridine receptor complementary DNA. *Nature* **336**, 134-139.

Tanabe T, Mikami A, Numa S & Beam KG (1990). Cardiac-type excitation contraction coupling in dysgenic skeletal muscle injected with cardiac dihydropyridine receptor cDNA. *Nature* **344**, 451-453.

Tang W, Sencer S & Hamilton SL (2002). Calmodulin modulation of proteins involved in excitation-contraction coupling. *Front Biosci* **7**, d1583-d1589.

Umazume Y (1991). Natori's skinned fiber. In: E Ozawa, T Masaki & Y Nabeshima (Eds), *Frontiers in muscle research: myogenesis, muscle contraction, and muscle dystrophy*. Chpt 10. Excerpta Medica, New York, USA. pp 261-274.

UNSW Embryology. Rat development.

<http://anatomy.med.unsw.edu.au/cbl/embryo/OtherEmb/Rat.htm>

Villa Moruzzi E, Bergamini E & Gori Bergamini Z (1981). Glycogen metabolism and the function of fast and slow muscles of the rat. *Pflugers Arch* **391**, 338-342.

Villa Moruzzi E & Bergamini E (1983). Effect of denervation on glycogen metabolism in fast and slow muscle of rat. *Muscle Nerve* **6**, 356-366.

Vollestad NK, Sejersted OM, Bahr R, Woods JJ & Bigland-Ritchie B (1988). Motor drive and metabolic responses during repeated submaximal contractions in humans. *J Appl Physiol* **64**, 1421-1427.

Walker JW, Somlyo AV, Goldman YE, Somlyo AP & Trentham DR (1987). Kinetics of smooth and skeletal muscle activation by laser pulse photolysis of caged inositol 1,4,5-trisphosphate. *Nature* **327**, 249-52.

Wanson JC & Drochman P (1968). Rabbit skeletal muscle glycogen. A morphological and biochemical study of glycogen β -particles isolated by the precipitation-centrifugation method. *J Cell Biol* **38**, 130-150.

Wanson JC & Drochmans P (1972). Role of the sarcoplasmic reticulum in glycogen metabolism. *J Cell Biol* **54**, 206-224.

Weihe WH (1987). The laboratory rat. In: T Poole (Ed), *The UFAW handbook on the care and management of laboratory animals*. 6th Ed. Longman Scientific & Technical, UK, pp. 309-330.

Weiss A & Leinwand LA (1996). The mammalian myosin heavy chain gene family. *Annu Rev Cell Dev Biol* **12**, 417-439.

Weiss S, Rossi R, Pellegrino MA, Bottinelli R & Geeves MA (2001). Differing ADP release rates from myosin heavy chain isoforms define the shortening velocity of skeletal muscle fibers. *J Biol Chem*. **276**, 45902-45908.

Winegrad S. (1971). Studies of cardiac muscle with high permeability to calcium produced by treatment with ethylenediaminetetraacetic acid. *J Gen Physiol* **58**, 71-93.

Witzmann FA, Kim DH & Fitts RH (1983). Effect of hindlimb immobilization on the fatigability of skeletal muscle. *J Appl Physiol* **54**, 1242-1248.

Wood DS, Zollman J & Reuben JP (1975). Human skeletal muscle: properties of the 'chemically skinned' fiber. *Science* **187**, 1075-1076.

Xu KY, Zweier JL & Becker LC (1995). Functional coupling between glycolysis and sarcoplasmic reticulum Ca^{2+} transport. *Circ Res* **77**, 88-97.

Xu KY & Becker LC (1998). Ultrastructural localization of glycolytic enzymes on sarcoplasmic reticulum vesicles. *J Histochem Cytochem* **46**, 419-427.

Yano K & Zarain-Herzberg A (1994). Sarcoplasmic reticulum calsequestrins: structural and functional properties. *Mol Cell Biochem* **135**, 61-70.

Zorato F, Sacchetto R & Margreth A (1994). Identification of two ryanodine receptor transcripts in neonatal, slow-, and fast-twitch rabbit skeletal muscles. *Biochem Biophys Res Com* **203**, 1725-1730.